

1 **Ice, Cloud, and Land Elevation Satellite 2 (ICESat-2)**

2
3 **Algorithm Theoretical Basis Document (ATBD)**

4
5 **for**

6
7 **Land - Vegetation Along-Track Products (ATL08)**

8
9
10
11 **Contributions by Land/Vegetation SDT Team Members**
12 **and ICESat-2 Project Science Office**

13 **(Amy Neuenschwander, Katherine Pitts, Benjamin Jelley, John Robbins,**
14 **Jonathan Markel, Sorin Popescu, Ross Nelson, David Harding, Dylan**
15 **Pederson, Brad Klotz, and Ryan Sheridan)**

16
17
18 **ATBD prepared by**

19 **Amy Neuenschwander and**

20 **Katherine Pitts**

21
22 **Winter 2021**

23 **(This ATBD Version corresponds to release 004 of the ICESat-2 ATL08**
24 **data)**

25
26
27 **Content reviewed: technical approach, assumptions, scientific soundness,**
28 **maturity, scientific utility of the data product**

31 **ATL08 algorithm and product change history**
 32

ATBD Version	Change
2016 Nov	Product segment size changed from 250 signal photons to 100 m using five 20m segments from ATL03 (Sec 2)
2016 Nov	Filtered signal classification flag removed from classed_pc_flag (Sec 2.3.2)
2016 Nov	DRAGANN signal flag added (Sec 2.3.5)
2016 Nov	Do not report segment statistics if too few ground photons within segment (Sec 4.15 (3))
2016 Nov	Product parameters added: h_canopy_uncertainty, landsat_flag, d_flag, delta_time_beg, delta_time_end, night_flag, msw_flag (Sec 2)
2017 May	Revised region boundaries to be separated by continent (Sec 2)
2017 May	Alternative DRAGANN parameter calculation added (Sec 4.3.1)
2017 May	Set canopy flag = 0 when <i>L-km</i> segment is over Antarctica or Greenland regions (Sec 4.4 (1))
2017 May	Change initial canopy filter search radius from 3 m to 15 m (Sec 4.9 (6))
2017 May	Product parameters removed: h_rel_ph, terrain_thresh
2017 May	Product parameters added: segment_id, segment_id_beg, segment_id_end, dem_flag, surf_type (Sec 2)
2017 July	Urban flag added (Sec 2.4.17)
2017 July	Dynamic point spread function added (Sec 4.11 (6))
2017 July	Methodology for processing <i>L-km</i> segments with buffer added (Sec 4.1 (2), Sec 4.17)
2017 July	Revised alternative DRAGANN methodology (see bolded text in Sec 4.3.1)
2017 July	Added post-DRAGANN filtering methodology (Sec 4.7)
2017 July	Updated SNR to be estimated from superset of ATL03 and DRAGANN found signal used for processing ATL08 (Sec 2.5.18)
2017 September	More details added to DRAGANN description (Sec 4.3), and corrections to DRAGANN implementation (Sec 3.1.1, Sec 4.3 (9))
2017 September	Added Appendix A – very detailed DRAGANN description
2017 September	Revised alternative DRAGANN methodology (see bolded text in Sec 4.3.1)
2017 September	Clarified SNR calculation (Sec 2.5.18, Sec 4.3 (18))
2017 September	Added cloud flag filtering option (Sec Error! Reference source not found.)
2017 September	Added top of canopy median surface filter (Sec 3.5 (a), Sec 4.10 (3), Sec 4.12 (1-3))

2017 September	Modified 500 canopy photon segment filter (Sec 3.5 (c), Sec 4.12 (6))
2017 November	Added solar_azimuth, solar_elevation, and n_seg_ph to Reference Data group; parameters were already in product (Sec 2.4)
2017 November	Specified number of ground photons threshold for relative canopy product calculations (Sec 4.16 (2)); no number of ground photons threshold for absolute canopy heights (Sec 4.16.1 (1))
2017 November	Changed the ATL03 signal used in superset from all ATL03 signal (signal_conf_ph flags 1-4) to the medium-high confidence flags (signal_conf_ph flags 3-4) (Sec 3.1, Sec 4.3 (17))
2017 November	Removed Date parameter from Table 2.4 since UTC date is in file metadata
2018 March	Clarified that cloud flag filtering option should be turned off by default (Sec Error! Reference source not found.)
2018 March	Changed h_diff_ref QA threshold from 10 m to 25 m (Table 5.2)
2018 March	Added absolute canopy height quartiles, canopy_h_quartile_abs (<i>Later removed</i>)
2018 March	Removed psf_flag from main product; psf_flag will only be a QAQC alert (Sec 5.2)
2018 March	Added an Asmooth filter based on the reference DEM value (Sec 4.6 (4-5))
2018 March	Changed relief calculation to 95 th – 5 th signal photon heights. (Sec 4.6 (6))
2018 March	Adjusted the Asmooth smoothing methodology (Sec 4.6 (8))
2018 March	Recalculate the Asmooth surface after filtering outlying noise from signal, then detrend signal height data (Sec 4.7 (3-4))
2018 March	Added option to run alternative DRAGANN process again in high noise cases (Sec 4.3.3)
2018 March	Changed global land cover reference to MODIS Global Mosaics product (Sec 2.4.14)
2018 March	Adjusted the top of canopy median filter thresholds based on SNR (Sec 4.12 (1-2))
2018 March	Added a final photon classification QA check (Sec 4.14, Table 5.2)
2018 March	Added slope adjusted terrain parameters (<i>Later removed</i>)
2018 June	Replaced slope adjusted terrain parameters with terrain best fit parameter (Sec 2.1.14, 4.15 (2.e))
2018 June	Clarified source for water mask (Sec 2.4.15)
2018 June	Clarified source for urban mask (Sec 2.4.17)
2018 June	Added expansion to the terrain_slope calculation (Sec 4.15)
2018 June	Removed canopy_d_quartile

2018 June	Removed canopy_quartile_heights and canopy_quartile_heights_abs, replaced with canopy_h_metrics (Secs 2.2.3, 4.16 (6), 4.16.1 (5))
2018 *** draft 1	Delta_time specified as mid-segment time, rather than mean segment time (Sec 2.4.5)
2018 *** draft 1	QA/QC products to be reported on a per orbit basis, rather than per region (Sec 5.2)
2018 *** draft 1	Added more detail to landsat_flag description (Sec 2.2.23)
2018 *** draft 1	Added psf_flag back into ATL08 product, as it is also needed for the QA product (Sec 2.5.12)
2018 *** draft 1	Specified that the sigma_h value reported here is the mean of the ATL03 reported sigma_h values (Sec 2.5.7)
2018 *** draft 1	Removed n_photons from all subgroups
2018 *** draft 1	Better defined the interpolation and smoothing methods used throughout: <ul style="list-style-type: none"> • Error! Reference source not found. (4): Interpolation – nearest • 4.6 (5): Interpolation – PCHIP • 4.6 (8): Smoothing – moving average • 4.7 (3): Interpolation – PCHIP • 4.7 (3): Smoothing – moving average • 4.8 (10): Smoothing – moving average • 4.8 (11): Interpolation – linear • 4.8 (12): Smoothing – moving average • 4.8 (13): Interpolation – linear • 4.8 (14): Smoothing – moving average • 4.8 (15): Smoothing – Savitzky-Golay • 4.8 (16): Interpolation – linear • 4.8 (21): Interpolation – PCHIP • 4.10 (10): Interpolation – linear • 4.11 (all): Smoothing – moving average • 4.10 (6.b): Interpolation – linear • 4.12 (1.a): Interpolation – linear • 4.12 (1.c): Smoothing – lowess • 4.12 (4): Interpolation – PCHIP • 4.12 (7): Interpolation – PCHIP • 4.12 (9): Smoothing – moving average • 4.15 (2.e.i.1): Interpolation – linear
2018 *** draft 1	Added ref_elev and ref_azimuth back in (it was mistakenly removed in a previous version; Secs 2.5.3, 2.5.4)
2018 *** draft 1	Clarified wording of h_canopy_quad definition (Sec 2.2.17)
2018 *** draft 1	Updated segment_snowcover description to match the ATL09 snow_ice parameter it references (Sec 2.4.16) and added product reference to Table 4.2

2018 *** draft 1	Added ph_ndx_beg (Sec 2.5.22); parameter was already on product
2018 *** draft 1	Added dem_removal_flag for QA purposes (Sec 2.4.11; Table 5.2)
2018 *** draft 2	Reformatted QA/QC trending and trigger alert list into a table for better clarification (Table 5.3)
2018 *** draft 2	Replaced n_photons in Table 5.2 with n_te_photons, n_ca_photons, and n_toc_photons
2018 *** draft 2	Removed beam_number from Table 2.5. Beam number and weak/strong designation within gtx group attributes.
2018 *** draft 2	Clarified calculation of h_te_best_fit (Sec 4.15 (2.e))
2018 *** draft 2	Changed h_canopy and h_canopy_abs to be 98 th percentile height (Table 2.2, Sec 2.2.5, Sec 2.2.6, Sec 4.16 (4), Sec 4.16.1 (3))
2018 *** draft 2	Separated h_canopy_metrics_abs from h_canopy_metrics (Table 2.2, Sec 2.2.3, Sec 4.16.1 (5))
2018 October	Removed 99 th percentile from h_canopy_metrics and h_canopy_metrics_abs (Table 2.2, Sec 2.2.3, Sec 2.2.4, Sec 4.16 (4), Sec 4.16.1 (5))
2018 December	Renamed and reworded Section 4.3.1 to better indicate that the DRAGANN preprocessing step is not optional
2018 December	Specified that DRAGANN should use along-track time, and added time rescaling step (Sec 4.3 (1 - 4))
2018 December	Added DRAGANN changes made to better capture sparse canopy in cases of low noise rates (Sec 4.3, Appendix A)
2018 December	Made corrections to DRAGANN description regarding the determination of the noise Gaussian (Sec 3.1.1, Sec 4.3)
2018 December	Removed h_median_canopy and h_median_canopy_abs, as they are equivalent to canopy_h_metrics(50) and canopy_h_metrics_abs(50) (Table 2.2, Sec 4.16 (5), Sec 4.16.1 (4))
2018 December	Removed the requirement that > 5% ground photons required to calculate relative canopy height parameters (Table 2.2, Sec 4.16 (2))
2018 December	Added canopy relative height confidence flag (canopy_rh_conf) based on the percentage of ground and canopy photons in a segment (Table 2.2, Sec 4.16 (2))
2018 December	Added ATL09 layer_flag to ATL08 output (Table 2.5, Table 4.2)
2019 February	Adjusted cloud filtering to be based on ATL09 backscatter analysis rather than cloud flags (Sec 4.1)
2019 March 5	Updated ATL09-based product descriptions reported on ATL08 product (Secs 2.5.13, 2.5.14, 2.5.15, 2.5.16)
2019 March 5	Updated cloud-based low signal filter methodology, and moved to first step of ATL08 processing (Sec 4.1)

2019 March 13	Replace canopy_closure with new landsat_perc parameter (Table 2.2, Sec 2.2.24)
2019 March 13	Change ATL08 product output regions to match ATL03 regions (Sec 2), but keep ATL08 regions internally and report in new parameter atl08_regions (Table 2.4, Sec 2.4.19)
2019 March 13	Add methodology for handling short ATL08 processing segments at the end of an ATL03 granule (Sec 4.2), and output distance the processing segment length is extended into new parameter last_seg_extend (Table 2.4, Sec 2.4.20)
2019 March 13	Add preprocessing step for removing atmospheric and ocean tide corrections from ATL03 heights (<i>Later removed</i>)
2019 March 27	Remove preprocessing step for removing atmospheric and ocean tide corrections from ATL03 heights, since those values are now removed from the ATL03 photon heights.
2019 March 27	Replaced ATL03 region figure with corrected version (Figure 2.2)
2019 March 27	Specified that at least 50 classed photons are required to create the 100 m land and canopy products (Secs 2, 4.15(1), 4.16(1))
2019 March 27	Clarified that any non-extended segments would report a land_seg_extend value of 0 (Sec 4.2, Sec 2.4.20)
2019 April 30	Fixed the error in Eqn 1.4 for the sigma topo value
2019 May 13	Specified for cloud flag carry-over from ATL09 that ATL08 will report the highest cloud flag if an 08 segment straddles two 09 segments. (Section 2.5)
2019 May 13	Changed parameter cloud_flag_asr to cloud_flag_atm since the cloud_flag_asr is likely not to work over land due to varying surface reflectance (Sec, 2.5)
2019 May 13	Add ATL09 parameter cloud_fold_flag to the ATL08 data product for future qa/qc checks for low clouds. (Secs, 2.5)
2019 May 13	Clarification on the calculation of gradient for slope that feeds into the calculation of the point spread function (Sec 4.11)
2019 July 8	Changed Landsat canopy cover percentage to 3 % (from original value of 5%) (Section 4.4)
2019 July 8	Added a QA method for DRAGANN flags to help remove false positives (now Section 4.3.1)
2019 July 8	Set the window size to 9 rather than SmoothSize for the final ground finding step. (Section 4.11 and 4.12)
2019 July 8	Added a brightness flag to land segments. (Section 2.4.21)
2019 November 12	Added subset_te_flag to (Section 2.1) which indicate 100 m segments that are populated by less than 100 m worth of data

2019 November 12	Added subset_can_flag (section 2.2) which indicate 100 m segments that are populated by less than 100 m worth of data
2020 January 5	Clarified the interpolation of values (latitude, longitude, delta time) when the 100 m segments are populated by less than 100 m worth of data. (Section 2.4.3 and 2.4.4)
2020 January 13	Fine-tuned the methodology to improve ground finding by first histogramming the photons to improve detecting the ground in cases of dense canopy. (Section 4.8)
2020 January 13	Updated ATL08 HDF5 file organization figure in Section 2.1
2020 February 14	Added sentence to avoid ATL03 data having a degraded PPD flag to beginning of Section 4
2020 February 14	Added documentation for removing signal photons due to cloud contamination by checking the reference DEM to beginning of Section 4
2020 February 14	Added full saturation flag and near saturation flag from ATL03 to ATL08 data product to Section 2.
2020 February 14	Added statement to clarify handling of remaining geosegments that do not fit within a 100 m window at the end of a 10-km processing window in Section 4.2
2020 April 15	Added ph_h parameter to photon group on data structure. ph_h is the photon height above the interpolated ground surface.
2020 May 15	Added sat_flag which is derived from the ATL03 product. The saturation flag indicates that the ATL08 segment experienced some saturation which is often an indicator for water
2020 May 15	Canopy height metrics (relative and absolute heights) were expanded to every 5% ranging from 5 - 95%.
2020 May 15	The Landsat canopy cover check to determine whether the algorithm should search for both ground and canopy or just ground has been disabled. Now the ATL08 algorithm will search for both ground and canopy points everywhere.
2020 June 15	Corrected the calculation of the absolute canopy heights
2020 June 15	Changed the search radius for initial top of canopy determination (Section 4.9)
2020 September 1	Incorporate the quality_ph flag from ATL03 into the ATL08 workflow (beginning of Section 4)
2020 September 1	Added the calculation of Terrain photon rate (photon_rate_te) for each ATL08 segment to the land product (Section 2.1.16)
2020 September 1	Added the calculation of canopy photon rate (photon_rate_can) for each ATL08 segment to the land product (Section 2.2.26)

2020 September 1	Changed the k-d tree search radius for the top of canopy from 15 m to 100 m. Section 4.9.6
-----------------------------	---

33

34

35 **Contents**

36 List of Tables..... 16

37 List of Figures..... 17

38 1 INTRODUCTION 19

39 1.1. Background 20

40 1.2 Photon Counting Lidar 22

41 1.3 The ICESat-2 concept..... 23

42 1.4 Height Retrieval from ATLAS 26

43 1.5 Accuracy Expected from ATLAS..... 28

44 1.6 Additional Potential Height Errors from ATLAS..... 30

45 1.7 Dense Canopy Cases 30

46 1.8 Sparse Canopy Cases 31

47 2. ATL08: DATA PRODUCT 32

48 2.1 Subgroup: Land Parameters 35

49 2.1.1 Georeferenced_segment_number_beg..... 36

50 2.1.2 Georeferenced_segment_number_end 36

51 2.1.3 Segment_terrain_height_mean..... 37

52 2.1.4 Segment_terrain_height_med 37

53 2.1.5 Segment_terrain_height_min 37

54 2.1.6 Segment_terrain_height_max..... 38

55 2.1.7 Segment_terrain_height_mode..... 38

56 2.1.8 Segment_terrain_height_skew 38

57 2.1.9 Segment_number_terrain_photons..... 38

58 2.1.10 Segment height_interp..... 38

59 2.1.11 Segment h_te_std..... 39

60 2.1.12 Segment_terrain_height_uncertainty 39

61 2.1.13 Segment_terrain_slope 39

62	2.1.14	Segment_terrain_height_best_fit.....	39
63	2.2	Subgroup: Vegetation Parameters.....	41
64	2.2.1	Georeferenced_segment_number_beg.....	43
65	2.2.2	Georeferenced_segment_number_end.....	44
66	2.2.3	Canopy_height_metrics_abs.....	44
67	2.2.4	Canopy_height_metrics.....	44
68	2.2.5	Absolute_segment_canopy_height.....	45
69	2.2.6	Segment_canopy_height.....	45
70	2.2.7	Absolute_segment_mean_canopy.....	45
71	2.2.8	Segment_mean_canopy.....	45
72	2.2.9	Segment_dif_canopy.....	46
73	2.2.10	Absolute_segment_min_canopy.....	46
74	2.2.11	Segment_min_canopy.....	46
75	2.2.12	Absolute_segment_max_canopy.....	46
76	2.2.13	Segment_max_canopy.....	47
77	2.2.14	Segment_canopy_height_uncertainty.....	47
78	2.2.15	Segment_canopy_openness.....	48
79	2.2.16	Segment_top_of_canopy_roughness.....	48
80	2.2.17	Segment_canopy_quadratic_height.....	48
81	2.2.18	Segment_number_canopy_photons.....	48
82	2.2.19	Segment_number_top_canopy_photons.....	48
83	2.2.20	Centroid_height.....	49
84	2.2.21	Segment_rel_canopy_conf.....	49
85	2.2.22	Canopy_flag.....	49
86	2.2.23	Landsat_flag.....	49
87	2.2.24	Landsat_perc.....	50
88	2.3	Subgroup: Photons.....	51

89	2.3.1	Indices_of_classed_photons.....	51
90	2.3.2	Photon_class.....	52
91	2.3.3	Georeferenced_segment_number.....	52
92	2.3.4	DRAGANN_flag.....	52
93	2.4	Subgroup: Reference data.....	52
94	2.4.1	Georeferenced_segment_number_beg.....	54
95	2.4.2	Georeferenced_segment_number_end.....	54
96	2.4.3	Segment_latitude.....	55
97	2.4.4	Segment_longitude.....	55
98	2.4.5	Delta_time.....	56
99	2.4.6	Delta_time_beg.....	56
100	2.4.7	Delta_time_end.....	56
101	2.4.8	Night_Flag.....	56
102	2.4.9	Segment_reference_DTM.....	56
103	2.4.10	Segment_reference_DEM_source.....	57
104	2.4.11	Segment_reference_DEM_removal_flag.....	57
105	2.4.12	Segment_terrain_difference.....	57
106	2.4.13	Segment_terrain_flag.....	57
107	2.4.14	Segment_landcover.....	57
108	2.4.15	Segment_watermask.....	58
109	2.4.16	Segment_snowcover.....	58
110	2.4.17	Urban_flag.....	58
111	2.4.18	Surface_type.....	58
112	2.4.19	ATL08_region.....	59
113	2.4.20	Last_segment_extend.....	59
114	2.5	Subgroup: Beam data.....	60
115	2.5.1	Georeferenced_segment_number_beg.....	62

116	2.5.2	Georeferenced_segment_number_end	62
117	2.5.3	Beam_coelevation.....	63
118	2.5.4	Beam_azimuth.....	63
119	2.5.5	ATLAS_Pointing_Angle	63
120	2.5.6	Reference_ground_track.....	63
121	2.5.7	Sigma_h	63
122	2.5.8	Sigma_along.....	64
123	2.5.9	Sigma_across.....	64
124	2.5.10	Sigma_topo	64
125	2.5.11	Sigma_ATLAS_LAND	64
126	2.5.12	PSF_flag	64
127	2.5.13	Layer_flag.....	64
128	2.5.14	Cloud_flag_atm.....	65
129	2.5.15	MSW.....	65
130	2.5.16	Cloud Fold Flag	66
131	2.5.17	Computed_Apparent_Surface_Reflectance	66
132	2.5.18	Signal_to_Noise_Ratio	66
133	2.5.19	Solar_Azimuth	66
134	2.5.20	Solar_Elevation	66
135	2.5.21	Number_of_segment_photons	66
136	2.5.22	Photon_Index_Begin	67
137	3	ALGORITHM METHODOLOGY.....	68
138	3.1	Noise Filtering.....	68
139	3.1.1	DRAGANN	69
140	3.2	Surface Finding.....	73
141	3.2.1	De-trending the Signal Photons.....	75
142	3.2.2	Canopy Determination	75

143	3.2.3	Variable Window Determination.....	77
144	3.2.4	Compute descriptive statistics.....	78
145	3.2.5	Ground Finding Filter (Iterative median filtering)	80
146	3.3	Top of Canopy Finding Filter	81
147	3.4	Classifying the Photons	82
148	3.5	Refining the Photon Labels.....	82
149	3.6	Canopy Height Determination	87
150	3.7	Link Scale for Data products.....	87
151	4.	ALGORITHM IMPLEMENTATION	88
152	4.1	Cloud based filtering	91
153	4.2	Preparing ATL03 data for input to ATL08 algorithm	94
154	4.3	Noise filtering via DRAGANN.....	95
155	4.3.1	DRAGANN Quality Assurance.....	98
156	4.3.2	Preprocessing to dynamically determine a DRAGANN parameter	99
157	4.3.3	Iterative DRAGANN processing.....	102
158	4.4	Is Canopy Present.....	103
159	4.5	Compute Filtering Window	103
160	4.6	De-trend Data	103
161	4.7	Filter outlier noise from signal	104
162	4.8	Finding the initial ground estimate	105
163	4.9	Find the top of the canopy (if canopy_flag = 1)	108
164	4.10	Compute statistics on de-trended data	109
165	4.11	Refine Ground Estimates.....	110
166	4.12	Canopy Photon Filtering.....	112
167	4.13	Compute individual Canopy Heights.....	114
168	4.14	Final photon classification QA check	114
169	4.15	Compute segment parameters for the Land Products	115

170	4.16	Compute segment parameters for the Canopy Products	118
171	4.16.1	Canopy Products calculated with absolute heights	119
172	4.17	Record final product without buffer	120
173	5	DATA PRODUCT VALIDATION STRATEGY	121
174	5.1	Validation Data	121
175	5.2	Internal QC Monitoring	124
176	6	REFERENCES	130
177			

178 **List of Tables**

179 Table 2.1. Summary table of land parameters on ATL08.....35

180 Table 2.2. Summary table of canopy parameters on ATL08.....41

181 Table 2.3. Summary table for photon parameters for the ATL08 product.....51

182 Table 2.4. Summary table for reference parameters for the ATL08 product.....53

183 Table 2.5. Summary table for beam parameters for the ATL08 product.....60

184 Table 3.1. Standard deviation ranges utilized to qualify the spread of photons within
185 moving window..... 79

186 Table 4.1. Input parameters to ATL08 classification algorithm.....89

187 Table 4.2. Additional external parameters referenced in ATL08 product.90

188 Table 5.1. Airborne lidar data vertical height (Z accuracy) requirements for
189 validation data. 121

190 Table 5.2. ATL08 parameter monitoring..... 124

191 Table 5.3. QA/QC trending and triggers. 128

192

193	List of Figures	
194	Figure 1.1. Various modalities of lidar detection. Adapted from Harding, 2009.....	23
195	Figure 1.2. Schematic of 6-beam configuration for ICESat-2 mission. The laser	
196	energy will be split into 3 laser beam pairs – each pair having a weak spot (1X) and a	
197	strong spot (4X).	25
198	Figure 1.3. Illustration of off-nadir pointing scenarios. Over land (green regions) in	
199	the mid-latitudes, ICESat-2 will be pointed away from the repeat ground tracks to	
200	increase the density of measurements over terrestrial surfaces.	26
201	Figure 1.4. Illustration of the point spread function, also referred to as Znoise, for a	
202	series of photons about a surface.....	28
203	Figure 2.1. HDF5 data structure for ATL08 products.....	33
204	Figure 2.2. ATL03 granule regions; graphic from ATL03 ATBD (Neumann et al.).	34
205	Figure 2.3. ATL08 product regions.....	35
206	Figure 2.4. Illustration of canopy photons (red dots) interaction in a vegetated area.	
207	Relative canopy heights, H_i , are computed by differencing the canopy photon height	
208	from an interpolated terrain surface.	41
209	Figure 3.1. Combination of noise filtering algorithms to create a superset of input	
210	data for surface finding algorithms.	69
211	Figure 3.2. Histogram of the number of photons within a search radius. This	
212	histogram is used to determine the threshold for the DRAGANN approach.....	71
213	Figure 3.3. Output from DRAGANN filtering. Signal photons are shown as blue.	73
214	Figure 3.4. Flowchart of overall surface finding method.	74
215	Figure 3.5. Plot of Signal Photons (black) from 2014 MABEL flight over Alaska and	
216	de-trended photons (red).	75
217	Figure 3.6. Shape Parameter for variable window size.	78
218	Figure 3.7. Illustration of the standard deviations calculated for each moving	
219	window to identify the amount of spread of signal photons within a given window.	
220	80
221	Figure 3.8. Three iterations of the ground finding concept for L -km segments with	
222	canopy.	81

223	Figure 3.9. Example of the intermediate ground and top of canopy surfaces	
224	calculated from MABEL flight data over Alaska during July 2014.....	84
225	Figure 3.10. Example of classified photons from MABEL data collected in Alaska	
226	2014. Red photons are photons classified as terrain. Green photons are classified as	
227	top of canopy. Canopy photons (shown as blue) are considered as photons lying	
228	between the terrain surface and top of canopy.....	85
229	Figure 3.11. Example of classified photons from MABEL data collected in Alaska	
230	2014. Red photons are photons classified as terrain. Green photons are classified as	
231	top of canopy. Canopy photons (shown as blue) are considered as photons lying	
232	between the terrain surface and top of canopy.....	86
233	Figure 3.12. Example of classified photons from MABEL data collected in Alaska	
234	2014. Red photons are photons classified as terrain. Green photons are classified as	
235	top of canopy. Canopy photons (shown as blue) are considered as photons lying	
236	between the terrain surface and top of canopy.....	86
237	Figure 5.1. Example of <i>L-km</i> segment classifications and interpolated ground	
238	surface.....	127
239		

240 **1 INTRODUCTION**

241 This document describes the theoretical basis and implementation of the
242 processing algorithms and data parameters for Level 3 land and vegetation heights
243 for the non-polar regions of the Earth. The ATL08 product contains heights for both
244 terrain and canopy in the along-track direction as well as other descriptive
245 parameters derived from the measurements. At the most basic level, a derived surface
246 height from the ATLAS instrument at a given time is provided relative to the WGS-84
247 ellipsoid. Height estimates from ATL08 can be compared with other geodetic data and
248 used as input to higher-level ICESat-2 products, namely ATL13 and ATL18. ATL13
249 will provide estimates of inland water-related heights and associated descriptive
250 parameters. ATL18 will consist of gridded maps for terrain and canopy features.

251 The ATL08 product will provide estimates of terrain heights, canopy heights,
252 and canopy cover at fine spatial scales in the along-track direction. Along-track is
253 defined as the direction of travel of the ICESat-2 satellite in the velocity vector.
254 Parameters for the terrain and canopy will be provided at a fixed step-size of 100 m
255 along the ground track referred to as a segment. A fixed segment size of 100 m was
256 chosen to provide continuity of data parameters on the ATL08 data product. From an
257 analysis perspective, it is difficult and cumbersome to attempt to relate canopy cover
258 over variable lengths. Furthermore, a segment size of 100 m will facilitate a simpler
259 combination of along-track data to create the gridded products.

260 We anticipate that the signal returned from the weak beam will be sufficiently
261 weak and may prohibit the determination of both a terrain and canopy segment
262 height, particularly over areas of dense vegetation. However, in more arid regions we
263 anticipate producing a terrain height for both the weak and strong beams.

264 In this document, section 1 provides a background of lidar in the ecosystem
265 community as well as describing photon counting systems and how they differ from
266 discrete return lidar systems. Section 2 provides an overview of the Land and
267 Vegetation parameters and how they are defined on the data product. Section 3
268 describes the basic methodology that will be used to derive the parameters for ATL08.

269 Section 4 describes the processing steps, input data, and procedure to derive the data
270 parameters. Section 5 will describe the test data and specific tests that NASA's
271 implementation of the algorithm should pass in order to determine a successful
272 implementation of the algorithm.

273

274 **1.1. Background**

275 The Earth's land surface is a complex mosaic of geomorphic units and land
276 cover types resulting in large variations in terrain height, slope, roughness, vegetation
277 height and reflectance, often with the variations occurring over very small spatial
278 scales. Documentation of these landscape properties is a first step in understanding
279 the interplay between the formative processes and response to changing conditions.
280 Characterization of the landscape is also necessary to establish boundary conditions
281 for models which are sensitive to these properties, such as predictive models of
282 atmospheric change that depend on land-atmosphere interactions. Topography, or
283 land surface height, is an important component for many height applications, both to
284 the scientific and commercial sectors. The most accurate global terrain product was
285 produced by the Shuttle Radar Topography Mission (SRTM) launched in 2000;
286 however, elevation data are limited to non-polar regions. The accuracy of SRTM
287 derived elevations range from 5 – 10 m, depending upon the amount of topography
288 and vegetation cover over a particular area. ICESat-2 will provide a global distribution
289 of geodetic measurements (of both the terrain surface and relative canopy heights)
290 which will provide a significant benefit to society through a variety of applications
291 including sea level change monitoring, forest structural mapping and biomass
292 estimation, and improved global digital terrain models.

293 In addition to producing a global terrain product, monitoring the amount and
294 distribution of above ground vegetation and carbon pools enables improved
295 characterization of the global carbon budget. Forests play a significant role in the
296 terrestrial carbon cycle as carbon pools. Events, such as management activities
297 (Krankina et al. 2012) and disturbances can release carbon stored in forest above

298 ground biomass (AGB) into the atmosphere as carbon dioxide, a greenhouse gas that
299 contributes to climate change (Ahmed et al. 2013). While carbon stocks in nations
300 with continuous national forest inventories (NFIs) are known, complications with NFI
301 carbon stock estimates exist, including: (1) ground-based inventory measurements
302 are time consuming, expensive, and difficult to collect at large-scales (Houghton
303 2005; Ahmed et al. 2013); (2) asynchronously collected data; (3) extended time
304 between repeat measurements (Houghton 2005); and (4) the lack of information on
305 the spatial distribution of forest AGB, required for monitoring sources and sinks of
306 carbon (Houghton 2005). Airborne lidar has been used for small studies to capture
307 canopy height and in those studies canopy height variation for multiple forest types
308 is measured to approximately 7 m standard deviation (Hall et al., 2011).

309 Although the spatial extent and changes to forests can be mapped with existing
310 satellite remote sensing data, the lack of information on forest vertical structure and
311 biomass limits the knowledge of biomass/biomass change within the global carbon
312 budget. Based on the global carbon budget for 2015 (Quere et al., 2015), the largest
313 remaining uncertainties about the Earth's carbon budget are in its terrestrial
314 components, the global residual terrestrial carbon sink, estimated at 3.0 ± 0.8
315 GtC/year for the last decade (2005-2014). Similarly, carbon emissions from land-use
316 changes, including deforestation, afforestation, logging, forest degradation and
317 shifting cultivation are estimated at 0.9 ± 0.5 GtC /year. By providing information on
318 vegetation canopy height globally with a higher spatial resolution than previously
319 afforded by other spaceborne sensors, the ICESat-2 mission can contribute
320 significantly to reducing uncertainties associated with forest vegetation carbon.

321 Although ICESat-2 is not positioned to provide global biomass estimates due
322 to its profiling configuration and somewhat limited detection capabilities, it is
323 anticipated that the data products for vegetation will be complementary to ongoing
324 biomass and vegetation mapping efforts. Synergistic use of ICESat-2 data with other
325 space-based mapping systems is one solution for extended use of ICESat-2 data.
326 Possibilities include NASA's Global Ecosystems Dynamics Investigation (GEDI) lidar

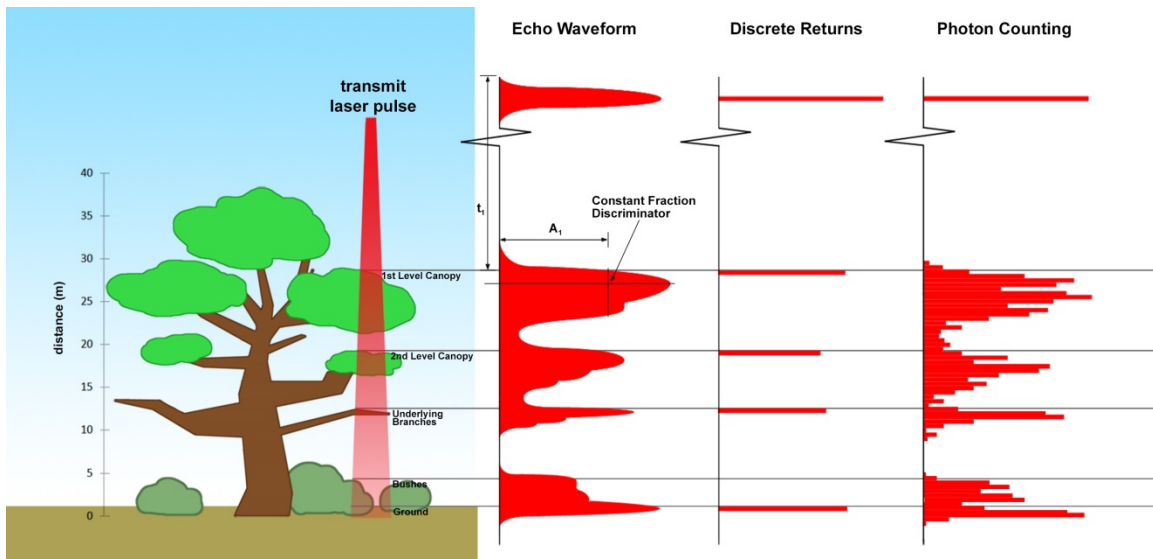
327 planned to fly onboard the International Space Station (ISS) or imaging sensors, such
328 as Landsat 8, or NASA/ISRO –NISAR radar mission.

329

330 **1.2 Photon Counting Lidar**

331 Rather than using an analog, full waveform system similar to what was utilized
332 on the ICESat/GLAS mission, ICESat-2 will employ a photon counting lidar. Photon
333 counting lidar has been used successfully for ranging for several decades in both the
334 science and defense communities. Photon counting lidar systems operate on the
335 concept that a low power laser pulse is transmitted and the detectors used are
336 sensitive at the single photon level. Due to this type of detector, any returned photon
337 whether from the reflected signal or solar background can trigger an event within the
338 detector. A discussion regarding discriminating between signal and background noise
339 photons is discussed later in this document. A question of interest to the ecosystem
340 community is to understand where within the canopy is the photon likely to be
341 reflected. Figure 1.1 is an example of three different laser detector modalities: full
342 waveform, discrete return, and photon counting. Full waveform sensors record the
343 entire temporal profile of the reflected laser energy through the canopy. In contrast,
344 discrete return systems have timing hardware that record the time when the
345 amplitude of the reflected signal energy exceeds a certain threshold amount. A photon
346 counting system, however, will record the arrival time associated with a single
347 photon detection that can occur anywhere within the vertical distribution of the
348 reflected signal. If a photon counting lidar system were to dwell over a surface for a
349 significant number of shots (i.e. hundreds or more), the vertical distribution of the
350 reflected photons will resemble a full waveform. Thus, while an individual photon
351 could be reflected from anywhere within the vertical canopy, the probability
352 distribution function (PDF) of that reflected photon would be the full waveform.
353 Furthermore, the probability of detecting the top of the tree is not as great as
354 detecting reflective surfaces positioned deeper into the canopy where the bulk of
355 leaves and branches are located. As one might imagine, the PDF will differ according

356 to canopy structure and vegetation physiology. For example, the PDF of a conifer tree
 357 will look different than broadleaf trees.



358

359 Figure 1.1. Various modalities of lidar detection. Adapted from Harding, 2009.

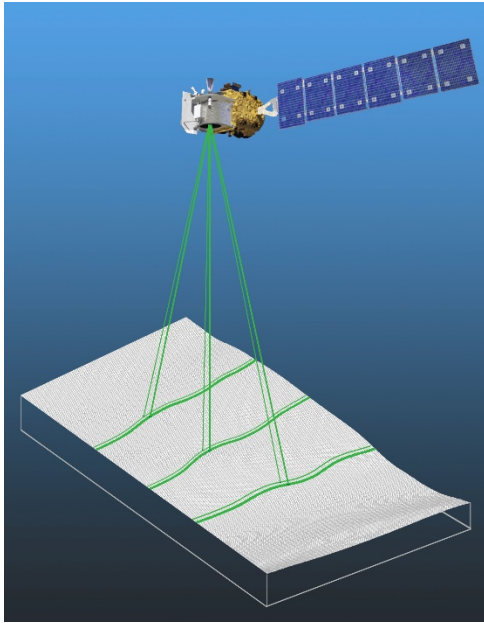
360 A cautionary note, the photon counting PDF that is illustrated in Figure 1.1 is
 361 merely an illustration if enough photons (i.e. hundreds of photons or more) were to
 362 be reflected from a target. In reality, due to the spacecraft speed, ATLAS will record 0
 363 – 4 photons per transmit laser pulse over vegetation.

364

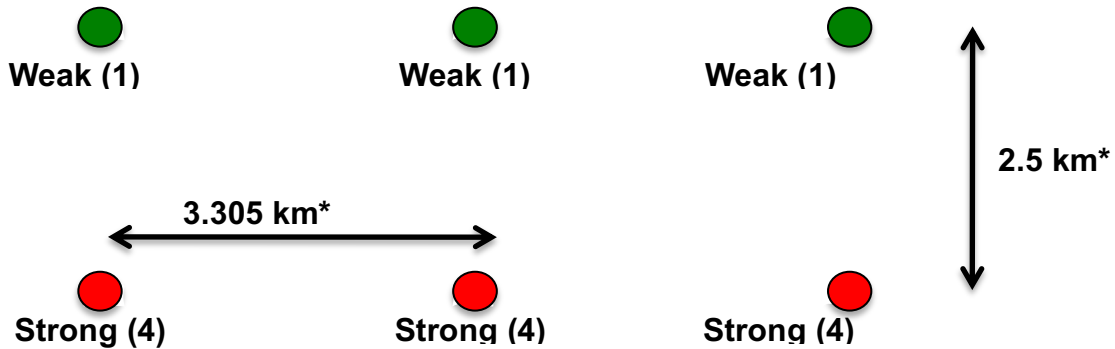
365 **1.3 The ICESat-2 concept**

366 The Advanced Topographic Laser Altimeter System (ATLAS) instrument
 367 designed for ICESat-2 will utilize a different technology than the GLAS instrument
 368 used for ICESat. Instead of using a high-energy, single-beam laser and digitizing the
 369 entire temporal profile of returned laser energy, ATLAS will use a multi-beam,
 370 micropulse laser (sometimes referred to as photon-counting). The travel time of each
 371 detected photon is used to determine a range to the surface which, when combined
 372 with satellite attitude and pointing information, can be geolocated into a unique XYZ
 373 location on or near the Earth’s surface. For more information on how the photons
 374 from ICESat-2 are geolocated, refer to ATL03 ATBD. The XYZ positions from ATLAS

375 are subsequently used to derive surface and vegetation properties. The ATLAS
376 instrument will operate at 532 nm in the green range of the electromagnetic (EM)
377 spectrum and will have a laser repetition rate of 10 kHz. The combination of the laser
378 repetition rate and satellite velocity will result in one outgoing laser pulse
379 approximately every 70 cm on the Earth's surface and each spot on the surface is ~13
380 m in diameter. Each transmitted laser pulse is split by a diffractive optical element in
381 ATLAS to generate six individual beams, arranged in three pairs (Figure 1.2). The
382 beams within each pair have different transmit energies ('weak' and 'strong', with an
383 energy ratio of approximately 1:4) to compensate for varying surface reflectance. The
384 beam pairs are separated by ~3.3 km in the across-track direction and the strong and
385 weak beams are separated by ~2.5 km in the along-track direction. As ICESat-2 moves
386 along its orbit, the ATLAS beams describe six tracks on the Earth's surface; the array
387 is rotated slightly with respect to the satellite's flight direction so that tracks for the
388 fore and aft beams in each column produce pairs of tracks - each separated by
389 approximately 90 m.



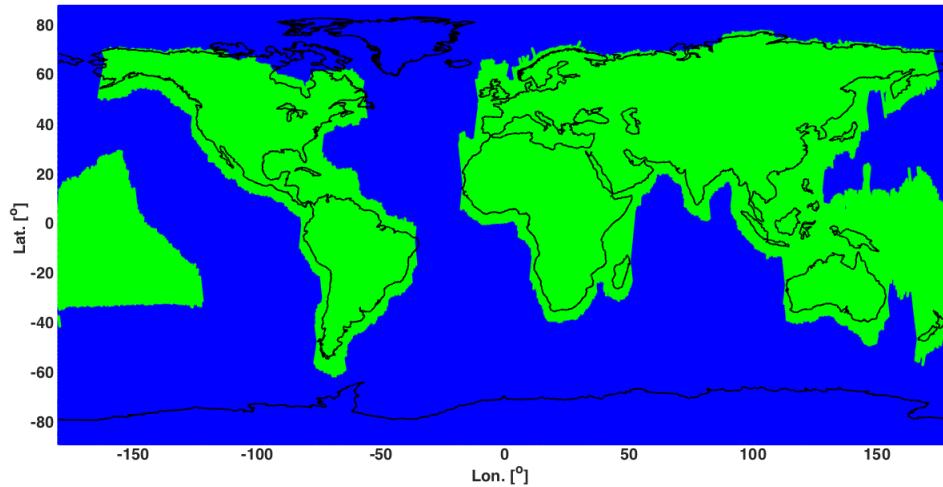
390



391

392 Figure 1.2. Schematic of 6-beam configuration for ICESat-2 mission. The laser energy will
 393 be split into 3 laser beam pairs – each pair having a weak spot (1X) and a strong spot (4X).

394 The motivation behind this multi-beam design is its capability to compute
 395 cross-track slopes on a per-orbit basis, which contributes to an improved
 396 understanding of ice dynamics. Previously, slope measurements of the terrain were
 397 determined via repeat-track and crossover analysis. The laser beam configuration as
 398 proposed for ICESat-2 is also beneficial for terrestrial ecosystems compared to GLAS
 399 as it enables a denser spatial sampling in the non-polar regions. To achieve a spatial
 400 sampling goal of no more than 2 km between equatorial ground tracks, ICESat-2 will
 401 be off-nadir pointed a maximum of 1.8 degrees from the reference ground track
 402 during the entire mission.



403

404 Figure 1.3. Illustration of off-nadir pointing scenarios. Over land (green regions) in the
 405 mid-latitudes, ICESat-2 will be pointed away from the repeat ground tracks to increase the
 406 density of measurements over terrestrial surfaces.

407 ICESat-2 is designed to densely sample the Earth’s surface, permitting
 408 scientists to measure and quantitatively characterize vegetation across vast
 409 expanses, e.g., nations, continents, globally. ICESat-2 will acquire synoptic
 410 measurements of vegetation canopy height, density, the vertical distribution of
 411 photosynthetically active material, leading to improved estimates of forest biomass,
 412 carbon, and volume. In addition, the orbital density, i.e., the number of orbits per unit
 413 area, at the end of the three year mission will facilitate the production of gridded
 414 global products. ICESat-2 will provide the means by which an accurate “snapshot” of
 415 global biomass and carbon may be constructed for the mission period.

416

417 **1.4 Height Retrieval from ATLAS**

418 Light from the ATLAS lasers reaches the earth’s surface as flat disks of down-
 419 traveling photons approximately 50 cm in vertical extent and spread over
 420 approximately 14 m horizontally. Upon hitting the earth’s surface, the photons are
 421 reflected and scattered in every direction and a handful of photons return to the

422 ATLAS telescope's focal plane. The number of photon events per laser pulse is a
423 function of outgoing laser energy, surface reflectance, solar conditions, and scattering
424 and attenuation in the atmosphere. For highly reflective surfaces (such as land ice)
425 and clear skies, approximately 10 signal photons from a single strong beam are
426 expected to be recorded by the ATLAS instrument for a given transmit laser pulse.
427 Over vegetated land where the surface reflectance is considerably less than snow or
428 ice surfaces, we expect to see fewer returned photons from the surface. Whereas
429 snow and ice surfaces have high reflectance at 532 nm (typical Lambertian
430 reflectance between 0.8 and 0.98 (Martino, GSFC internal report, 2010)), canopy and
431 terrain surfaces have much lower reflectance (typically around 0.3 for soil and 0.1 for
432 vegetation) at 532 nm. As a consequence we expect to see 1/3 to 1/9 as many photons
433 returned from terrestrial surfaces as from ice and snow surfaces. For vegetated
434 surfaces, the number of reflected signal photon events per transmitted laser pulse is
435 estimated to range between 0 to 4 photons.

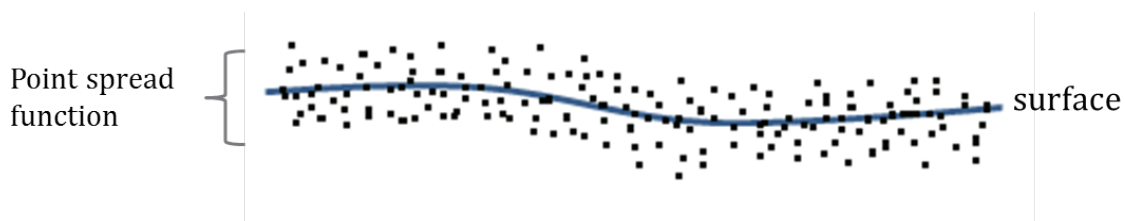
436 The time measured from the detected photon events are used to compute a
437 range, or distance, from the satellite. Combined with the precise pointing and attitude
438 information about the satellite, the range can be geolocated into a XYZ point (known
439 as a geolocated photon) above the WGS-84 reference ellipsoid. In addition to
440 recording photons from the reflected signal, the ATLAS instrument will detect
441 background photons from sunlight which are continually entering the telescope. A
442 primary objective of the ICESat-2 data processing software is to correctly
443 discriminate between signal photons and background photons. Some of this
444 processing occurs at the ATL03 level and some of it also occurs within the software
445 for ATL08. At ATL03, this discrimination is done through a series of three steps of
446 progressively finer resolution with some processing occurring onboard the satellite
447 prior to downlink of the raw data. The ATL03 data product produces a classification
448 between signal and background (i.e. noise) photons, and further discussion on that
449 classification process can be read in the ATL03 ATBD. In addition, not all geophysical
450 corrections (e.g. ocean tide) are applied to the position of the individual geolocated
451 photons at the ATL03 level, but they are provided on the ATL03 data product if there

452 exists a need to apply them. Thus, in general, all of the heights processed in the ATL08
453 algorithm consists of the ATL03 heights with respect to the WGS-84 ellipsoid, with
454 geophysical corrections applied, as specified in Chapter 6 of the ATL03 ATBD.

455

456 **1.5 Accuracy Expected from ATLAS**

457 There are a variety of elements that contribute to the elevation accuracy that
458 are expected from ATLAS and the derived data products. Elevation accuracy is a
459 composite of ranging precision of the instrument, radial orbital uncertainty,
460 geolocation knowledge, forward scattering in the atmosphere, and tropospheric path
461 delay uncertainty. The ranging precision seen by ATLAS will be a function of the laser
462 pulse width, the surface area potentially illuminated by the laser, and uncertainty in
463 the timing electronics. The requirement on radial orbital uncertainty is specified to
464 be less than 4 cm and tropospheric path delay uncertainty is estimated to be 3 cm. In
465 the case of ATLAS, the ranging precision for flat surfaces, is expected to have a
466 standard deviation of approximately 25 cm. The composite of each of the errors can
467 also be thought of as the spread of photons about a surface (see Figure 1.4) and is
468 referred to as the point spread function or Znoise.



469

470 Figure 1.4. Illustration of the point spread function, also referred to as Znoise, for a series
471 of photons about a surface.

472 The estimates of σ_{orbit} , $\sigma_{troposphere}$, $\sigma_{forwardscattering}$, $\sigma_{pointing}$, and σ_{timing}
473 for a photon will be represented on the ATL03 data product as the final geolocated
474 accuracy in the X, Y, and Z (or height) direction. In reality, these parameters have
475 different temporal and spatial scales, however until ICESat-2 is on orbit, it is uncertain
476 how these parameters will vary over time. As such, Equation 1.1 may change once the

477 temporal aspects of these parameters are better understood. For a preliminary
 478 quantification of the uncertainties, Equation 1.1 is valid to incorporate the instrument
 479 related factors.

$$480 \quad \sigma_Z = \sqrt{\sigma_{Orbit}^2 + \sigma_{trop}^2 + \sigma_{forwardscattering}^2 + \sigma_{pointing}^2 + \sigma_{timing}^2} \quad \text{Eqn. 1.1}$$

481

482 Although σ_Z on the ATL03 product represents the best understanding of the
 483 uncertainty for each geolocated photon, it does not incorporate the uncertainty
 484 associated with local slope of the topography. The slope component to the geolocation
 485 uncertainty is a function of both the geolocation knowledge of the pointing (which is
 486 required to be less than 6.5 m) multiplied by the tangent of the surface slope. In a case
 487 of flat topography (≤ 1 degree slope), $\sigma_Z \leq 25$ cm, whereas in the case of a 10 degree
 488 surface slope, $\sigma_Z = 119$ cm. The uncertainty associated with the local slope will be
 489 combined with σ_Z to produce the term $\sigma_{AtlasLand}$.

$$490 \quad \sigma_{AtlasLand} = \sqrt{\sigma_Z^2 + \sigma_{topo}^2} \quad \text{Eqn. 1.2}$$

$$491 \quad \sigma_{topo} = \sigma_{topo} = \sqrt{\left(6.5 \tan(\theta_{surfaceslope})\right)^2} \quad \text{Eqn.}$$

492 1.3

493 Ultimately, the uncertainty that will be reported on the data product ATL08
 494 will include the $\sigma_{AtlasLand}$ term and the local rms values of heights computed within
 495 each data parameter segment. For example, calculations of terrain height will be
 496 made on photons classified as terrain photons (this process is described in the
 497 following sections). The uncertainty of the terrain height for a segment is described
 498 in Equation 1.4, where the root mean square term of $\sigma_{AtlasLand}$ and rms of terrain
 499 heights are normalized by the number of terrain photons for that given segment.

$$500 \quad \sigma_{ATL08segment} = \sqrt{\sigma_{AtlasLand}^2 + \sigma_{Zrmssegment_class}^2} \quad \text{Eqn. 1.4}$$

501

502 **1.6 Additional Potential Height Errors from ATLAS**

503 Some additional potential height errors in the ATL08 terrain and vegetation
504 product can come from a variety of sources including:

505 a. Vertical sampling error. ATLAS height estimates are based on a
506 random sampling of the surface height distribution. Photons may
507 be reflected from anywhere within the PDF of the reflecting surface;
508 more specifically, anywhere from within the canopy. A detailed
509 look at the potential effect of vertical sampling error is provided in
510 Neuenschwander and Magruder (2016).

511 b. Background noise. Random noise photons are mixed with the
512 signal photons so classified photons will include random outliers.

513 c. Complex topography. The along-track product may not always
514 represent complex surfaces, particularly if the density of ground
515 photons does not support an accurate representation.

516 d. Vegetation. Dense vegetation may preclude reflected photon
517 events from reaching the underlying ground surface. An incorrect
518 estimation of the underlying ground surface will subsequently lead
519 to an incorrect canopy height determination.

520 e. Misidentified photons. The product from ATL03 combined with
521 additional noise filtering may not identify the correct photons as
522 signal photons.

523

524 **1.7 Dense Canopy Cases**

525 Although the height accuracy produced from ICESat-2 is anticipated to be
526 superior to other global height products (e.g. SRTM), for certain biomes photon

527 counting lidar data as it will be collected by the ATLAS instrument present a challenge
528 for extracting both the terrain and canopy heights, particularly for areas of dense
529 vegetation. Due to the relatively low laser power, we anticipate that the along-track
530 signal from ATLAS may lose ground signal under dense forest (e.g. >96% canopy
531 closure) and in situations where cloud cover obscures the terrestrial signal. In areas
532 having dense vegetation, it is likely that only a handful of photons will be returned
533 from the ground surface with the majority of reflections occurring from the canopy.
534 A possible source of error can occur with both the canopy height estimates and the
535 terrain heights if the vegetation is particularly dense and the ground photons were
536 not correctly identified.

537

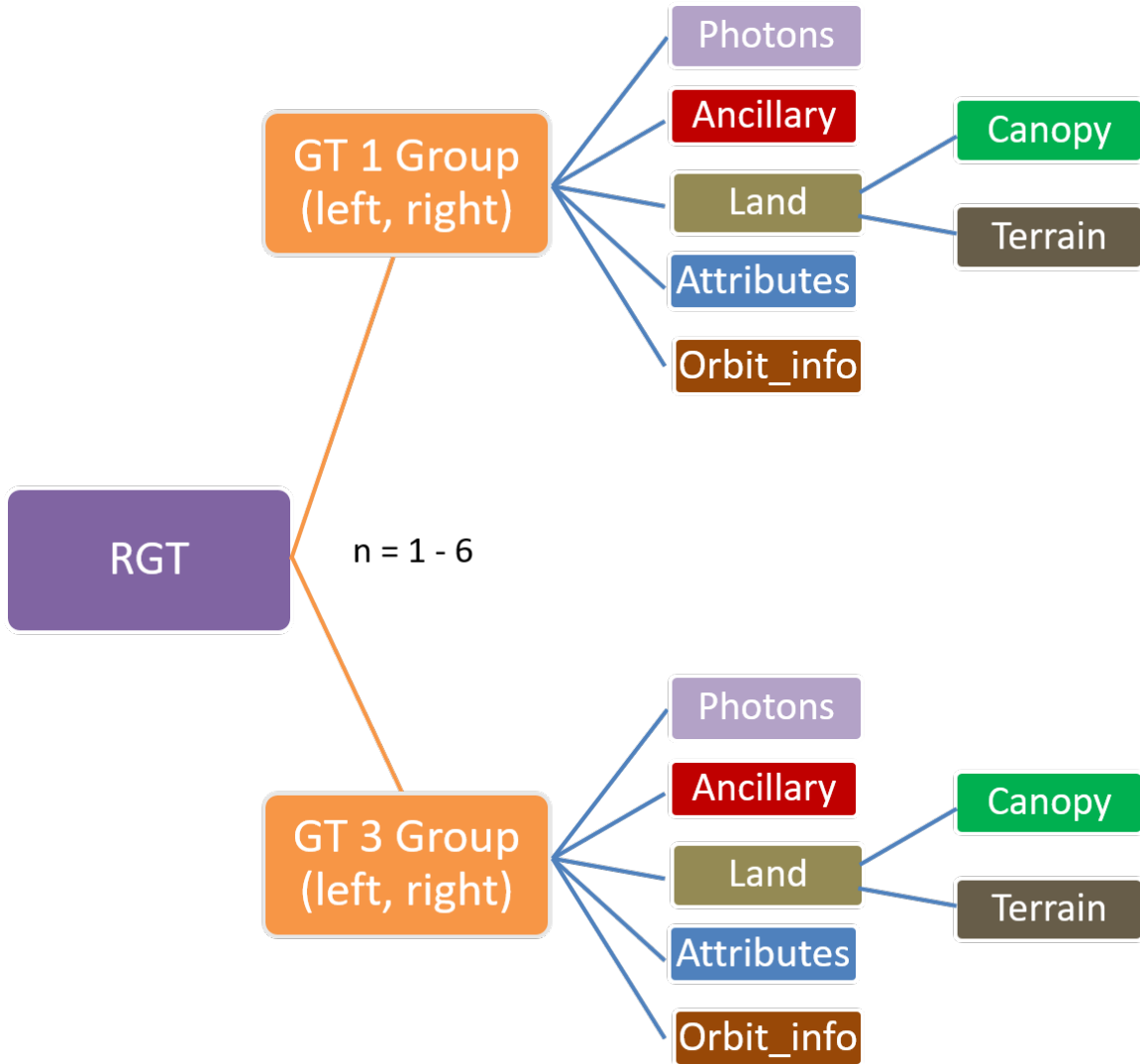
538 **1.8 Sparse Canopy Cases**

539 Conversely, sparse canopy cases also pose a challenge to vegetation height
540 retrievals. In these cases, expected reflected photon events from sparse trees or
541 shrubs may be difficult to discriminate between solar background noise photons. The
542 algorithms being developed for ATL08 operate under the assumption that signal
543 photons are close together and noise photons will be more isolated in nature. Thus,
544 signal (in this case canopy) photons may be incorrectly identified as solar background
545 noise on the data product. Due to the nature of the photon counting processing,
546 canopy photons identified in areas that have extremely low canopy cover <15% will
547 be filtered out and reassigned as noise photons.

548

549 **2. ATL08: DATA PRODUCT**

550 The ATL08 product will provide estimates of terrain height, canopy height,
551 and canopy cover at fine spatial scales in the along-track direction. In accordance with
552 the HDF-driven structure of the ICESat-2 products, the ATL08 product will
553 characterize each of the six Ground Tracks (GT) associated with each Reference
554 Ground Track (RGT) for each cycle and orbit number. Each ground track group has a
555 distinct beam number, distance from the reference track, and transmit energy
556 strength, and all beams will be processed independently using the same sequence of
557 steps described within ATL08. Each ground track group (GT) on the ATL08 product
558 contains subgroups for land and canopy heights segments as well as beam and
559 reference parameters useful in the ATL08 processing. In addition, the labeled photons
560 that are used to determine the data parameters will be indexed back to the ATL03
561 products such that they are available for further, independent analysis. A layout of
562 the ATL08 HDF product is shown in Figure 2.1. The six GTs are numbered from left to
563 right, regardless of satellite orientation.



564

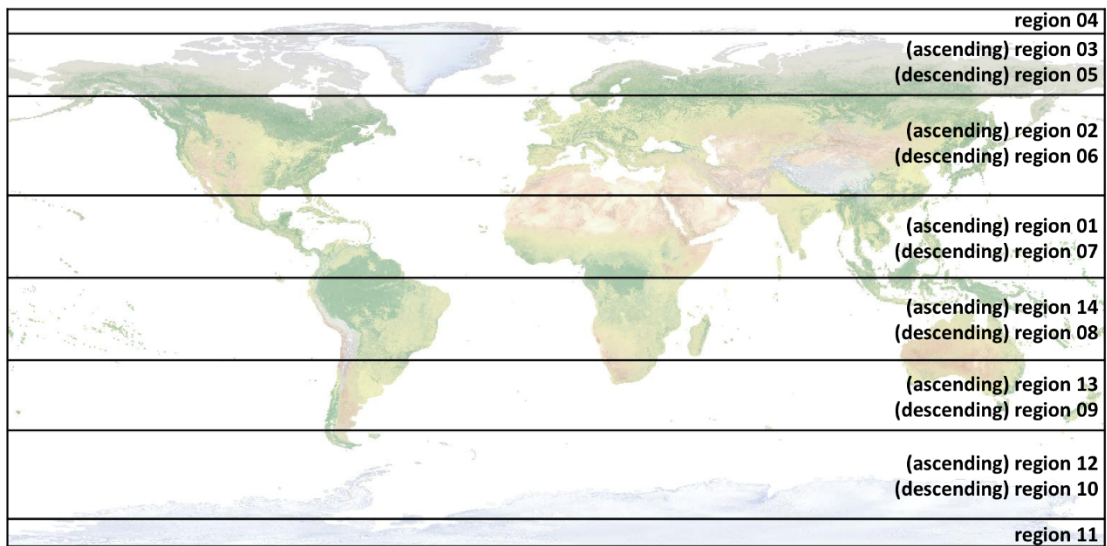
565 Figure 2.1. HDF5 data structure for ATL08 products

566

567 For each data parameter, terrain surface elevation and canopy heights will be
 568 provided at a fixed segment size of 100 meters along the ground track. Based on the
 569 satellite velocity and the expected number of reflected photons for land surfaces, each
 570 segment should have more than 100 signal photons, but in some instances there may
 571 be less than 100 signal photons per segment. If a segment has less than 50 classed
 572 (i.e., labeled by ATL08 as ground, canopy, or top of canopy) photons we feel this
 573 would not accurately represent the surface. Thus, an invalid value will be reported in

574 all height fields. In the event that there are more than 50 classed photons, but a terrain
 575 height cannot be determined due to an insufficient number of ground photons, (e.g.
 576 lack of photons penetrating through dense canopy), the only reported terrain height
 577 will be the interpolated surface height.

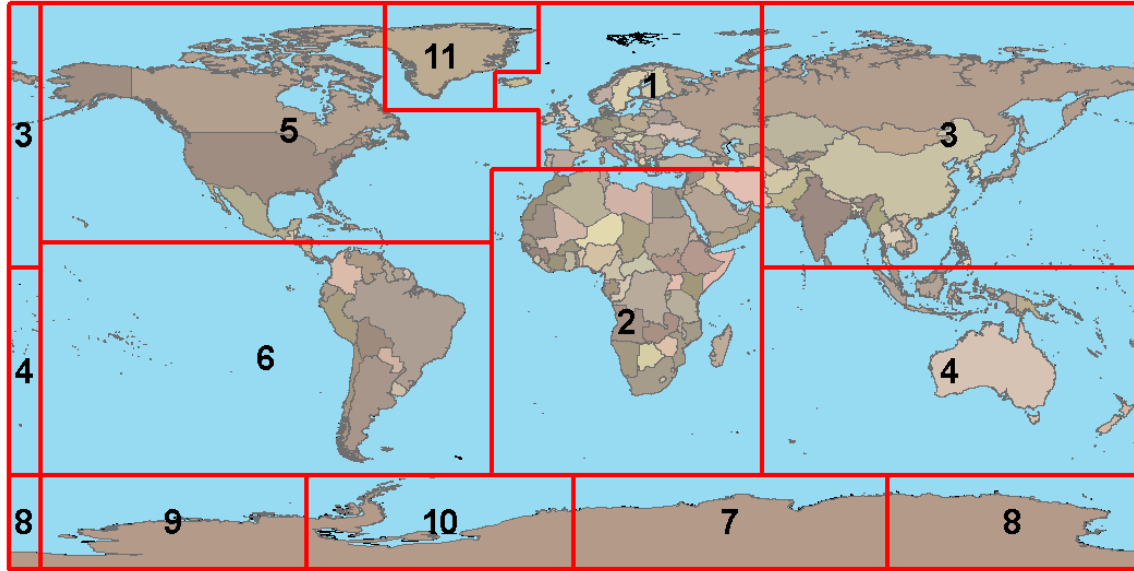
578 The ATL08 product will be produced per granule based on the ATL03 defined
 579 regions (see Figure 2.2). Thus, the ATL08 file/name convention scheme will match
 580 the file/naming convention for ATL03 –in attempt for reducing complexity to allow
 581 users to examine both data products.



582

583 Figure 2.2. ATL03 granule regions; graphic from ATL03 ATBD (Neumann et al.).

584 The ATL08 product additionally has its own internal regions, which are
 585 roughly assigned by continent, as shown by Figure 2.3. For the regions covering
 586 Antarctica (regions 7, 8, 9, 10) and Greenland (region 11), the ATL08 algorithm will
 587 assume that no canopy is present. These internal ATL08 regions will be noted in the
 588 ATL08 product (see parameter atl08_region in Section 2.4.19). Note that the regions
 589 for each ICESat-2 product are not the same.



590

591 Figure 2.3. ATL08 product regions.

592

593 **2.1 Subgroup: Land Parameters**

594 ATL08 terrain height parameters are defined in terms of the absolute height
 595 above the reference ellipsoid.

596 Table 2.1. Summary table of land parameters on ATL08.

Group	Data type	Description	Source
segment_id_beg	Integer	First along-track segment_id number in 100-m segment	ATL03
segment_id_end	Integer	Last along-track segment_id number in 100-m segment	ATL03
h_te_mean	Float	Mean terrain height for segment	computed
h_te_median	Float	Median terrain height for segment	computed
h_te_min	Float	Minimum terrain height for segment	computed
h_te_max	Float	Maximum terrain height for segment	computed
h_te_mode	Float	Mode of terrain height for segment	computed
h_te_skew	Float	Skew of terrain height for segment	computed

n_te_photons	Integer	Number of ground photons in segment	computed
h_te_interp	Float	Interpolated terrain surface height at mid-point of segment	computed
h_te_std	Float	Standard deviation of ground heights about the interpolated ground surface	computed
h_te_uncertainty	Float	Uncertainty of ground height estimates. Includes all known uncertainties such as geolocation, pointing angle, timing, radial orbit errors, etc.	computed from Equation 1.4
terrain_slope	Float	Slope of terrain within segment	computed
h_te_best_fit	Float	Best fit terrain elevation at the 100 m segment mid-point location	computed
subset_te_flag	Integer	Quality flag indicating the terrain photons populating the 100 m segment statistics are derived from less than 100 m worth of photons	computed
photon_rate_te	Float	Calculated photon rate for ground photons within each segment	computed

597

598 **2.1.1 Georeferenced_segment_number_beg**

599 (parameter = segment_id_beg). The first along-track segment_id in each 100-m
600 segment. Each 100-m segment consists of five sequential 20-m segments provided
601 from the ATL03 product, which are labeled as segment_id. The segment_id is a seven
602 digit number that uniquely identifies each along track segment, and is written at the
603 along-track geolocation segment rate (i.e. ~20m along track). The four digit RGT
604 number can be combined with the seven digit segment_id number to uniquely define
605 any along-track segment number. Values are sequential, with 0000001 referring to
606 the first segment after the equatorial crossing of the ascending node.

607 **2.1.2 Georeferenced_segment_number_end**

608 (parameter = segment_id_end). The last along-track segment_id in each 100-m
609 segment. Each 100-m segment consists of five sequential 20-m segments provided

610 from the ATL03 product, which are labeled as `segment_id`. The `segment_id` is a seven
611 digit number that uniquely identifies each along track segment, and is written at the
612 along-track geolocation segment rate (i.e. ~20m along track). The four digit RGT
613 number can be combined with the seven digit `segment_id` number to uniquely define
614 any along-track segment number. Values are sequential, with 0000001 referring to
615 the first segment after the equatorial crossing of the ascending node.

616 **2.1.3** `Segment_terrain_height_mean`

617 (parameter = `h_te_mean`). Estimated mean of the terrain height above the
618 reference ellipsoid derived from classified ground photons within the 100 m segment.
619 If a terrain height cannot be directly determined within the segment (i.e. there are not
620 a sufficient number of ground photons), only the interpolated terrain height will be
621 reported. Required input data is classified point cloud (i.e. photons labeled as either
622 canopy or ground in the ATL08 processing). This parameter will be derived from only
623 classified ground photons.

624 **2.1.4** `Segment_terrain_height_med`

625 (parameter = `h_te_median`). Median terrain height above the reference
626 ellipsoid derived from the classified ground photons within the 100 m segment. If
627 there are not a sufficient number of ground photons, an invalid value will be reported
628 –no interpolation will be done. Required input data is classified point cloud (i.e.
629 photons labeled as either canopy or ground in the ATL08 processing). This parameter
630 will be derived from only classified ground photons.

631 **2.1.5** `Segment_terrain_height_min`

632 (parameter = `h_te_min`). Minimum terrain height above the reference ellipsoid
633 derived from the classified ground photons within the 100 m segment. If there are
634 not a sufficient number of ground photons, an invalid value will be reported –no
635 interpolation will be done. Required input data is classified point cloud (i.e. photons
636 labeled as either canopy or ground in the ATL08 processing). This parameter will be
637 derived from only classified ground photons.

638 **2.1.6** Segment_terrain_height_max

639 (parameter = h_te_max). Maximum terrain height above the reference
640 ellipsoid derived from the classified ground photons within the 100 m segment. If
641 there are not a sufficient number of ground photons, an invalid value will be reported
642 –no interpolation will be done. Required input data is classified point cloud (i.e.
643 photons labeled as either canopy or ground in the ATL08 processing). This parameter
644 will be derived from only classified ground photons.

645 **2.1.7** Segment_terrain_height_mode

646 (parameter = h_te_mode). Mode of the classified ground photon heights above
647 the reference ellipsoid within the 100 m segment. If there are not a sufficient number
648 of ground photons, an invalid value will be reported –no interpolation will be done.
649 Required input data is classified point cloud (i.e. photons labeled as either canopy or
650 ground in the ATL08 processing). This parameter will be derived from only classified
651 ground photons.

652 **2.1.8** Segment_terrain_height_skew

653 (parameter = h_te_skew). The skew of the classified ground photons within the
654 100 m segment. If there are not a sufficient number of ground photons, an invalid
655 value will be reported –no interpolation will be done. Required input data is classified
656 point cloud (i.e. photons labeled as either canopy or ground in the ATL08 processing).
657 This parameter will be derived from only classified ground photons.

658 **2.1.9** Segment_number_terrain_photons

659 (parameter = n_te_photons). Number of terrain photons identified in segment.

660 **2.1.10** Segment_height_interp

661 (parameter = h_te_interp). Interpolated terrain surface height above the
662 reference ellipsoid from ATL08 processing at the mid-point of each segment. This
663 interpolated surface is the FINALGROUND estimate (described in section 4.9).

664 **2.1.11 Segment h_te_std**

665 (parameter = h_te_std). Standard deviations of terrain points about the
666 interpolated ground surface within the segment. Provides an indication of surface
667 roughness.

668 **2.1.12 Segment_terrain_height_uncertainty**

669 (parameter = h_te_uncertainty). Uncertainty of the mean terrain height for the
670 segment. This uncertainty incorporates all systematic uncertainties (e.g. timing,
671 orbits, geolocation, etc.) as well as uncertainty from errors of identified photons. This
672 parameter is described in Section 1, Equation 1.4. If there are not a sufficient number
673 of ground photons, an invalid value will be reported –no interpolation will be done.
674 Required input data is classified point cloud (i.e. photons labeled as either canopy or
675 ground in the ATL08 processing). This parameter will be derived from only classified
676 ground photons. The $\sigma_{segmentclass}$ term in Equation 1.4 represents the standard
677 deviation of the terrain height residuals about the FINALGROUND estimate.

678 **2.1.13 Segment_terrain_slope**

679 (parameter = terrain_slope). Slope of terrain within each segment. Slope is
680 computed from a linear fit of the terrain photons. It estimates the rise [m] in relief
681 over each segment [100 m]; e.g., if the slope value is 0.04, there is a 4 m rise over the
682 100 m segment. Required input data are the classified terrain photons.

683 **2.1.14 Segment_terrain_height_best_fit**

684 (parameter = h_te_best_fit). The best fit terrain elevation at the mid-point
685 location of each 100 m segment. The mid-segment terrain elevation is determined by
686 selecting the best of three fits – linear, 3rd order and 4th order polynomials – to the
687 terrain photons and interpolating the elevation at the mid-point location of the 100
688 m segment. For the linear fit, a slope correction and weighting is applied to each
689 ground photon based on the distance to the slope height at the center of the segment.

690 **2.1.15 Subset_te_flag {1:5}**

691 (parameter = subset_te_flag). This flag indicates the quality distribution of
692 identified terrain photons within each 100 m on a gesegment basis. The purpose of
693 this flag is to provide the user with an indication whether the photons contributing to
694 the terrain estimate are evenly distributed or only partially distributed (i.e. due to
695 cloud cover or signal attenuation). A 100 m ATL08 segment is comprised of 5 geo-
696 segments and we are populating a flag for each geosegment. subset_te_flags:

697 -1: no data within geosegment available for analysis

698 0: indicates no ground photons within geosegment

699 1: indicates ground photons within geosegment

700 For example, an 100 m ATL08 segment might have the following
701 subset_te_flags: {-1 -1 0 1 1} which would translate that no signal photons (canopy or
702 ground) were available for processing in the first two geosegments. Geosegment 3
703 was found to have photons, but none were labeled as ground photons. Geosegment 4
704 and 5 had valid labeled ground photons. Again, the motivation behind this flag is to
705 inform the user that, in this example, the 100 m estimate are being derived from only
706 40 m worth of data.

707 **2.1.16 Segment Terrain Photon Rate**

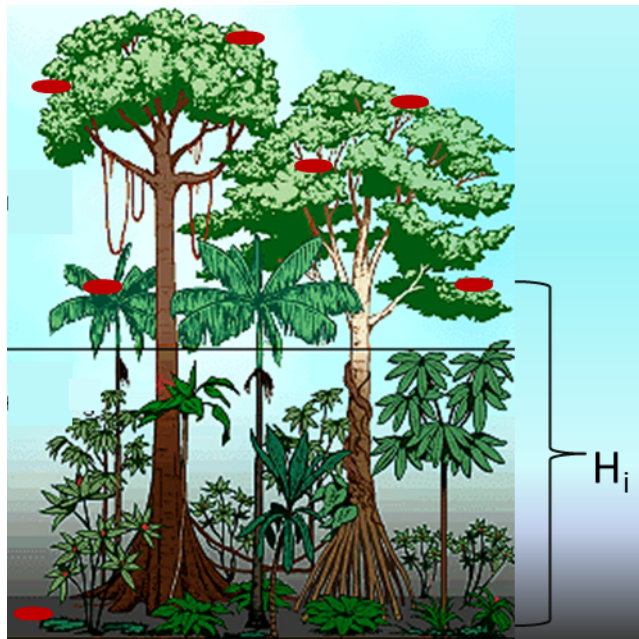
708 (parameter = photon_rate_te). This value indicates the terrain photon rate
709 within each ATL08 segment. This value is calculated as the total number of terrain
710 photons divided by the total number of laser shots within each ATL08 segment. The
711 number of laser shots is defined as the number of unique Delta_Time values within
712 each segment.

713

714 **2.2 Subgroup: Vegetation Parameters**

715 Canopy parameters will be reported on the ATL08 data product in terms of both
 716 the absolute height above the reference ellipsoid as well as the relative height above
 717 an estimated ground. The relative canopy height, H_i , is computed as the height from
 718 an identified canopy photon minus the interpolated ground surface for the same
 719 horizontal geolocation (see Figure 2.3). Thus, each identified signal photon above an
 720 interpolated surface (including a buffer distance based on the instrument point
 721 spread function) is by default considered a canopy photon. Canopy parameters will
 722 only be computed for segments where more than 5% of the classed photons are
 723 classified as canopy photons.

724



725

726 Figure 2.4. Illustration of canopy photons (red dots) interaction in a vegetated area.
 727 Relative canopy heights, H_i , are computed by differencing the canopy photon height from
 728 an interpolated terrain surface.

729 Table 2.2. Summary table of canopy parameters on ATL08.

Group	Data type	Description	Source
-------	-----------	-------------	--------

segment_id_beg	Integer	First along-track segment_id number in 100-m segment	ATL03
segment_id_end	Integer	Last along-track segment_id number in 100-m segment	ATL03
canopy_h_metrics_abs	Float	Absolute (H##) canopy height metrics calculated at the following percentiles: 5, 10, 15, 20, 25, 30, 35, 40, 45, 50, 55, 60, 65, 70, 75, 80, 85, 90, 95.	computed
canopy_h_metrics	Float	Relative (RH##) canopy height metrics calculated at the following percentiles: 5, 10, 15, 20, 25, 30, 35, 40, 45, 50, 55, 60, 65, 70, 75, 80, 85, 90, 95.	computed
h_canopy_abs	Float	98% height of all the individual absolute canopy heights (height above WGS84 ellipsoid) for segment.	computed
h_canopy	Float	98% height of all the individual relative canopy heights (height above terrain) for segment.	computed
h_mean_canopy_abs	Float	Mean of individual absolute canopy heights within segment	computed
h_mean_canopy	Float	Mean of individual relative canopy heights within segment	computed
h_dif_canopy	Float	Difference between h_canopy and canopy_h_metrics(50)	computed
h_min_canopy_abs	Float	Minimum of individual absolute canopy heights within segment	computed
h_min_canopy	Float	Minimum of individual relative canopy heights within segment	computed
h_max_canopy_abs	Float	Maximum of individual absolute canopy heights within segment. Should be equivalent to H100	computed
h_max_canopy	Float	Maximum of individual relative canopy heights within segment. Should be equivalent to RH100	computed
h_canopy_uncertainty	Float	Uncertainty of the relative canopy height (h_canopy)	computed
canopy_openness	Float	STD of relative heights for all photons classified as canopy photons within the segment to provide inference of canopy openness	computed
toc_roughness	Float	STD of relative heights of all photons classified as top of canopy within the segment	computed
h_canopy_quad	Float	Quadratic mean canopy height	computed
n_ca_photons	Integer4	Number of canopy photons within 100 m segment	computed

n_toc_photons	Integer4	Number of top of canopy photons within 100 m segment	computed
centroid_height	Float	Absolute height above reference ellipsoid associated with the centroid of all signal photons	computed
canopy_rh_conf	Integer	Canopy relative height confidence flag based on percentage of ground and canopy photons within a segment: 0 (<5% canopy), 1 (>5% canopy, <5% ground), 2 (>5% canopy, >5% ground)	computed
canopy_flag	Integer	Flag indicating that canopy was detected using the Landsat Tree Cover Continuous Fields data product	computed
landsat_flag	Integer	Flag indicating that Landsat Tree Cover Continuous Fields data product had more than 50% values >100 for L-km segment	computed
landsat_perc	Float	Average percentage value of the valid (value <= 100) Landsat Tree Cover Continuous Fields product for each 100 m segment	
subset_can_flag	Integer	Quality flag indicating the canopy photons populating the 100 m segment statistics are derived from less than 100 m worth of photons	computed
photon_rate_can	Float	Photon rate of canopy photons within each 100 m segment	computed

730

731 **2.2.1** Georeferenced_segment_number_beg

732 (parameter = segment_id_beg). The first along-track segment_id in each 100-m
733 segment. Each 100-m segment consists of five sequential 20-m segments provided
734 from the ATL03 product, which are labeled as segment_id. The segment_id is a seven
735 digit number that uniquely identifies each along track segment, and is written at the
736 along-track geolocation segment rate (i.e. ~20m along track). The four digit RGT
737 number can be combined with the seven digit segment_id number to uniquely define
738 any along-track segment number. Values are sequential, with 0000001 referring to
739 the first segment after the equatorial crossing of the ascending node.

740 **2.2.2** Georeferenced_segment_number_end

741 (parameter = segment_id_end). The last along-track segment_id in each 100-m
742 segment. Each 100-m segment consists of five sequential 20-m segments provided
743 from the ATL03 product, which are labeled as segment_id. The segment_id is a seven
744 digit number that uniquely identifies each along track segment, and is written at the
745 along-track geolocation segment rate (i.e. ~20m along track). The four digit RGT
746 number can be combined with the seven digit segment_id number to uniquely define
747 any along-track segment number. Values are sequential, with 0000001 referring to
748 the first segment after the equatorial crossing of the ascending node.

749 **2.2.3** Canopy_height_metrics_abs

750 (parameter = canopy_h_metrics_abs). The absolute height metrics (H##) of
751 classified canopy photons (labels 2 and 3) above the ellipsoid. The height metrics are
752 sorted based on a cumulative distribution and calculated at the following percentiles:
753 10, 15, 20, 25, 30, 35, 40, 45, 50, 55, 60,65, 70, 75, 80, 85, 90, 95. These height metrics
754 are often used in the literature to characterize vertical structure of vegetation. One
755 important distinction of these canopy height metrics compared to those derived from
756 other lidar systems (e.g., LVIS or GEDI) is that the ICESat-2 canopy height metrics are
757 heights above the ground surface. These metrics do not include the ground photons.
758 Required input data are the relative canopy heights of all canopy photons above the
759 estimated terrain surface and the mid-segment elevation. The absolute canopy
760 heights metrics are determined by adding the relative canopy height metric to the
761 best-fit terrain (h_te_bestfit).

762 **2.2.4** Canopy_height_metrics

763 (parameter = canopy_h_metrics). Relative height metrics above the estimated
764 terrain surface (RH##) of classified canopy photons (labels 2 and 3). The height
765 metrics are sorted based on a cumulative distribution and calculated at the following
766 percentiles: 10, 15, 20, 25, 30, 35, 40, 45, 50, 55, 60, 65, 70, 75, 80, 85, 90, 95. These
767 height metrics are often used in the literature to characterize vertical structure of
768 vegetation. One important distinction of these canopy height metrics compared to

769 those derived from other lidar systems (e.g., LVIS or GEDI) is that the ICESat-2 canopy
770 height metrics are heights above the ground surface. These metrics do not include the
771 ground photons. Required input data are relative canopy heights above the estimated
772 terrain surface for all canopy photons.

773 **2.2.5** Absolute_segment_canopy_height

774 (parameter = h_canopy_abs). The absolute 98% height of classified canopy
775 photon heights (labels 2 and 3) above the ellipsoid. The relative height from classified
776 canopy photons are sorted into a cumulative distribution, and the height associated
777 with the 98% height above the h_te_bestfit for that segment is reported.

778 **2.2.6** Segment_canopy_height

779 (parameter = h_canopy). The relative 98% height of classified canopy photon
780 heights (labels 2 and 3) above the estimated terrain surface. Relative canopy heights
781 have been computed by differencing the canopy photon height from the estimated
782 terrain surface in the ATL08 processing. The relative canopy heights are sorted into
783 a cumulative distribution, and the height associated with the 98% height is reported.

784 **2.2.7** Absolute_segment_mean_canopy

785 (parameter = h_mean_canopy_abs). The absolute mean canopy height for the
786 segment. relative canopy heights are the photons heights for canopy photons (labels
787 2 and 3) above the estimated terrain surface. These relative heights are averaged and
788 then added to h_te_bestfit.

789 **2.2.8** Segment_mean_canopy

790 (parameter = h_mean_canopy). The mean canopy height for the segment.
791 Relative canopy heights have been computed by differencing the canopy photon
792 height (labels 2 and 3) from the estimated terrain surface in the ATL08 processing.
793 These heights are averaged.

794 **2.2.9** Segment_dif_canopy

795 (parameter = h_dif_canopy). Difference between h_canopy and
796 canopy_h_metrics(50). This parameter is one metric used to describe the vertical
797 distribution of the canopy within the segment.

798 **2.2.10** Absolute_segment_min_canopy

799 (parameter = h_min_canopy_abs). The minimum absolute canopy height for
800 the segment. Relative canopy heights are the photons heights for canopy photons
801 (labels 2 and 3) above the estimated terrain surface. Required input data is classified
802 point cloud (i.e. photons labeled as either canopy or ground in the ATL08 processing).
803 The minimum relative canopy height for each segment is added to h_te_bestfit and
804 reported as the absolute minimum canopy height.

805 **2.2.11** Segment_min_canopy

806 (parameter = h_min_canopy). The minimum relative canopy height for the
807 segment. Canopy heights are the photons heights for canopy photons (labels 2 and 3)
808 differenced from the estimated terrain surface. Required input data is classified point
809 cloud (i.e. photons labeled as either canopy or ground in the ATL08 processing).

810 **2.2.12** Absolute_segment_max_canopy

811 (parameter = h_max_canopy_abs). The maximum absolute canopy height for
812 the segment. This parameter is equivalent to H100 metric reported in the literature.
813 This parameter, however, has the potential for error as random solar background
814 noise may not have been fully rejected. It is recommended that h_canopy or
815 h_canopy_abs (i.e., the 98% canopy height) be considered as the top of canopy
816 measurement. Required input data is classified point cloud (i.e. photons labeled as
817 either canopy or ground in the ATL08 processing). The absolute max canopy height
818 is the maximum relative canopy height added to h_te_bestfit.

819 **2.2.13 Segment_max_canopy**

820 (parameter = h_max_canopy). The maximum relative canopy height for the
821 segment. Canopy heights are the photons heights for canopy photons (labels 2 and 3)
822 differenced from the estimated terrain surface. This product is equivalent to RH100
823 metric reported in the literature. This parameter, however, has the potential for error
824 as random solar background noise may not have been fully rejected. It is
825 recommended that h_canopy or h_canopy_abs (i.e., the 98% canopy height) be
826 considered as the top of canopy measurement. Required input data is classified point
827 cloud (i.e. photons labeled as either canopy or ground in the ATL08 processing).

828 **2.2.14 Segment_canopy_height_uncertainty**

829 (parameter = h_canopy_uncertainty). Uncertainty of the relative canopy
830 height for the segment. This uncertainty incorporates all systematic uncertainties
831 (e.g. timing, orbits, geolocation, etc.) as well as uncertainty from errors of identified
832 photons. This parameter is described in Section 1, Equation 1.4. If there are not a
833 sufficient number of ground photons, an invalid value will be reported –no
834 interpolation will be done. In the case for canopy height uncertainty, the parameter
835 $\sigma_{segmentclass}$ is comprised of both the terrain uncertainty within the segment but also
836 the top of canopy residuals. Required input data is classified point cloud (i.e. photons
837 labeled as either top of canopy or ground in the ATL08 processing). This parameter
838 will be derived from only classified top of canopy photons, label = 3. The canopy
839 height uncertainty is derived from Equation 1.4, shown below as Equation 1.5,
840 represents the standard deviation of the terrain points and the standard deviation of
841 the top of canopy height photons.

842
$$\sigma_{ATL08_{segment_ch}} = \frac{\sqrt{\sigma_{AtlasLand}^2 + \sigma_{Zrms_{segment_terrain}}^2 + \sigma_{Zrms_{segment_toc}}^2}}{n_{photons_{segment_terrain}} + n_{photons_{segment_toc}}} \quad \text{Eqn 1.5}$$

843

844 **2.2.15 Segment_canopy_openness**

845 (parameter = canopy_openness). Standard deviation of relative canopy
846 heights within each segment. This parameter will potentially provide an indicator of
847 canopy openness (label = 2 and 3) as a greater standard deviation of heights indicates
848 greater penetration of the laser energy into the canopy. Required input data is
849 classified point cloud (i.e. photons labeled as either canopy or ground in the ATL08
850 processing).

851 **2.2.16 Segment_top_of_canopy_roughness**

852 (parameter = toc_roughness). Standard deviation of relative top of canopy
853 heights (label = 3) within each segment. This parameter will potentially provide an
854 indicator of canopy variability. Required input data is classified point cloud (i.e.
855 photons labeled as the top of the canopy in the ATL08 processing).

856 **2.2.17 Segment_canopy_quadratic_height**

857 (parameter = h_canopy_quad). The quadratic mean relative height of relative
858 canopy heights. The quadratic mean height is computed as:

859
$$qmh = \sqrt{\frac{\sum_{i=1}^{n_{ca_photons}} h_i^2}{n_{ca_photons}}}$$

860 **2.2.18 Segment_number_canopy_photons**

861 (parameter = n_ca_photons). Number of canopy photons (label 2 and 3) within
862 each segment. Required input data is classified point cloud (i.e. photons labeled as
863 either canopy or ground in the ATL08 processing).

864 **2.2.19 Segment_number_top_canopy_photons**

865 (parameter = n_toc_photons). Number of top of canopy photons (label = 3)
866 within each segment. Required input data is classified point cloud (i.e. photons
867 labeled as top of canopy in the ATL08 processing).

868 **2.2.20** Centroid_height

869 (parameter = centroid_height). Optical centroid of all photons classified as
870 either canopy or ground points (label = 1 2 or 3) within a segment. The heights used
871 in this calculation are absolute heights above the reference ellipsoid. This parameter
872 is equivalent to the centroid height produced on ICESat GLA14.

873 **2.2.21** Segment_rel_canopy_conf

874 (parameter = canopy_rh_conf). Canopy relative height confidence flag based
875 on percentage of ground photons and percentage of canopy photons (label 2 and 3),
876 relative to the total classified (ground and canopy, label = 1 2 and 3) photons within
877 a segment: 0 (<5% canopy), 1 (>5% canopy and <5% ground), 2 (>5% canopy and
878 >5% ground). This is a measure based on the quantity, not the quality, of the
879 classified photons in each segment.

880 **2.2.22** Canopy_flag

881 (parameter = canopy_flag). Flag indicating that canopy was detected using the
882 Landsat Continuous Cover product for the *L-km* segment. Currently, if more than 3%
883 of the Landsat CC pixels along the profile have canopy in them, we make the
884 assumption canopy is present along the entire *L-km* segment. Beginning in release
885 004, the canopy_flag is no longer used to determine how the ATL08 ground and
886 canopy finding software operates.

887 **2.2.23** Landsat_flag

888 (parameter = landsat_flag). Flag indicating that more than 50% of the Landsat
889 Tree Cover Continuous Fields product have values >100 (indicating water, cloud,
890 shadow, or filled values) for the *L-km* segment. Canopy is assumed present along the
891 *L-km* segment if landsat_flag is 1.

892 **2.2.24 Landsat_perc**

893 (parameter = landsat_perc). Average percentage value of the valid (value <=
894 100) Landsat Tree Cover Continuous Fields product pixels that overlap within each
895 100 m segment.

896 **2.2.25 Subset_can_flag {1:5}**

897 (parameter = subset_can_flag). This flag indicates the distribution of identified
898 canopy photons (label 2 and 3) within each 100 m. The purpose of this flag is to
899 provide the user with an indication whether the photons contributing to the canopy
900 height estimates are evenly distributed or only partially distributed (i.e. due to cloud
901 cover or signal attenuation). A 100 m ATL08 segment is comprised of 5 geo-segments.
902 subset_can_flags:

903 -1: no data within geosegment available for analysis

904 0: indicates no canopy photons within geosegment

905 1: indicates canopy photons within geosegment

906 For example, a 100 m ATL08 segment might have the following
907 subset_can_flags: {-1 -1 -1 1 1} which would translate that no photons (canopy or
908 ground) were available for processing in the first three geosegments. Geosegment 4
909 and 5 had valid labeled canopy photons. Again, the motivation behind this flag is to
910 inform the user that, in this example, the 100 m estimate are being derived from only
911 40 m worth of data.

912 **2.2.26 Segment Canopy Photon Rate**

913 (parameter = photon_rate_can). This value indicates the canopy photon rate
914 within each ATL08 segment. This value is calculated as the total number of canopy
915 photons (label =2 and 3) divided by the total number of unique laser shots within
916 each ATL08 segment. The number of laser shots is defined as the number of unique
917 Delta_Time values within each segment.

918

919

920 **2.3 Subgroup: Photons**

921 The subgroup for photons contains the classified photons that were used to
922 generate the parameters within the land or canopy subgroups. Each photon that is
923 identified as being likely signal will be classified as: 0 = noise, 1 = ground, 2 = canopy,
924 or 3 = top of canopy. The index values for each classified photon will be provided such
925 that they can be extracted from the ATL03 data product for independent evaluation.

926 Table 2.3. Summary table for photon parameters for the ATL08 product.

Group	Data Type	Description	Source
classed_PC_indx	Float	Indices of photons tracking back to ATL03 that surface finding software identified and used within the creation of the data products.	ATL03
classed_PC_flag	Integer	Classification flag for each photon as either noise, ground, canopy, or top of canopy.	computed
ph_segment_id	Integer	Georeferenced bin number (20-m) associated with each photon	ATL03
ph_h	Float	Height of photon above interpolated ground surface	computed
d_flag	Integer	Flag indicating whether DRAGANN labeled the photon as noise or signal	computed

927

928 **2.3.1 Indices_of_classed_photons**

929 (parameter = classed_PC_indx). Indices of photons tracking back to ATL03 that
930 surface finding software identified and used within the creation of the data products
931 for a given segment.

932 **2.3.2 Photon_class**

933 (parameter = classed_PC_flag). Classification flags for a given segment. 0 =
934 noise, 1 = ground, 2 = canopy, 3 = top of canopy. The final ground and canopy
935 classification are flags 1-3. The full canopy is the combination of flags 2 and 3.

936 **2.3.3 Georeferenced_segment_number**

937 (parameter = ph_segment_id). The segment_id associated with every photon in
938 each 100-m segment. Each 100-m segment consists of five sequential 20-m segments
939 provided from the ATL03 product, which are labeled as segment_id. The segment_id
940 is a seven digit number that uniquely identifies each along track segment, and is
941 written at the along-track geolocation segment rate (i.e. ~20m along track). The four
942 digit RGT number can be combined with the seven digit segment_id number to
943 uniquely define any along-track segment number. Values are sequential, with
944 0000001 referring to the first segment after the equatorial crossing of the ascending
945 node.

946 **2.3.4 Photon Height**

947 (parameter = ph_h). Height of the photon above the interpolated ground
948 surface at the location of the photon.

949 **2.3.5 DRAGANN_flag**

950 (parameter = d_flag). Flag indicating the labeling of DRAGANN noise filtering for
951 a given photon. 0 = noise, 1=signal.

952

953 **2.4 Subgroup: Reference data**

954 The reference data subgroup contains parameters and information that are
955 useful for determining the terrain and canopy heights that are reported on the
956 product. In addition to position and timing information, these parameters include the
957 reference DEM height, reference landcover type, and flags indicating water or snow.

958 Table 2.4. Summary table for reference parameters for the ATL08 product.

Group	Data Type	Description	Source
segment_id_beg	Integer	First along-track segment_id number in 100-m segment	ATL03
segment_id_end	Integer	Last along-track segment_id number in 100-m segment	ATL03
latitude	Float	Center latitude of signal photons within each segment	ATL03
longitude	Float	Center longitude of signal photons within each segment	ATL03
delta_time	Float	Mid-segment GPS time in seconds past an epoch. The epoch is provided in the metadata at the file level	ATL03
delta_time_beg	Float	Delta time of the first photon in the segment	ATL03
delta_time_end	Float	Delta time of the last photon in the segment	ATL03
night_flag	Integer	Flag indicating whether the measurements were acquired during night time conditions	computed
dem_h	Float4	Reference DEM elevation	external
dem_flag		Source of reference DEM	external
dem_removal_flag	Integer	Quality check flag to indicate > 20% photons removed due to large distance from dem_h	computed
h_dif_ref	Float4	Difference between h_te_median and dem_h	computed
terrain_flg	Integer	Terrain flag quality check to indicate a deviation from the reference DTM	computed
segment_landcover	Integer4	Reference landcover for segment derived from best global landcover product available	external
segment_watermask	Integer4	Water mask indicating inland water produced from best sources available	external
segment_snowcover	Integer4	Daily snow cover mask derived from best sources	external
urban_flag	Integer	Flag indicating segment is located in an urban area	external
surf_type	Integer1	Flags describing surface types: 0=not type, 1=is type.	ATL03

		Order of array is land, ocean, sea ice, land ice, inland water.	
atl08_region	Integer	ATL08 region(s) encompassed by ATL03 granule being processed	computed
last_seg_extend	Float	The distance (km) that the last ATL08 processing segment in a file is either extended or overlapped with the previous ATL08 processing segment	computed
brightness_flag	Integer	Flag indicating that the ground surface is bright (e.g. snow-covered or other bright surfaces)	computed

959

960 **2.4.1 Georeferenced_segment_number_beg**

961 (parameter = segment_id_beg). The first along-track segment_id in each 100-m
 962 segment. Each 100-m segment consists of five sequential 20-m segments provided
 963 from the ATL03 product, which are labeled as segment_id. The segment_id is a seven
 964 digit number that uniquely identifies each along track segment, and is written at the
 965 along-track geolocation segment rate (i.e. ~20m along track). The four digit RGT
 966 number can be combined with the seven digit segment_id number to uniquely define
 967 any along-track segment number. Values are sequential, with 0000001 referring to
 968 the first segment after the equatorial crossing of the ascending node.

969 **2.4.2 Georeferenced_segment_number_end**

970 (parameter = segment_id_end). The last along-track segment_id in each 100-m
 971 segment. Each 100-m segment consists of five sequential 20-m segments provided
 972 from the ATL03 product, which are labeled as segment_id. The segment_id is a seven
 973 digit number that uniquely identifies each along track segment, and is written at the
 974 along-track geolocation segment rate (i.e. ~20m along track). The four digit RGT
 975 number can be combined with the seven digit segment_id number to uniquely define
 976 any along-track segment number. Values are sequential, with 0000001 referring to
 977 the first segment after the equatorial crossing of the ascending node.

978 **2.4.3** Segment_latitude

979 (parameter = latitude). Center latitude of signal photons within each segment.
980 Each 100 m segment consists of 5 20m ATL03 geosegments. In most cases, there will
981 be signal photons in each of the 5 geosegments necessary for calculating a latitude
982 value. For instances where the 100 m ATL08 is not fully populated with photons (e.g.
983 photons drop out due to clouds or signal attenuation), the latitude will be interpolated
984 to the mid-point of the 100 m segment. To implement this interpolation, we confirm
985 that each 100 m segment is comprised of at least 3 unique ATL03 geosegments IDs,
986 indicating that data is available near the mid-point of the land segment. If less than 3
987 ATL03 segments are available, the coordinate is interpolated based on the ratio of
988 delta time at the centermost ATL03 segment and that of the centermost photon, thus
989 applying the centermost photon's coordinates to represent the land segment with a
990 slight adjustment. In some instances, the latitude and longitude will require
991 extrapolation to estimate a mid-100 m segment location. It is possible that in these
992 extremely rare cases, the latitude and longitude could not represent the true center
993 of the 100 m segment. We encourage the user to investigate the parameters
994 segment_te_flag and segment_can_flag which provide information as to the number
995 and distribution of signal photons within each 100 m segment.

996 **2.4.4** Segment_longitude

997 (parameter = longitude). Center longitude of signal photons within each
998 segment. Each 100 m segment consists of 5 20m geosegments. In most cases, there
999 will be signal photons in each of the 5 geosegments necessary for calculating a
1000 longitude value. For instances where the 100 m ATL08 is not fully populated with
1001 photons (e.g. photons drop out due to clouds or signal attenuation), the latitude will
1002 be interpolated to the mid-point of the 100 m segment. To implement this
1003 interpolation, we confirm that each 100 m segment is comprised of at least 3 unique
1004 ATL03 geosegments IDs, indicating that data is available near the mid-point of the
1005 land segment. If less than 3 ATL03 segments are available, the coordinate is
1006 interpolated based on the ratio of delta time at the centermost ATL03 segment and

1007 that of the centermost photon, thus applying the centermost photon's coordinates to
1008 represent the land segment with a slight adjustment. In some instances, the latitude
1009 and longitude will require extrapolation to estimate a mid-100 m segment location. It
1010 is possible that in these extremely rare cases, the latitude and longitude could not
1011 represent the true center of the 100 m segment. We encourage the user to investigate
1012 the parameters `segment_te_flag` and `segment_can_flag` which provide information as to
1013 the number and distribution of signal photons within each 100 m segment.

1014 **2.4.5** `Delta_time`

1015 (parameter = `delta_time`). Mid-segment GPS time for the segment in seconds
1016 past an epoch. The epoch is listed in the metadata at the file level.

1017 **2.4.6** `Delta_time_beg`

1018 (parameter = `delta_time_beg`). Delta time for the first photon in the segment
1019 in seconds past an epoch. The epoch is listed in the metadata at the file level.

1020 **2.4.7** `Delta_time_end`

1021 (parameter = `delta_time_end`). Delta time for the last photon in the segment
1022 in seconds past an epoch. The epoch is listed in the metadata at the file level.

1023 **2.4.8** `Night_Flag`

1024 (parameter = `night_flag`). Flag indicating the data were acquired in night
1025 conditions: 0 = day, 1 = night. Night flag is set when solar elevation is below 0.0
1026 degrees.

1027 **2.4.9** `Segment_reference_DTM`

1028 (parameter = `dem_h`). Reference terrain height value for segment determined
1029 by the "best" DEM available based on data location. All heights in ICESat-2 are
1030 referenced to the WGS 84 ellipsoid unless clearly noted otherwise. DEM is taken from
1031 a variety of ancillary data sources: GIMP, GMTED, MSS. The DEM source flag indicates
1032 which source was used.

1033 **2.4.10** Segment_reference_DEM_source

1034 (parameter = dem_flag). Indicates source of the reference DEM height. Values:
1035 0=None, 1=GIMP, 2=GMTED, 3=MSS.

1036 **2.4.11** Segment_reference_DEM_removal_flag

1037 (parameter = dem_removal_flag). Quality check flag to indicate > 20%
1038 classified photons removed from land segment due to large distance from dem_h.

1039 **2.4.12** Segment_terrain_difference

1040 (parameter = h_dif_ref). Difference between h_te_median and dem_h. Since the
1041 mean terrain height is more sensitive to outliers, the median terrain height will be
1042 evaluated against the reference DEM. This parameter will be used as an internal data
1043 quality check with the notion being that if the difference exceeds a threshold (TBD) a
1044 terrain quality flag (terrain_flg) will be triggered.

1045 **2.4.13** Segment_terrain flag

1046 (parameter = terrain_flg). Terrain flag to indicate confidence in the derived
1047 terrain height estimate. If h_dif_ref exceeds a threshold (TBD) the terrain_flg
1048 parameter will be set to 1. Otherwise, it is 0.

1049 **2.4.14** Segment_landcover

1050 (parameter = segment_landcover). Segment landcover will be based on best
1051 available global landcover product used for reference. One potential source is the 0.5
1052 km global mosaics of the standard MODIS land cover product (Channan et al, 2015;
1053 Friedl et al, 2010; available online at <http://glcf.umd.edu/data/lc/index.shtml>). Here,
1054 17 classes are defined ranging from evergreen (needle and broadleaf forest),
1055 deciduous (needle and broadleaf forest), shrublands, woodlands, savanna and
1056 grasslands, agriculture, to urban. The most current year processed for this product is
1057 based on MODIS measurements from 2012.

1058 **2.4.15 Segment_watermask**

1059 (parameter = segment_watermask). Water mask (i.e., flag) indicating inland
1060 water as referenced from the Global Raster Water Mask at 250 m spatial resolution
1061 (Carroll et al, 2009; available online at <http://glcf.umd.edu/data/watermask/>). 0 =
1062 no water; 1 = water.

1063 **2.4.16 Segment_snowcover**

1064 (parameter = segment_snowcover). Daily snowcover mask (i.e., flag)
1065 indicating a likely presence of snow or ice within each segment produced from best
1066 available source used for reference. The snow mask will be the same snow mask as
1067 used for ATL09 Atmospheric Products: NOAA snow-ice flag. 0=ice free water;
1068 1=snow free land; 2=snow; 3=ice.

1069 **2.4.17 Urban_flag**

1070 (parameter = urban_flag). The urban flag indicates that a segment is likely
1071 located over an urban area. In these areas, buildings may be misclassified as canopy,
1072 and thus the canopy products may be incorrect. The urban flag is sourced from the
1073 “urban and built up” classification on the MODIS land cover product (Channan et al,
1074 2015; Friedl et al, 2010; available online at
1075 <http://glcf.umd.edu/data/lc/index.shtml>). 0 = not urban; 1 = urban.

1076 **2.4.18 Surface_type**

1077 (parameter = surf_type). The surface type for a given segment is determined at
1078 the major frame rate (every 200 shots, or ~140 meters along-track) and is a two-
1079 dimensional array surf_type(n, nsurf), where n is the major frame number, and nsurf
1080 is the number of possible surface types such that surf_type(n, isurf) is set to 0 or 1
1081 indicating if surface type isurf is present (1) or not (0), where isurf = 1 to 5 (land,
1082 ocean, sea ice, land ice, and inland water) respectively.

1083 **2.4.19** ATL08_region

1084 (parameter = atl08_region). The ATL08 regions that encompass the ATL03
1085 granule being processed through the ATL08 algorithm. The ATL08 regions are shown
1086 by Figure 2.3. In ATL08 regions 11 (Greenland) and 7 - 10 (Antarctica), the
1087 canopy_flag is automatically set to false for ATL08 processing.

1088 **2.4.20** Last_segment_extend

1089 (parameter = last_seg_extend). The distance (km) that the last ATL08 10 km
1090 processing segment is either extended beyond 10 km or uses data from the previous
1091 10 km processing segment to allow for enough data for processing the ATL03 photons
1092 through the ATL08 algorithm. If the last portion of an ATL03 granule being processed
1093 would result in a segment with less than 3.4 km (170 geosegments) worth of data,
1094 that last portion is added to the previous 10 km processing window to be processed
1095 together as one extended ATL08 processing segment. The resulting last_seg_extend
1096 value would be a positive value of distance beyond 10 km that the ATL08 processing
1097 segment was extended by. If the last ATL08 processing segment would be less than
1098 10 km but greater than 3.4 km, a portion extending from the start of current ATL08
1099 processing segment backwards into the previous ATL08 processing segment would
1100 be added to the current ATL08 processing segment to make it 10 km in length. The
1101 distance of this backward data gathering would be reported in last_seg_extend as a
1102 negative distance value. Only new 100 m ATL08 segment products generated from
1103 this backward extension would be reported. All other segments that are not extended
1104 will report a last_seg_extend value of 0.

1105 **2.4.21** Brightness_flag

1106 (parameter = brightness_flag). Based upon the classification of the photons
1107 within each 100 m, this parameter flags ATL08 segments where the mean number of
1108 ground photons per shot exceed a value of 3. This calculation can be made as the total
1109 number of ground photons divided by the number of ATLAS shots within the 100 m
1110 segment. A value of 0 = indicates non-bright surface, value of 1 indicates bright
1111 surface, and a value of 2 indicates "undetermined" due to clouds or other factors. The

1112 brightness is computed initially on the 10 km processing segment. If the ground
 1113 surface is determined to be bright for the entire 10 km segment, the brightness is then
 1114 calculated at the 100 m segment size.

1115

1116 **2.5 Subgroup: Beam data**

1117 The subgroup for beam data contains basic information on the geometry and
 1118 pointing accuracy for each beam.

1119 Table 2.5. Summary table for beam parameters for the ATL08 product.

Group	Data Type	Units	Description	Source
segment_id_beg	Integer		First along-track segment_id number in 100-m segment	ATL03
segment_id_end	Integer		Last along-track segment_id number in 100-m segment	ATL03
ref_elev	Float		Elevation of the unit pointing vector for the reference photon in the local ENU frame in radians. The angle is measured from East-North plane and positive towards up	ATL03
ref_azimuth	Float		Azimuth of the unit pointing vector for the reference photon in the ENU frame in radians. The angle is measured from North and positive toward East.	ATL03
atlas_pa	Float		Off nadir pointing angle of the spacecraft	ATL03
rgt	Integer		The reference ground track (RGT) is the track on the earth at which the vector bisecting laser beams 3 and 4 is pointed during repeat operations	ATL03

sigma_h	Float	Total vertical uncertainty due to PPD and POD	ATL03
sigma_along	Float	Total along-track uncertainty due to PPD and POD knowledge	ATL03
sigma_across	Float	Total cross-track uncertainty due to PPD and POD knowledge	ATL03
sigma_topo	Float	Uncertainty of the geolocation knowledge due to local topography (Equation 1.3)	computed
sigma_atlas_land	Float	Total uncertainty that includes sigma_h plus the geolocation uncertainty due to local slope Equation 1.2	computed
psf_flag	integer	Flag indicating sigma_atlas_land (aka PSF) as computed in Equation 1.2 exceeds a value of 1m.	computed
layer_flag	Integer	Cloud flag indicating presence of clouds or blowing snow	ATL09
cloud_flag_atm	Integer	Cloud confidence flag from ATL09 indicating clear skies	ATL09
msw_flag	Integer	Multiple scattering warning product produced on ATL09	ATL09
cloud_fold_flag	integer	Cloud flag to indicate potential of high clouds that have “folded” into the lower range bins	ATL09
asr	Float	Apparent surface reflectance	ATL09
snr	Float	Background signal to noise level	Computed
solar_azimuth	Float	The azimuth (in degrees) of the sun position vector from the reference photon bounce point position in the local ENU frame. The angle is measured from	ATL03g

solar_elevation	Float	North and is positive towards East. The elevation of the sun position vector from the reference photon bounce point position in the local ENU frame. The angle is measured from the East-North plane and is positive Up.	ATL03g
n_seg_ph	Integer	Number of photons within each land segment	computed
ph_ndx_beg	Integer	Photon index begin	computed
sat_flag	Integer	Flag derived from full_sat_fract and near_sat_fract on the ATL03 data product	computed

1120

1121 **2.5.1 Georeferenced_segment_number_beg**

1122 (parameter = segment_id_beg). The first along-track segment_id in each 100-m
 1123 segment. Each 100-m segment consists of five sequential 20-m segments provided
 1124 from the ATL03 product, which are labeled as segment_id. The segment_id is a seven
 1125 digit number that uniquely identifies each along track segment, and is written at the
 1126 along-track geolocation segment rate (i.e. ~20m along track). The four digit RGT
 1127 number can be combined with the seven digit segment_id number to uniquely define
 1128 any along-track segment number. Values are sequential, with 0000001 referring to
 1129 the first segment after the equatorial crossing of the ascending node.

1130 **2.5.2 Georeferenced_segment_number_end**

1131 (parameter = segment_id_end). The last along-track segment_id in each 100-m
 1132 segment. Each 100-m segment consists of five sequential 20-m segments provided
 1133 from the ATL03 product, which are labeled as segment_id. The segment_id is a seven
 1134 digit number that uniquely identifies each along track segment, and is written at the
 1135 along-track geolocation segment rate (i.e. ~20m along track). The four digit RGT
 1136 number can be combined with the seven digit segment_id number to uniquely define

1137 any along-track segment number. Values are sequential, with 0000001 referring to
1138 the first segment after the equatorial crossing of the ascending node.

1139 **2.5.3** Beam_coelevation

1140 (parameter = ref_elev). Elevation of the unit pointing vector for the reference
1141 photon in the local ENU frame in radians. The angle is measured from East-North
1142 plane and positive towards up.

1143 **2.5.4** Beam_azimuth

1144 (parameter = ref_azimuth). Azimuth of the unit pointing vector for the
1145 reference photon in the ENU frame in radians. The angle is measured from North and
1146 positive toward East.

1147 **2.5.5** ATLAS_Pointing_Angle

1148 (parameter = atlas_pa). Off nadir pointing angle (in radians) of the satellite to
1149 increase spatial sampling in the non-polar regions.

1150 **2.5.6** Reference_ground_track

1151 (parameter = rgt). The reference ground track (RGT) is the track on the earth
1152 at which the vector bisecting laser beams 3 and 4 (or GT2L and GT2R) is pointed
1153 during repeat operations. Each RGT spans the part of an orbit between two ascending
1154 equator crossings and are numbered sequentially. The ICESat-2 mission has 1387
1155 RGTs, numbered from 0001xx to 1387xx. The last two digits refer to the cycle number.

1156 **2.5.7** Sigma_h

1157 (parameter = sigma_h). Total vertical uncertainty due to PPD (Precise Pointing
1158 Determination), POD (Precise Orbit Determination), and geolocation errors.
1159 Specifically, this parameter includes radial orbit error, σ_{Orbit} , tropospheric errors,
1160 σ_{Trop} , forward scattering errors, $\sigma_{forwardscattering}$, instrument timing errors, σ_{timing} ,
1161 and off-nadir pointing geolocation errors. The component parameters are pulled
1162 from ATL03 and ATL09. Sigma_h is the root sum of squares of these terms as detailed

1163 in Equation 1.1. The σ_h reported here is the mean of the σ_h values reported
1164 within the five ATL03 geosegments that are used to create the 100 m ATL08 segment.

1165 **2.5.8** σ_{along}

1166 (parameter = σ_{along}). Total along-track uncertainty due to PPD and POD
1167 knowledge. This parameter is pulled from ATL03.

1168 **2.5.9** σ_{across}

1169 (parameter = σ_{across}). Total cross-track uncertainty due to PPD and
1170 POD knowledge. This parameter is pulled from ATL03.

1171 **2.5.10** σ_{topo}

1172 (parameter = σ_{topo}). Uncertainty in the geolocation due to local surface
1173 slope as described in Equation 1.3. The local slope is multiplied by the 6.5 m
1174 geolocation uncertainty factor that will be used to determine the geolocation
1175 uncertainty. The geolocation error will be computed from a 100 m sample due to the
1176 local slope calculation at that scale.

1177 **2.5.11** $\sigma_{\text{ATLAS_LAND}}$

1178 (parameter = $\sigma_{\text{atlas_land}}$). Total vertical geolocation error due to
1179 ranging, and local surface slope. The parameter is computed for ATL08 as described
1180 in Equation 1.2. The geolocation error will be computed from a 100 m sample due to
1181 the local slope calculation at that scale.

1182 **2.5.12** PSF_flag

1183 (parameter = psf_flag). Flag indicating that the point spread function
1184 (computed as $\sigma_{\text{atlas_land}}$) has exceeded 1m.

1185 **2.5.13** Layer_flag

1186 (parameter = layer_flag). Flag is a combination of multiple ATL09 flags and
1187 takes daytime/nighttime into consideration. A value of 1 means clouds or blowing

1188 snow is likely present. A value of 0 indicates the likely absence of clouds or blowing
1189 snow. If no ATL09 product is available for an ATL08 segment, an invalid value will be
1190 reported. Since the cloud flags from the ATL09 product are reported at an along-track
1191 distance of 250 m, we will report the highest value of the ATL09 flags at the ATL08
1192 resolution (100 m). Thus, if a 100 m ATL08 segment straddles two values from
1193 ATL09, the highest cloud flag value will be reported on ATL08. This reporting strategy
1194 holds for all the cloud flags reported on ATL08.

1195 **2.5.14** Cloud_flag_atm

1196 (parameter = cloud_flag_atm). Cloud confidence flag from ATL09 that indicates
1197 the number of cloud or aerosol layers identified in each 25Hz atmospheric profile. If
1198 the flag is greater than 0, aerosols or clouds could be present.

1199 **2.5.15** MSW

1200 (parameter = msw_flag). Multiple scattering warning flag with values from -1 to
1201 5 as computed in the ATL09 atmospheric processing and delivered on the ATL09 data
1202 product. If no ATL09 product is available for an ATL08 segment, an invalid value will
1203 be reported. MSW flags:

1204 -1 = signal to noise ratio too low to determine presence of
1205 cloud or blowing snow
1206 0 = no_scattering
1207 1 = clouds at > 3 km
1208 2 = clouds at 1-3 km
1209 3 = clouds at < 1 km
1210 4 = blowing snow at < 0.5 optical depth
1211 5 = blowing snow at >= 0.5 optical depth

1212 **2.5.16** Cloud Fold Flag

1213 (parameter = cloud_fold_flag). Clouds occurring higher than 14 to 15 km in the
1214 atmosphere will be folded down into the lower portion of the atmospheric profile.

1215 **2.5.17** Computed_Apparent_Surface_Reflectance

1216 (parameter = asr). Apparent surface reflectance computed in the ATL09
1217 atmospheric processing and delivered on the ATL09 data product. If no ATL09
1218 product is available for an ATL08 segment, an invalid value will be reported.

1219 **2.5.18** Signal_to_Noise_Ratio

1220 (parameter = snr). The Signal to Noise Ratio of geolocated photons as
1221 determined by the ratio of the superset of ATL03 signal and DRAGANN found signal
1222 photons used for processing the ATL08 segments to the background photons (i.e.,
1223 noise) within the same ATL08 segments.

1224 **2.5.19** Solar_Azimuth

1225 (parameter = solar_azimuth). The azimuth (in degrees) of the sun position
1226 vector from the reference photon bounce point position in the local ENU frame. The
1227 angle is measured from North and is positive towards East.

1228 **2.5.20** Solar_Elevation

1229 (parameter = solar_elevation). The elevation of the sun position vector from
1230 the reference photon bounce point position in the local ENU frame. The angle is
1231 measured from the East-North plane and is positive up.

1232 **2.5.21** Number_of_segment_photons

1233 (parameter = n_seg_ph). Number of photons in each land segment.

1234 **2.5.22 Photon_Index_Begin**

1235 (parameter = ph_ndx_beg). Index (1-based) within the photon-rate data of
1236 the first photon within this each land segment.

1237 **2.5.23 Saturation Flag**

1238 (parameter = sat_flag) Saturation flag derived from the ATL03 saturation
1239 flags full_sat_frac. The saturation flags on the ATL03 data product (full_sat_frac)
1240 are the percentage of photons determined to be saturated within each geosegment.
1241 For the ATL08 saturation flag, a value of 0 will indicate no saturation. A value of 1
1242 will indicate the average of all 5 geosegment full_sat_frac values was over 0.2. This
1243 value of 1 is an indication of standing water or saturated soils. If an ATL08 segment
1244 is not fully populated with 5 values for full_sat_frac, a value of -1 will be set.

1245 sat_flag: -1 indicates not enough valid data to make determination

1246 0 indicates no saturation in ATL08 segment

1247 1 indicates saturation in ATL08 segment

1248

1249

1250

1251

1252 3 ALGORITHM METHODOLOGY

1253 For the ecosystem community, identification of the ground and canopy surface
1254 is by far the most critical task, as meeting the science objective of determining global
1255 canopy heights hinges upon the ability to detect both the canopy surface and the
1256 underlying topography. Since a space-based photon counting laser mapping system
1257 is a relatively new instrument technology for mapping the Earth's surface, the
1258 software to accurately identify and extract both the canopy surface and ground
1259 surface is described here. The methodology adopted for ATL08 establishes a
1260 framework to potentially accept multiple approaches for capturing both the upper
1261 and lower surface of signal photons. One method used is an iterative filtering of
1262 photons in the along-track direction. This method has been found to preserve the
1263 topography and capture canopy photons, while rejecting noise photons. An advantage
1264 of this methodology is that it is self-parameterizing, robust, and works in all
1265 ecosystems if sufficient photons from both the canopy and ground are available. For
1266 processing purposes, along-track data signal photons are parsed into L -km segment
1267 of the orbit which is recommended to be 10 km in length.

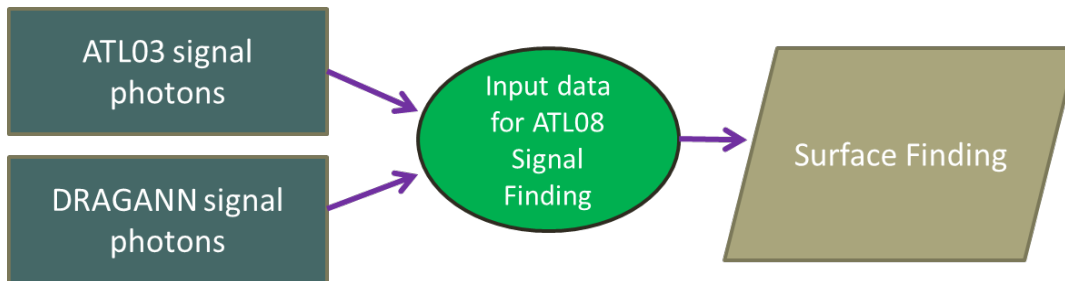
1268

1269 3.1 Noise Filtering

1270 Solar background noise is a significant challenge in the analysis of photon
1271 counting laser data. Range measurement data created from photon counting lidar
1272 detectors typically contain far higher noise levels than the more common photon
1273 integrating detectors available commercially in the presence of passive, solar
1274 background photons. Given the higher detection sensitivity for photon counting
1275 devices, a background photon has a greater probability of triggering a detection event
1276 over traditional integral measurements and may sometimes dominate the dataset.
1277 Solar background noise is a function of the surface reflectance, topography, solar
1278 elevation, and atmospheric conditions. Prior to running the surface finding
1279 algorithms used for ATL08 data products, the superset of output from the GSFC
1280 medium-high confidence classed photons (ATL03 signal_conf_ph: flags 3-4) and the

1281 output from DRAGANN will be considered as the input data set. ATL03 input data
1282 requirements include the latitude, longitude, height, segment delta time, segment ID,
1283 and a preliminary signal classification for each photon. The motivation behind
1284 combining the results from two different noise filtering methods is to ensure that all
1285 of the potential signal photons for land surfaces will be provided as input to the
1286 surface finding software. The description of the methodology for the ATL03
1287 classification is described separately in the ATL03 ATBD. The methodology behind
1288 DRAGANN is described in the following section.

1289



1290

1291 Figure 3.1. Combination of noise filtering algorithms to create a superset of input data for
1292 surface finding algorithms.

1293

1294 3.1.1 DRAGANN

1295 The Differential, Regressive, and Gaussian Adaptive Nearest Neighbor
1296 (DRAGANN) filtering technique was developed to identify and remove noise photons
1297 from the photon counting data point cloud. DRAGANN utilizes the basic premise that
1298 signal photons will be closer in space than random noise photons. The first step of the
1299 filtering is to implement an adaptive nearest neighbor search. By using an adaptive
1300 method, different thresholds can be applied to account for variable amounts of
1301 background noise and changing surface reflectance along the data profile. This search
1302 finds an effective radius by computing the probability of finding P number of points
1303 within a search area. For MABEL and mATLAS, P=20 points within the search area

1304 was empirically derived but found to be an effective and efficient number of
1305 neighbors.

1306 There may be cases, however, where the value of P needs to be changed. For
1307 example, during night acquisitions it is anticipated that the background noise rate will
1308 be considerably low. Since DRAGANN is searching for two distributions in
1309 neighborhood searching space, the software could incorrectly identify signal photons
1310 as noise photons. The parameter P, however, can be determined dynamically from
1311 estimations of the signal and noise rates from the photon cloud. In cases of low
1312 background noise (night), P would likely be changed to a value lower than 20.
1313 Similarly, in cases of high amounts of solar background, P may need to be increased
1314 to better capture the signal and avoid classifying small, dense clusters of noise as
1315 signal. In this case, however, it is likely that noise photons near signal photons will
1316 also be misclassified as signal. The method for dynamically determining a P value is
1317 explained further in section 4.3.1.

1318 After P is defined, a histogram of the number of neighbors within a search
1319 radius for each point is generated. The distribution of neighbor radius occurrences is
1320 analyzed to determine the noise threshold.

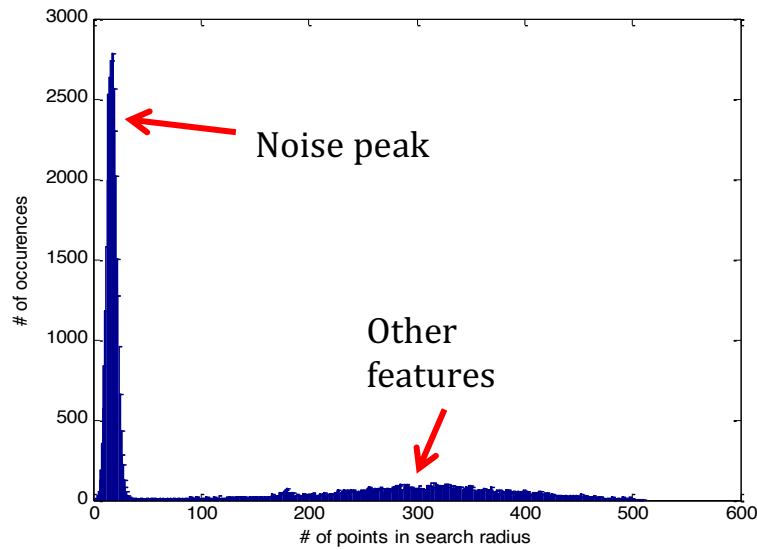
1321
$$\frac{P}{N_{total}} = \frac{V}{V_{total}} \quad \text{Eqn. 3.1}$$

1322
1323 where N_{total} is the total number of photons in the point cloud, V is the volume of the
1324 nearest neighborhood search, and V_{total} is the bounding volume of the enclosed point
1325 cloud. For a 2-dimensional data set, V becomes

1326
1327
$$V = \pi r^2 \quad \text{Eqn. 3.2}$$

1328
1329 where r is the radius. A good practice is to first normalize the data set along each
1330 dimension before running the DRAGANN filter. Normalization prevents the algorithm
1331 from favoring one dimension over the others in the radius search (e.g., when the
1332 latitude and longitude are in degrees and height is in meters).

1333



1334

1335 Figure 3.2. Histogram of the number of photons within a search radius. This histogram is
1336 used to determine the threshold for the DRAGANN approach.

1337

1338 Once the radius has been computed, DRAGANN counts the number of points
1339 within the radius for each point and histograms that set of values. The distribution of
1340 the number of points, Figure 3.2, reveals two distinct peaks; a noise peak and a signal
1341 peak. The motivation of DRAGANN is to isolate the signal photons by determining a
1342 threshold based on the number of photons within the search radius. The noise peak
1343 is characterized as having a large number of occurrences of photons with just a few
1344 neighboring photons within the search radius. The signal photons comprise the broad
1345 second peak. The first step in determining the threshold between the noise and signal
1346 is to implement Gaussian fitting to the number of photons distribution (i.e., the
1347 distribution shown in Figure 3.2). The Gaussian function has the form

1348

1349

$$g(x) = ae^{-\frac{(x-b)^2}{2c^2}} \quad \text{Eqn. 3.3}$$

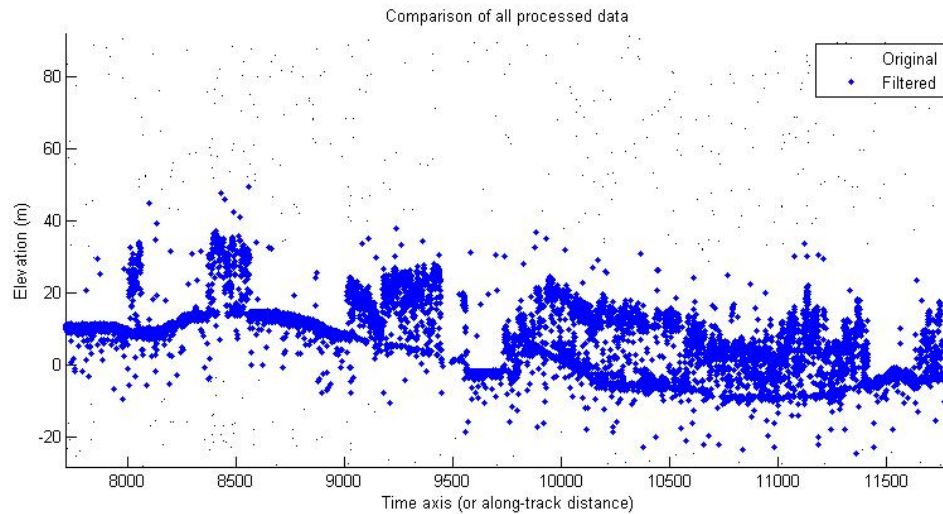
1350

1351 where a is the amplitude of the peak, b is the center of the peak, and c is the standard
1352 deviation of the curve. A first derivative sign crossing method is one option to identify
1353 peaks within the distribution.

1354 To determine the noise and signal Gaussians, up to ten Gaussian curves are fit
1355 to the histogram using an iterative process of fitting and subtracting the max-
1356 amplitude peak component from the histogram until all peaks have been extracted.
1357 Then, the potential Gaussians pass through a rejection process to eliminate those with
1358 poor statistical fits or other apparent errors (Goshtasby and O'Neill, 1994; Chauve et
1359 al. 2008). A Gaussian with an amplitude less than $1/5$ of the previous Gaussian and
1360 within two standard deviations of the previous Gaussian should be rejected. Once the
1361 errant Gaussians are rejected, the final two remaining are assumed to represent the
1362 noise and signal. These are separated based on the remaining two Gaussian
1363 components within the histogram using the logic that the leftmost Gaussian is noise
1364 (low neighbor counts) and the other is signal (high neighbor counts).

1365 The intersection of these two Gaussians (noise and signal) determines a data
1366 threshold value. The threshold value is the parameter used to distinguish between
1367 noise points and signal points when the point cloud is re-evaluated for surface finding.
1368 In the event that only one curve passes the rejection process, the threshold is set at
1369 1σ above the center of the noise peak.

1370 An example of the noise filtered product from DRAGANN is shown in Figure
1371 3.3. The signal photons identified in this process will be combined with the coarse
1372 signal finding output available on the ATL03 data product.



1373

1374 Figure 3.3. Output from DRAGANN filtering. Signal photons are shown as blue.

1375 Figure 3.3 provides an example of along-track (profiling) height data collected
 1376 in September 2012 from the MABEL (ICESat-2 simulator) over vegetation in North
 1377 Carolina. The photons have been filtered such that the signal photons returned from
 1378 vegetation and the ground surface are remaining. Noise photons that are adjacent to
 1379 the signal photons are also retained in the input dataset; however, these should be
 1380 classified as noise photons during the surface finding process. It is possible that some
 1381 additional outlying noise may be retained during the DRAGANN process when noise
 1382 photons are densely grouped, and these photons should be filtered out before the
 1383 surface finding process. Estimates of the ground surface and canopy height can then
 1384 be derived from the signal photons.

1385

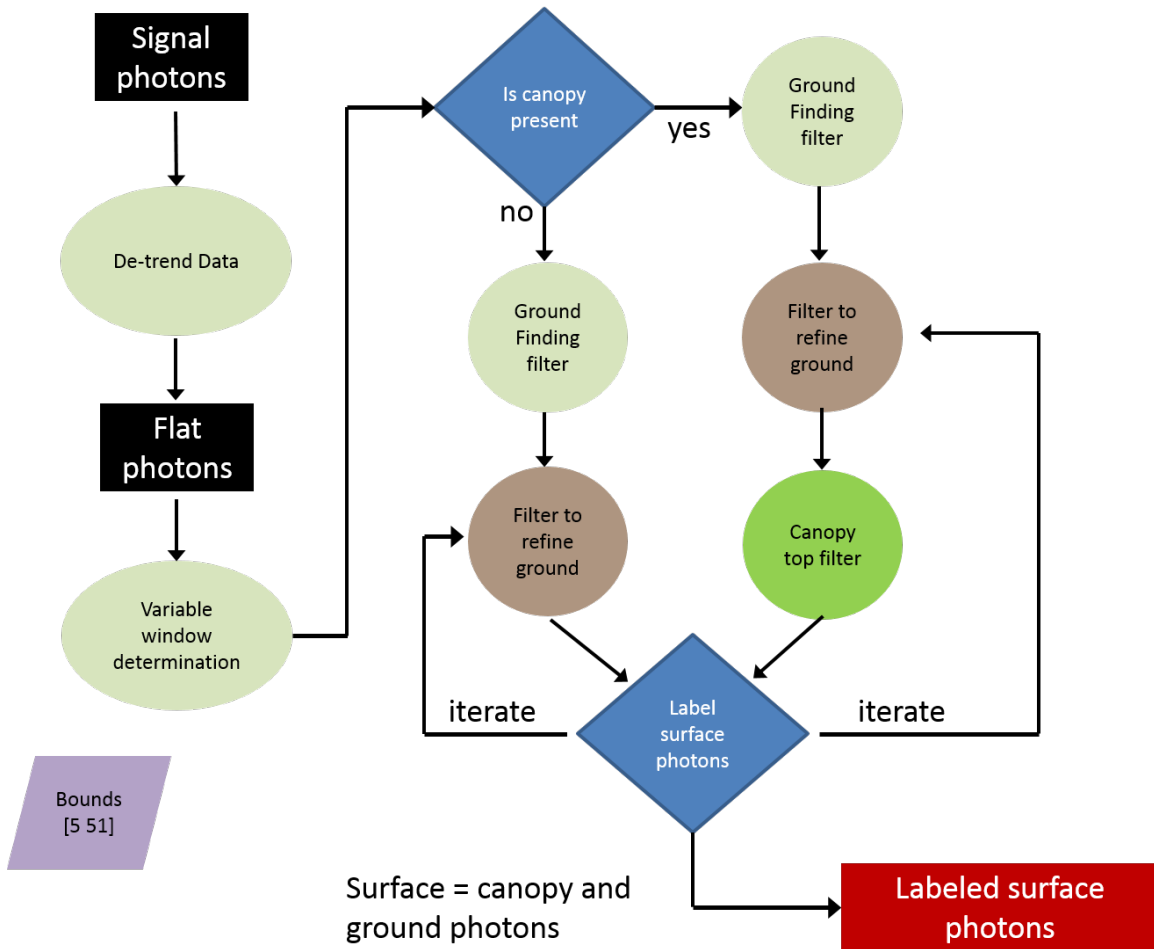
1386 **3.2 Surface Finding**

1387 Once the signal photons have been determined, the objective is to find the
 1388 ground and canopy photons from within the point cloud. With the expectation that
 1389 one algorithm may not work everywhere for all biomes, we are employing a
 1390 framework that will allow us to combine the solutions of multiple algorithms into one
 1391 final composite solution for the ground surface. The composite ground surface
 1392 solution will then be utilized to classify the individual photons as ground, canopy, top

1393 of canopy, or noise. Currently, the framework described here utilizes one algorithm
 1394 for finding the ground surface and canopy surface. Additional methods, however,
 1395 could be integrated into the framework at a later time. Figure 3.4 below describes the
 1396 framework.

1397

1398



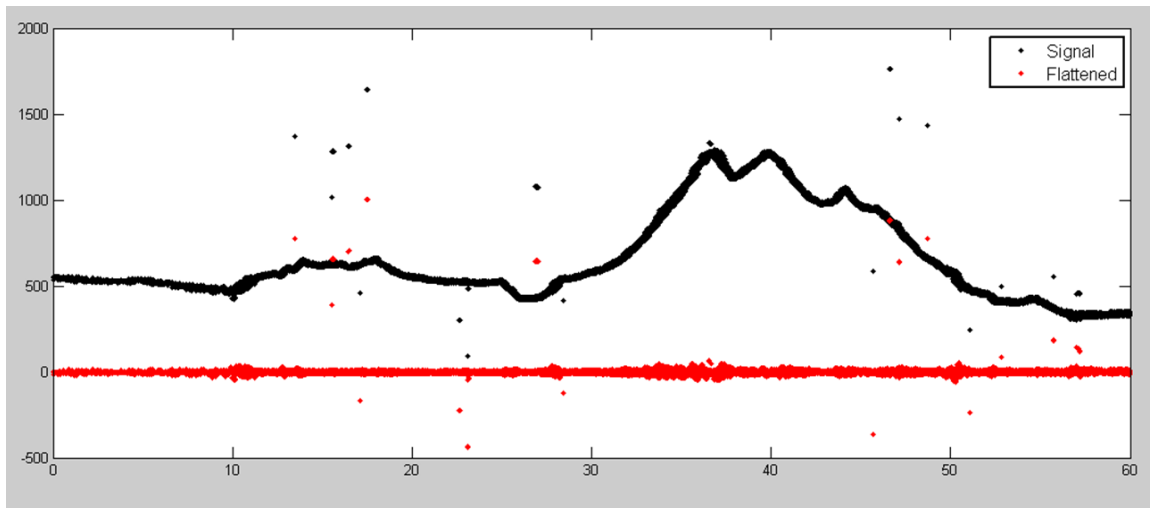
1399

1400 Figure 3.4. Flowchart of overall surface finding method.

1401

1402 3.2.1 De-trending the Signal Photons

1403 An important step in the success of the surface finding algorithm is to remove
1404 the effect of topography on the input data, thus improving the performance of the
1405 algorithm. This is done by de-trending the input signal photons by subtracting a
1406 heavily smoothed “surface” that is derived from the input data. Essentially, this is a
1407 low pass filter of the original data and most of the analysis to detect the canopy and
1408 ground will subsequently be implemented on the high pass data. The amount of
1409 smoothing that is implemented in order to derive this first surface is dependent upon
1410 the relief. For segments where the relief is high, the smoothing window size is
1411 decreased so topography isn’t over-filtered.



1412

1413 Figure 3.5. Plot of Signal Photons (black) from 2014 MABEL flight over Alaska and
1414 de-trended photons (red).

1415

1416 3.2.2 Canopy Determination

1417 A key factor in the success of the surface finding algorithm is for the software
1418 to automatically **account for the presence of canopy** along a given L -km segment.
1419 Due to the large volume of data, this process has to occur in an automated fashion,
1420 allowing the correct methodology for extracting the surface to be applied to the data.
1421 In the absence of canopy, the iterative filtering approach to finding ground works

1422 extremely well, but if canopy does exist, we need to accommodate for that fact when
1423 we are trying to recover the ground surface.

1424 Currently, the Landsat Tree Cover Continuous Fields dataset from the 2000
1425 epoch is used to set a canopy flag within the ATL08 algorithm. Each of these Landsat
1426 Tree Cover tiles contain 30 m pixels indicating the percentage canopy cover for
1427 vegetation over 5 m high in that pixel area. The 2000 epoch is used over the newer
1428 2005 epoch due to “striping” in the 2005 tiles, caused by the failure of the scan line
1429 corrector (SLC) in 2003. The striping artifacts result in inconsistent pixel values
1430 across a landscape which in turn can result in a tenfold difference in the average
1431 canopy cover percentage calculated between the epochs for a flight segment. There is
1432 currently available a 2015 Tree Cover Beta Release that utilizes Landsat 8 data. This
1433 new release of the 2015 Tree Cover product will replace the 2000 epoch for setting
1434 the canopy flag in the ATL08 algorithm. The Tree Cover data are available via ftp at
1435 <http://glcf.umd.edu/data/landsatTreecover/>.

1436 For each L - km segment of ATLAS data, a comparison is made between the
1437 midpoint location of the segment and the midpoint locations of the WRS Landsat tiles
1438 to find the closest tile that encompasses the L - km segment. Using the closest found
1439 tile, each signal photon’s X-Y location is used to identify the corresponding Landsat
1440 pixel. Multiple instances of the same pixels found for the L - km segment are discarded,
1441 and the percentage canopy values of the unique pixels determined to be under the L -
1442 km segment are averaged to produce an average canopy cover percentage for that
1443 segment. If the average canopy cover percentage for a segment is over 3% (threshold
1444 subject to change under further testing), then the ATL08 algorithm will assume the
1445 presence of canopy and identify both ground and vegetation photons in that
1446 segment’s output. Else, the ATL08 algorithm uses a simplified calculation to identify
1447 only ground photons in that segment.

1448 The canopy flag determines if the algorithm will calculate only ground photons
1449 (canopy flag = 0) or both ground and vegetation photons (canopy flag = 1) for each L -
1450 km segment.

1451 For ATL08 product regions over Antarctica (regions 7, 8, 9, 10) and Greenland
1452 (region 11), the algorithm will assume only ground photons (canopy flag = 0) (see
1453 Figure 2.2).

1454

1455 3.2.3 Variable Window Determination

1456 The method for generating a best estimated terrain surface will vary depending
1457 upon whether canopy is present. *L-km segments* without canopy are much easier to
1458 analyze because the ground photons are usually continuous. *L-km segments* with
1459 canopy, however, require more scrutiny as the number of signal photons from ground
1460 are fewer due to occlusion by the vegetation.

1461 There are some common elements for finding the terrain surface for both cases
1462 (canopy/no canopy) and with both methods. In both cases, we will use a variable
1463 windowing span to compute statistics as well as filter and smooth the data. For
1464 clarification, the window size is variable for each *L-km segment*, but it is constant
1465 within the *L-km segment*. For the surface finding algorithm, we will employ a
1466 Savitzky-Golay smoothing/median filtering method. Using this filter, we compute a
1467 variable smoothing parameter (or window size). It is important to bound the filter
1468 appropriately as the output from the median filter can lose fidelity if the scan is over-
1469 filtered.

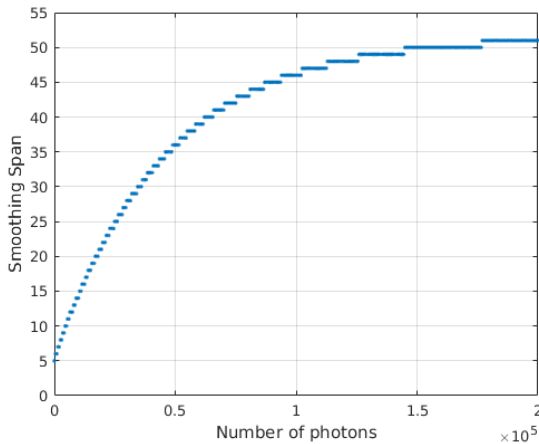
1470 We have developed an empirically-determined shape function, bound between
1471 [5 51], that sets the window size (*Sspan*) based on the number of photons within each
1472 *L-km segment*.

$$1473 \quad Sspan = \text{ceil}[5 + 46 * (1 - e^{-a*length})] \quad \text{Eqn. 3.4}$$

$$1474 \quad a = \frac{\log\left(1 - \frac{21}{51-5}\right)}{-28114} \approx 21 \times 10^{-6} \quad \text{Eqn. 3.5}$$

1475 where *a* is the shape parameter and *length* is the total number of photons in the *L-km*
1476 segment. The shape parameter, *a*, was determined using data collected by MABEL and

1477 is shown in Figure 3.6. It is possible that the model of the shape function, or the
1478 filtering bounds, will need to be adjusted once ICESat-2/ATLAS is on orbit and
1479 collecting data.



1480

1481 Figure 3.6. Shape Parameter for variable window size.

1482

1483 3.2.4 Compute descriptive statistics

1484 To help characterize the input data and initialize some of the parameters used
1485 in the algorithm, we employ a moving window to compute descriptive statistics on
1486 the de-trended data. The moving window's width is the smoothing span function
1487 computed in Equation 5 and the window slides $\frac{1}{4}$ of its size to allow of overlap
1488 between windows. By moving the window with a large overlap helps to ensure that
1489 the approximate ground location is returned. The statistics computed for each
1490 window step include:

- 1491 • Mean height
- 1492 • Min height
- 1493 • Max height
- 1494 • Standard deviation of heights
- 1495

1496 Dependent upon the amount of vegetation within each window, the estimated
 1497 ground height is estimated using different statistics. A standard deviation of the
 1498 photon elevations computed within each moving window are used to classify the
 1499 vertical spread of photons as belonging to one of four classes with increasing amounts
 1500 of variation: open, canopy level 1, canopy level 2, canopy level 3. The canopy indices
 1501 are defined in Table 3.1.

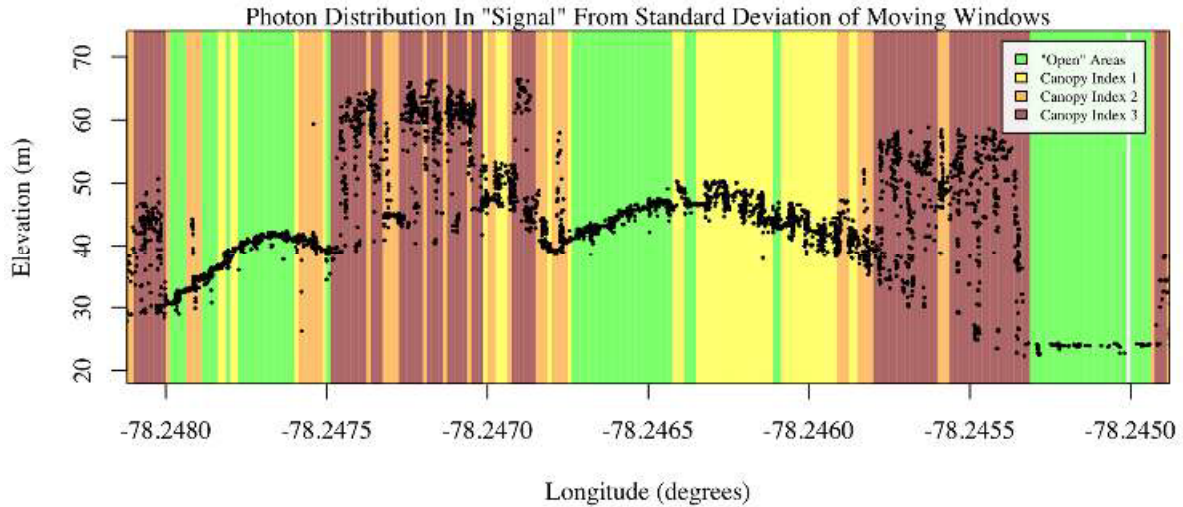
1502

1503 Table 3.1. Standard deviation ranges utilized to qualify the spread of photons within
 1504 moving window.

Name	Definition	Lower Limit	Upper Limit
Open	Areas with little or no spread in signal photons determined due to low standard deviation	N/A	Photons falling within 1 st quartile of Standard deviation
Canopy Level 1	Areas with small spread in signal photons	1 st quartile	Median
Canopy Level 2	Areas with a medium amount of spread	Median	3 rd quartile
Canopy Level 3	Areas with high amount of spread in signal photons	3 rd quartile	N/A

1505

1506



1507

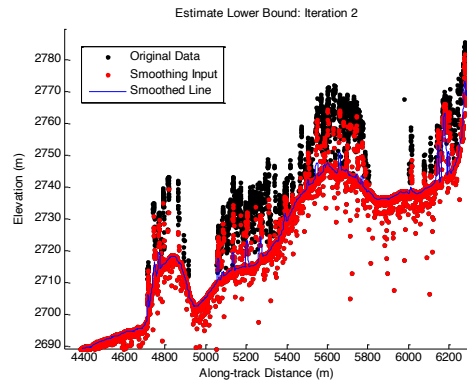
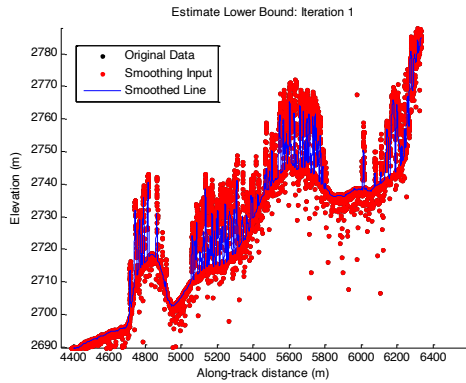
1508 Figure 3.7. Illustration of the standard deviations calculated for each moving window to
 1509 identify the amount of spread of signal photons within a given window.

1510

1511 3.2.5 Ground Finding Filter (Iterative median filtering)

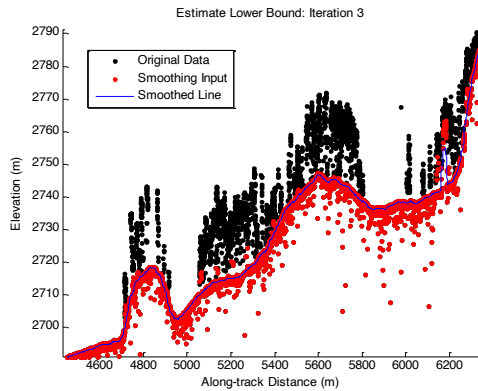
1512 A combination of an iterative median filtering and smoothing filter approach
 1513 will be employed to derive the output solution of both the ground and canopy
 1514 surfaces. The input to this process is the set of de-trended photons. Finding the
 1515 ground in the presence of canopy often poses a challenge because often there are
 1516 fewer ground photons underneath the canopy. The algorithm adopted here uses an
 1517 iterative median filtering approach to retain/eliminate photons for ground finding in
 1518 the presence of canopy. When canopy exists, a smoothed line will lay somewhere
 1519 between the canopy top and the ground. This fact is used to iteratively label points
 1520 above the smoothed line as canopy. The process is repeated five times to eliminate
 1521 canopy points that fall above the estimated surface as well as noise points that fall
 1522 below the ground surface. An example of iterative median filtering is shown in Figure
 1523 3.8. The final median filtered line is the preliminary surface estimate. A limitation of
 1524 this approach, however, is in cases of dense vegetation and few photons reaching the
 1525 ground surface. In these instances, the output of the median filter may lie within the
 1526 canopy.

1527



1528

1529



1530

1531 Figure 3.8. Three iterations of the ground finding concept for L -km segments with canopy.

1532

1533 3.3 Top of Canopy Finding Filter

1534 Finding the top of the canopy surface uses the same methodology as finding
1535 the ground surface, except now the de-trended data are “flipped” over. The “flip”
1536 occurs by multiplying the photons heights by -1 and adding the mean of all the heights
1537 back to the data. The same procedure used to find the ground surface can be used to
1538 find the indices of the top of canopy points.

1539

1540 **3.4 *Classifying the Photons***

1541 Once a composite ground surface is determined, photons falling within the
1542 point spread function of the surface are labeled as ground photons. Based on the
1543 expected performance of ATLAS, the point spread function should be approximately
1544 35 cm rms. Signal photons that are not labeled as ground and are below the ground
1545 surface (buffered with the point spread function) are considered noise, but keep the
1546 signal label.

1547 The top of canopy photons that are identified can be used to generate an upper
1548 canopy surface through a shape-preserving surface fitting method. All signal photons
1549 that are not labeled ground and lie above the ground surface (buffered with the point
1550 spread function) and below the upper canopy surface are considered to be canopy
1551 photons (and thus labeled accordingly). Signal photons that lie above the top of
1552 canopy surface are considered noise, but keep the signal label.

1553

1554 FLAGS, 0 = noise
1555 1 = ground
1556 2 = canopy
1557 3 = TOC (top of canopy)

1558

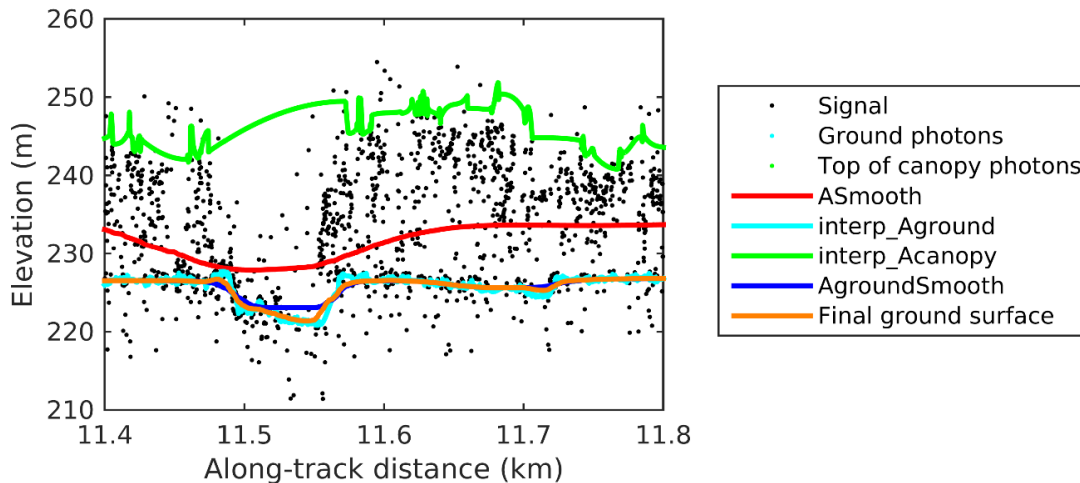
1559 The final ground and canopy classifications are flags 1 – 3. The full canopy is
1560 the combination of flags 2 and 3.

1561

1562 **3.5 *Refining the Photon Labels***

1563 During the first iteration of the algorithm, it is possible that some photons are
1564 mislabeled; most likely this would be noise photons mislabeled as canopy. To reject
1565 these mislabeled photons, we apply three criteria:

- 1566 a) If top of canopy photons are 2 standard deviations above a
1567 smoothed median top of canopy surface
1568 b) If there are less than 3 canopy indices within a 15m radius



1583

1584 Figure 3.9. Example of the intermediate ground and top of canopy surfaces calculated from
 1585 MABEL flight data over Alaska during July 2014.

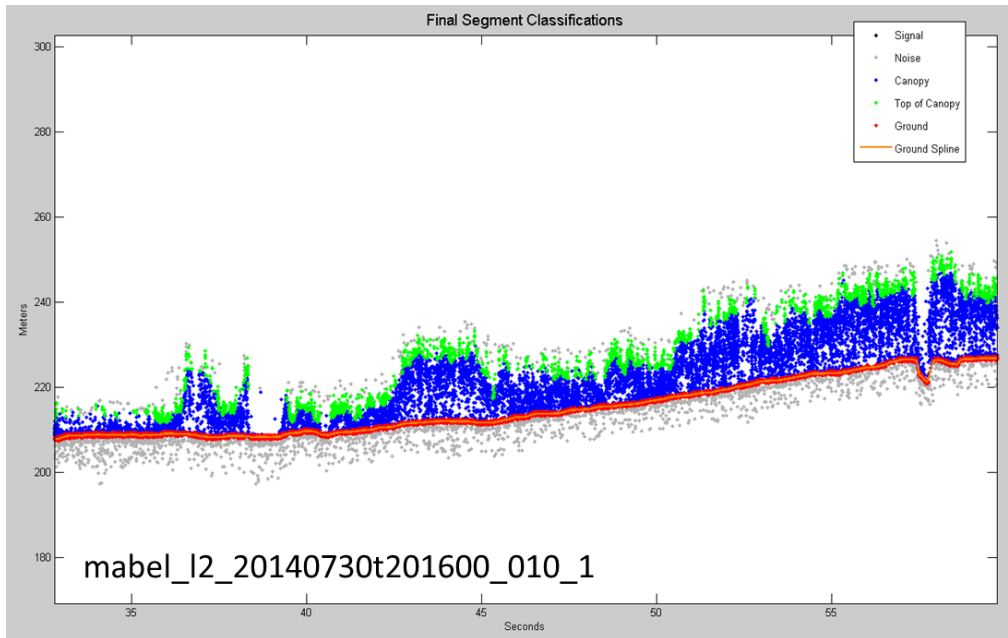
1586

1587 During the first round of ground surface refinement, where there are canopy
 1588 photons identified in the segment, the ground surface at that location is defined by
 1589 the smoothed ground surface (AgroundSmooth) value. Else, if there is a location
 1590 along-track where the standard deviation of the ground-only photons is greater than
 1591 the 75% quartile for all signal photon standard deviations (i.e., canopy level 3), then
 1592 the ground surface at that location is a weighted average between the interpolated
 1593 ground surface (Interp_Aground*1/3) and the smoothed interpolated ground surface
 1594 (AgroundSmooth*2/3). For all remaining locations long the segment, the ground
 1595 surface is the average of the interpolated ground surface (Interp_Aground) and the
 1596 heavily smoothed surface (ASmooth).

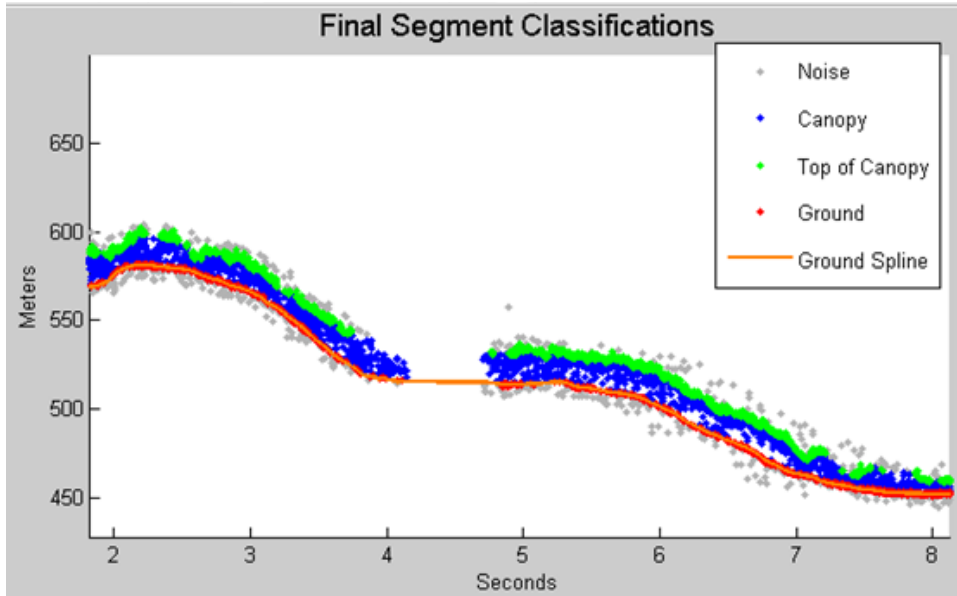
1597 The second round of ground surface refinement is simpler than the first.
 1598 Where there are canopy photons identified in the segment, the ground surface at that
 1599 location is defined by the smoothed ground surface (AgroundSmooth) value again.
 1600 For all other locations, the ground surface is defined by the interpolated ground
 1601 surface (Interp_Aground). This composite ground surface is run through the median
 1602 and smoothing filters again.

1603 The pseudocode for this surface refining process can be found in section 4.11.

1604 Examples of the ground and canopy photons for several MABEL lines are
1605 shown in Figures 3.10 – 3.12.



1606
1607 Figure 3.10. Example of classified photons from MABEL data collected in Alaska 2014.
1608 Red photons are photons classified as terrain. Green photons are classified as top of canopy.
1609 Canopy photons (shown as blue) are considered as photons lying between the terrain
1610 surface and top of canopy.



1611

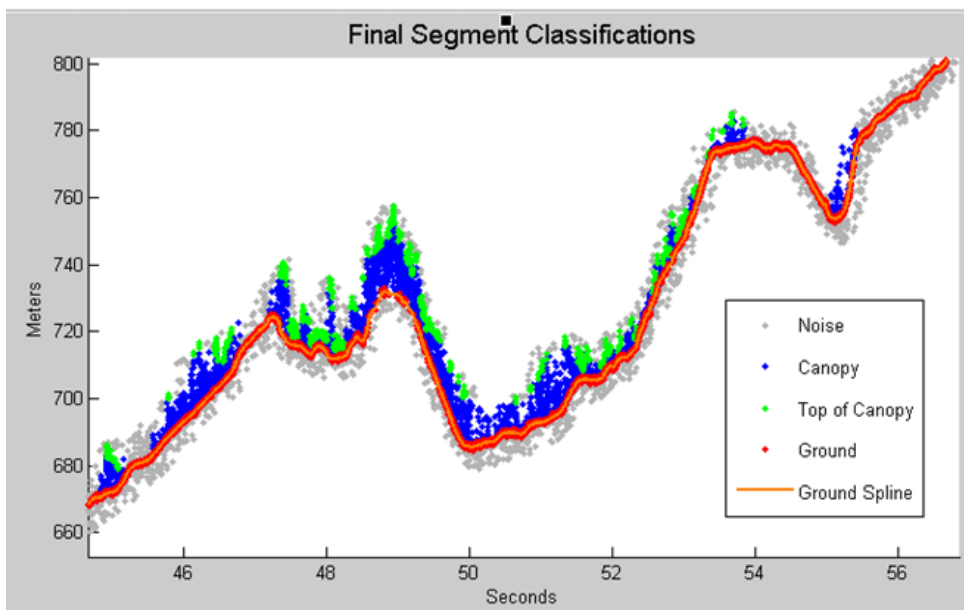
1612 Figure 3.11. Example of classified photons from MABEL data collected in Alaska 2014.

1613 Red photons are photons classified as terrain. Green photons are classified as top of canopy.

1614 Canopy photons (shown as blue) are considered as photons lying between the terrain

1615 surface and top of canopy.

1616



1617

1618 Figure 3.12. Example of classified photons from MABEL data collected in Alaska 2014.

1619 Red photons are photons classified as terrain. Green photons are classified as top of canopy.

1620 Canopy photons (shown as blue) are considered as photons lying between the terrain
1621 surface and top of canopy.

1622

1623 **3.6 Canopy Height Determination**

1624 Once a final ground surface is determined, canopy heights for individual
1625 photons are computed by removing the ground surface height for that photon's
1626 latitude/longitude. These relative canopy height values will be used to compute the
1627 canopy statistics on the ATL08 data product.

1628

1629 **3.7 Link Scale for Data products**

1630 The link scale for each segment within which values for vegetation parameters
1631 will be derived will be defined over a fixed distance of 100 m. A fixed segment length
1632 ensures that canopy and terrain metrics are consistent between segments, in addition
1633 to increased ease of use of the final products. A size of 100 m was selected as it should
1634 provide approximately 140 photons (a statistically sufficient number) from which to
1635 make the calculations for terrain and canopy height.

1636

1637 **4. ALGORITHM IMPLEMENTATION**

1638 Prior to running the surface finding algorithms used for ATL08 data products, the
1639 superset of output from the GSFC medium-high confidence classed photons (ATL03
1640 signal_conf_ph: flags 3-4) and the output from DRAGANN will be considered as the input
1641 data set. ATL03 input data requirements include the along-track time, latitude, longitude,
1642 height, and classification for each photon. The motivation behind combining the results
1643 from two different noise filtering methods is to ensure that all of the potential signal
1644 photons for land surfaces will be provided as input to the surface finding software.

1645 Some additional quality checks are also described here prior to implementing the
1646 ATL08 software. The first check utilizes the POD_PPD flag on ATL03. In instances where
1647 the satellite is maneuvering or the pointing/ranging solutions are suspect, ATL08 will not
1648 use those data. Thus, data will only flow to the ATL08 algorithm when the POD_PPD flag
1649 is set to 0 which indicates ‘nominal’ conditions.

1650 A second quality check pertains to the flags set on the ATL03 photon quality flag
1651 (quality_ph). Currently, ATL03 quality_ph flags are described as:

1652 0 = nominal conditions

1653 1 = possible after-pulse (this identifies the after pulses that occur between 2.3 and
1654 5 m below the surface)

1655 2 = possible late impulse response effect (this flag identifies additional detector
1656 effects 5 – 50 m below the surface).

1657 3 = possible TEP crossing.

1658 For this release of the software, we want to mention that there are cases of after-pulsing
1659 that occur 0.5 – 2.3 m below the surface that are considered nominal with the quality_ph
1660 flag. The output from the DRAGANN algorithm (i.e. the DRAGANN flag) will be set to a
1661 value of 0 when ATL03 quality_ph flags are greater than 0 such that they are ignored in
1662 the ATL08 algorithm.

1663

1664 A third quality check pertains to the signal photons (DRAGANN + ATL03 signal
 1665 confidence photons) and whether those heights are near the surface heights. To pass this
 1666 check, signal photons that lie 120 m above the reference DEM will be disregarded. Signal
 1667 photons lying below the reference DEM will be allowed to continue for additional ATL08
 1668 processing. The motivation for this quality check is to eliminate ICESat-2 photons that are
 1669 reflecting from clouds rather than the true surface.

1670 Table 4.1. Input parameters to ATL08 classification algorithm.

Name	Data Type	Long Name	Units	Description	Source
delta_time	DOUBLE	GPS elapsed time	seconds	Elapsed GPS seconds since start of the granule for a given photon. Use the metadata attribute granule_start_seconds to compute full gps time.	ATL03
lat_ph	FLOAT	latitude of photon	degrees	Latitude of each received photon. Computed from the ECEF Cartesian coordinates of the bounce point.	ATL03
lon_ph	FLOAT	longitude of photon	degrees	Longitude of each received photon. Computed from the ECEF Cartesian coordinates of the bounce point.	ATL03
h_ph	FLOAT	height of photon	meters	Height of each received photon, relative to the WGS-84 ellipsoid.	ATL03
sigma_h	FLOAT	height uncertainty	m	Estimated height uncertainty (1-sigma) for the reference photon.	ATL03
signal_conf_ph	UINT_1_LE	photon signal confidence	counts	Confidence level associated with each photon event selected as signal (0-noise, 1- added to allow for buffer but algorithm classifies as background, 2-low, 3-med, 4-high).	ATL03
segment_id	UNIT_32	along-track segment ID number	unitless	A seven-digit number uniquely identifying each along-track segment. These are sequential, starting with one for the first segment after an ascending equatorial crossing node.	ATL03

cab_prof	FLOAT	Calibrated Attenuated Backscatter	unitless	Calibrated Attenuated Backscatter from 20 to -1 km with vertical resolution of 30m	ATL09
dem_h	FLOAT	DEM Height	meters	Best available DEM (in priority of GIMP/ANTARCTIC/GMTED/MS S) value at the geolocation point. Height is in meters above the WGS84 Ellipsoid.	ATL09
Landsat tree cover	UINT_8	Landsat Tree Cover Continuous Fields	percentage	Percentage of woody vegetation greater than 5 meters in height across a 30 meter pixel	Global Land Cover Facility (Sexton, 2013)

1671

1672 Table 4.2. Additional external parameters referenced in ATL08 product.

Name	Data Type	Long Name	Units	Description	Source
atlas_pa				Off nadir pointing angle of the spacecraft	
ground_track				Ground track, as numbered from left to right: 1 = 1L, 2 = 1R, 3 = 2L, 4 = 2R, 5 = 3L, 6 = 3R	
dem_h				Reference DEM height	ANC06
ref_azimuth	FLOAT	azimuth	radians	Azimuth of the unit pointing vector for the reference photon in the local ENU frame in radians. The angle is measured from north and positive towards east.	ATL03
ref_elev	FLOAT	elevation	radians	Elevation of the unit pointing vector for the reference photon in the local ENU frame in radians. The angle is measured from east-north plane and positive towards up.	ATL03
rgt	INTEGER_2	reference ground track	unitless	The reference ground track (RGT) is the track on the Earth at which a specified unit vector within the observatory is pointed. Under nominal operating conditions, there will be no	ATL03

				data collected along the RGT, as the RGT is spanned by GT2L and GT2R. During slews or off-pointing, it is possible that ground tracks may intersect the RGT. The ICESat-2 mission has 1,387 RGTs.	
sigma_along	DOUBLE	along-track geolocation uncertainty	meters	Estimated Cartesian along-track uncertainty (1-sigma) for the reference photon.	ATL03
sigma_across	DOUBLE	across-track geolocation uncertainty	meters	Estimated Cartesian across-track uncertainty (1-sigma) for the reference photon.	ATL03
surf_type	INTEGER_1	surface type	unitless	Flags describing which surface types this interval is associated with. 0=not type, 1=is type. Order of array is land, ocean, sea ice, land ice, inland water.	ATL03, Section 4
layer_flag	Integer	Consolidated cloud flag	unitless	Flag indicating the presence of clouds or blowing snow with good confidence	ATL09
cloud_flag_asr	Integer(3)	Cloud probability from ASR	unitless	Cloud confidence flag, from 0 to 5, indicating low, med, or high confidence of clear or cloudy sky	ATL09
msw_flag	Byte(3)	Multiple scattering warning flag	unitless	Flag with values from 0 to 5 indicating presence of multiple scattering, which may be due to blowing snow or cloud/aerosol layers.	ATL09
asr	Float(3)	Apparent surface reflectance	unitless	Surface reflectance as modified by atmospheric transmission	ATL09
snow_ice	INTEGER_1	Snow Ice Flag	unitless	NOAA snow-ice flag. 0=ice free water; 1=snow free land; 2=snow; 3=ice	ATL09

1673

1674 **4.1 Cloud based filtering**

1675 It is possible for the presence of clouds to affect the number of surface photon
1676 returns through signal attenuation, or to cause false positive classifications of
1677 ground or canopy photons on low cloud returns. Either of these cases would reduce

1678 the accuracy of the ATL08 product. To improve the performance of the ATL08
1679 algorithm, ideally all clouds would be identified prior to processing through the
1680 ATL08 algorithm. There will be instances, however, where low lying clouds (e.g.
1681 <800 m above the ground surface) may be difficult to identify. Currently, ATL08
1682 provides an ATL09 derived cloud flag (layer_flag) on its 100 m product and
1683 encourages the user to make note of the presence of clouds when using ATL08
1684 output. Unfortunately at present, a review of on-orbit data from ATL03 and ATL09
1685 indicate that the cloud layer flag is not being set correctly in the ATL09 algorithm.
1686 Ultimately, the final cloud based filtering process used in the ATL08 algorithm will
1687 most likely be derived from parameters/flag on the ATL09 data product. Until the
1688 ATL09 cloud flags are proven reliable, however, a preliminary cloud screening
1689 method is presented below. This methodology utilizes the calibrated attenuated
1690 backscatter on the ATL09 data product to identify (and subsequently remove for
1691 processing) clouds or other problematic issues (i.e. incorrectly telemetered
1692 windows). Using this new method, telemetered windows identified as having either
1693 low or no surface signal due to the presence of clouds (likely above the telemetered
1694 band), as well as photon returns suspected to be clouds instead of surface returns,
1695 will be omitted from the ATL08 processing. This process, however, will not identify
1696 the extremely low clouds (i.e. <800 m). The steps are as follows:

- 1697 1. Match up the ATL09 calibrated attenuated backscatter (cab_prof) columns to
1698 the ATL03 granule being processed using segment ID.
- 1699 2. Flip the matching cab_prof vertical columns so that the elevation bins go
1700 from low to high.
- 1701 3. For each of the matching ATL09 cab_prof vertical columns, perform a cubic
1702 Savitsky-Golay smoothing filter with a span size of 15 vertical bins. Call this
1703 cab_smooth.
- 1704 4. Perform the same smoothing filter on each horizontal row of the cab_smooth
1705 output, this time using a span size of 7 horizontal bins. Call this
1706 cab_smoother.

- 1707 5. Create a low_signal logical array the length of the number of matching ATL09
1708 columns and set to false.
- 1709 6. For each column of cab_smoother:
- 1710 a. Set any values below 0 to 0.
- 1711 b. Set a logical array of cab_smoother bins that are below 15 km in
1712 elevation to true. Call this cab15.
- 1713 c. Using the ATL09 dem_h value for that column, find the ATL09
1714 cab_smoother bins that are 240 m above and 240 m below (~8 ATL09
1715 vertical bins each direction) the dem_h value. The bins found here that
1716 are also within cab15 are designated as sfc_bins.
- 1717 d. Find the maximum peak value of cab_smoother within the sfc_bins, if
1718 any. This will represent the surface peak.
- 1719 e. Find the maximum value of cab_smoother that is higher in elevation
1720 than the sfc_bins and within cab15, if any. This will represent the
1721 cloud peak.
- 1722 f. If there is no surface peak, set the low_signal flag to true.
- 1723 g. If there are both surface and cloud peak values returned, determine a
1724 surface peak / cloud peak ratio. If that ratio is less than or equal to 0.4,
1725 set low_signal flag for that column to true.
- 1726 7. After each matching ATL09 column of cab_smoother has been analyzed for
1727 low signal, assign the low_signal flag to an ATL03 photon resolution logical
1728 array by matching up the ATL03 photon segment_id values to the ATL09
1729 range of segment IDs for each ATL09 cab_prof column.
- 1730 8. For each ATL09 cab_prof column where the low_signal flag was not set, check
1731 for any ATL03 photons greater than 800 meters (TBD) in elevation away
1732 (higher or lower) from the ATL09 dem_h value. Assign an ATL03 photon
1733 resolution too_far_signal flag to true when this conditional is met.
- 1734 9. A logical array mask is created for any ATL03 photons that have either the
1735 low_signal flag or the too_far_signal flag set to true such that those photons
1736 will not be further processed by the ATL08 function.

1737

1738 **4.2 Preparing ATL03 data for input to ATL08 algorithm**

- 1739 1. At times, cloud attenuation will lead to a reduced L-km with a length that is
1740 not a multiple of 100 meters. If the last 100m land segment of the L-km
1741 segment contains fewer than 5 ATL03 20m geosegments and the current L-
1742 km segment is not the last one of the granule, do not report output for this
1743 last 100m land segment. Retain the starting geosegment of this land segment
1744 and begin the next L-km segment here.
- 1745 2. Break up data into *L-km* segments. Segments equivalent of 10 km in along-
1746 track distance of an orbit would be appropriate.
- 1747 a. If the last portion of an ATL03 granule being processed would result
1748 in an *L-km* segment with less than 3.4 km (170 geosegments) worth of
1749 data, that last portion is added to the previous *L-km* processing
1750 window to be processed together as one extended *L-km* processing
1751 segment.
- 1752 i. The resulting **last_seg_extend** value would be reported as a
1753 positive value of distance beyond 10 km that the ATL08
1754 processing segment was extended by.
- 1755 b. If the last *L-km* segment would be less than 10 km but greater than 3.4
1756 km, a portion extending from the start of current *L-km* processing
1757 segment backwards into the previous *L-km* processing segment would
1758 be added to the current ATL08 processing segment to make it 10 km
1759 in length. Only new 100 m ATL08 segment products generated from
1760 this backward extension would be reported.
- 1761 i. The distance of this backward data gathering would be
1762 reported in **last_seg_extend** as a negative distance value.
- 1763 c. All other segments that are not extended will report a last_seg_extend
1764 value of 0.

- 1765 3. Add a buffer of 200 m (or 10 segment_id's) to both ends of each L -km
 1766 segment. The total processing segment length is $(L\text{-km} + 2*\text{buffer})$, but will
 1767 be referred to as L -km segments for simplicity.
 1768 a. The first L -km segment from an ATL03 granule would only have a
 1769 buffer at the end, and the last L -km segment from an ATL03 granule
 1770 would only have a buffer at the beginning.
 1771 4. The input data for ATL08 algorithm is X, Y, Z, T (where T is time).

1772

1773 **4.3 Noise filtering via DRAGANN**

1774 DRAGANN will use ATL03 photons with all signal classification flags (0-4). These
 1775 will include both signal and noise photons. This section give a broad overview of the
 1776 DRAGANN function. See Appendix A for more details.

- 1777 1. Determine the relative along-track time, ATT, of each geolocated photon
 1778 from the beginning of each L -km segment.
 1779 2. Rescale the ATT with equal-time spacing between each data photon, keeping
 1780 the relative beginning and end time values the same.
 1781 3. Normalize the height and rescaled ATT data from 0 – 1 for each L -km
 1782 segment based on the min/max of each field. So, $\text{normtime} = (\text{time} -$
 1783 $\text{mintime})/(\text{maxtime} - \text{mintime})$.
 1784 4. Build a kd-tree based on normalized Z and normalized and rescaled ATT.
 1785 5. Determine the search radius starting with Equation 3.1. P =[determined by
 1786 preprocessor; see Sec 4.3.1], and $V_{\text{total}} = 1$. N_{total} is the number of photons
 1787 within the data L -km segment. Solve for V .
 1788 6. Now that you know V , determine the radius using Equation 3.2.
 1789 7. Compute the number of neighbors for each photon using this search radius.
 1790 8. Generate a histogram of the neighbor count distribution. As illustrated in
 1791 Figure 3.2, the noise peak is the first peak (usually with the highest
 1792 amplitude).
 1793 9. Determine the 10 highest peaks of the histogram.

1794 10. Fit Gaussians to the 10 highest peaks. For each peak,
1795 a. Compute the amplitude, a , which is located at peak position b .
1796 b. Determine the width, c , by stepping one bin at a time away from b and
1797 finding the last histogram value that is $> \frac{1}{2}$ the amplitude, a .
1798 c. Use the amplitude and width to fit a Gaussian to the peak of the
1799 histogram, as described in Equation 3.3.
1800 d. Subtract the Gaussian from the histogram, and move on to calculate
1801 the next highest peak's Gaussian.
1802 e. Reject Gaussians that are too near (< 2 standard deviations) and
1803 amplitude too low ($< 1/5$ previous amplitude) from the previous
1804 signal Gaussian.

1805 11. Reject any of the returned Gaussians with imaginary components.

1806 12. Determine if there is a narrow noise Gaussian at the beginning of the
1807 histogram. These typically occur when there is little noise, such as during
1808 nighttime passes.

1809 a. Search for the Gaussian with the highest amplitude, a , in the first 5%
1810 of the histogram
1811 b. Check if the highest amplitude is $\geq 1/10$ of the maximum of all
1812 Gaussian amplitudes
1813 c. Check if the width, c , of the Gaussian with the highest amplitude is \leq
1814 4 bins
1815 d. If these three conditions are met, save the $[a,b,c]$ values as $[a_0,b_0,c_0]$.
1816 e. If the three conditions are not met, search again within the first 10%.
1817 Repeat the process, incrementing the percentage of histogram
1818 searched by 5% up to 30%. As soon as the conditions are met, save
1819 the $[a_0,b_0,c_0]$ values and break out of the percentage histogram search
1820 loop.

1821 13. If a narrow noise peak was found, sort the remaining Gaussians from largest
1822 to smallest area, estimated by $a*c$, then append $[a_0,b_0,c_0]$ to the beginning of
1823 the sorted $[a,b,c]$ arrays. If a narrow noise peak was not found, sort all
1824 Gaussians by largest to smallest area.

- 1825 a. If a narrow noise peak was not found, check in sorted order if one of
1826 the Gaussians are in the first 10% of the histogram. If so, it becomes
1827 the first Gaussian.
- 1828 b. Reject any Gaussians that are fully contained within another.
- 1829 c. Reject Gaussians whose centers are within 3 standard deviations of
1830 another, unless only two Gaussians remain
- 1831 14. If there are two or more Gaussians remaining, they are referred to as
1832 Gaussian 1 and Gaussian 2, assumed to be the noise and signal Gaussians.
- 1833 15. Determine the threshold value that will define the cutoff between noise and
1834 signal.
- 1835 a. If the absolute difference of the two Gaussians becomes near zero,
1836 defined as $< 1e-8$, set the first bin index where that occurs, past the
1837 first Gaussian peak location, as the threshold. This would typically be
1838 set if the two Gaussians are far away from each other.
- 1839 b. Else, the threshold value is the intersection of the two Gaussians,
1840 which can be estimated as the first bin index past the first Gaussian
1841 peak location where there is a minimum absolute difference between
1842 the two Gaussians.
- 1843 c. If there is only one Gaussian, it is assumed to be the noise Gaussian,
1844 and the threshold is set to $b + c$.
- 1845 16. Label all photons having a neighbor count above the threshold as signal.
- 1846 17. Label all photons having a neighbor count below the threshold as noise.
- 1847 18. Reject noise photons.
- 1848 19. Retain signal photons for feeding into next step of processing.
- 1849 20. Use Logical OR to combine DRAGANN signal photons with ATL03 medium-
1850 high confidence signal photons (flags 3-4) as ATL08 signal photons.
- 1851 21. Calculate a signal to noise ratio (SNR) for the L - km segment by dividing the
1852 number of ATL08 signal photons by the number of noise (i.e., all – signal)
1853 photons.

1854 **4.3.1 DRAGANN Quality Assurance**

1855 Based upon on-orbit data, there are instances where only noise photons are selected
1856 as signal photons following running through DRAGANN. These instances usually
1857 occur to telemetered windows with low signal, signal attenuation near the surface
1858 due to fog, haze (or other atmospheric properties). If any d_flag results in the 10 km
1859 = 1

- 1860 1. For each 20 m segment_id that has a d_flag = 1, build a histogram of 5 m
1861 height bins using the height of only the DRAGANN-flagged photons
1862 (d_flag=1)
- 1863 2. If the number of bins indicates that all d_flag photons fall within the same
1864 vertical 60 m, do nothing and move to the next geosegment.
- 1865 3. If the d_flag photons fall outside of 60 m, calculate the median and
1866 standard deviation of the histogram counts.
- 1867 4. If the maximum value of the histogram counts is greater than the median
1868 + 3*standard deviation, a surface peak has been detected based on the
1869 relative photon density within the 5 meter steps. Else, set all d_flag = 0
1870 for this geosegment.
- 1871 5. Set all d_flag = 0 from 3 height bins below the detected peak to the bottom
1872 of the telemetry window.
- 1873 6. Starting with the peak count bin (surface), step upwards bin by bin and
1874 check if 12 bin counts (60 meters of height bins) above surface are less
1875 than 0.5 * histogram median. If so, for all photons above current height in
1876 loop + 60 meters, set all d_flag = 0 and exit bin-by-bin loop.
- 1877 7. Starting with one bin above the peak count bin (surface), again step
1878 upwards bin by bin. For each iteration, calculate the standard deviation of
1879 the bin counts including only the current bin to the highest height bin and
1880 call this noise standard deviation. If all remaining vertical height bins
1881 from current bin to highest height bin are less than 2* histogram
1882 standard deviation, or if the noise standard deviation is less than 1.0, or if
1883 this bin and the next 2 higher bins each have counts less than the peak bin

1884 count (entire histogram) – 3*histogram standard deviation, then set all
1885 $d_flag = 0$ for all heights above this level.
1886 8. For a final check, construct a new histogram, with median and standard
1887 deviation, using the corrected d_flag results and only where $d_flag = 1$. If
1888 the histogram median is greater than 0.0 and the standard deviation is
1889 greater than $0.75*median$, set all d_flag in this geosegment = 0. This
1890 indicates results not well constrained about a detectible surface.
1891

1892 **4.3.2 Preprocessing to dynamically determine a DRAGANN parameter**

1893 While a default value of $P=20$ was found to work well when testing with MABEL
1894 flight data, further testing with simulated data showed that $P=20$ is not sufficient in
1895 cases of very low or very high noise. Additional testing with real ATL03 data have
1896 shown the ground signal to be much stronger, and the canopy signal to be much
1897 weaker, than originally anticipated. Therefore, a preprocessing step for dynamically
1898 calculating P and running the core DRAGANN function is described in this
1899 subsection. This assumes L -km to be 10 km (with additional L -km buffering).

- 1900 1. Define a DRAGANN processing window of 170 segments (~ 3.4 km),
1901 and a buffer of 10 segments (~ 200 m).
- 1902 2. The buffer is applied to both sides of each DRAGANN processing
1903 window to create buffered DRAGANN processing windows
1904 (referenced as “buffered window” for the rest of this section) that will
1905 overlap the DRAGANN processing windows next to them.
- 1906 3. For each buffered window within the L -km segment, calculate a
1907 histogram of points with 1 m elevation bins.
- 1908 4. For each buffered window histogram, calculate the median counts.
- 1909 5. Bins with counts below the buffered window median count value are
1910 estimated to be noise. Calculate the mean count of noise bins.
- 1911 6. Bins with counts above the buffered window median count value are
1912 estimated to be signal. Calculate the mean count of signal bins.
- 1913 7. Determine the time elapsed over the buffered window.

- 1914 8. Calculate estimated noise and signal rates for each buffered window
 1915 by multiplying each window's mean counts of noise bins and signal
 1916 bins, determined from steps 5 and 6 above, by 1/(elapsed time) to
 1917 return the rates in terms of points/meter[elevation]/second[across].
- 1918 9. Calculate a noise ratio for each window by dividing the noise rate by
 1919 the signal rate.
- 1920 10. If, for all the buffered windows in the L -km segment, the noise rate is
 1921 less than 20 and the noise ratio is less than 0.15; OR any noise rate is
 1922 0; OR any signal rate is greater than 1000: re-calculate steps 3-9
 1923 using the entire L -km segment. Continue with the following steps
 1924 using results from the one L -km window (instead of multiple buffered
 1925 windows).
- 1926 11. Now, determine the DRAGANN parameter, P , for each buffered
 1927 window based on the following conditionals:
- 1928 a. If the signal rate is NaN (i.e., an invalid value), set the signal
 1929 index array to empty and move on to the next buffered
 1930 window.
- 1931 b. If noise rate < 20 || noise ratio < 0.15:
 1932 $P = \text{signal rate}$
 1933 If signal rate is < 5, $P = 5$; if signal rate > 20, $P = 20$
- 1934 c. Else $P = 20$.
- 1935 12. Run DRAGANN on the buffered window points using the calculated P .
- 1936 13. If DRAGANN fails to find a signal (i.e., only one Gaussian found), run
 1937 DRAGANN again with $P = 10$.
- 1938 14. If DRAGANN still fails to find a signal, try to determine P a second time
 1939 using the following conditionals:
- 1940 a. If (noise rate ≥ 20) ...
 1941 && (signal rate > 100) ...
 1942 && (signal rate < 250),
 1943 $P = (\text{signal rate})/2$

```

1944         b. Else if signal rate >= 250,
1945             if noise rate >= 250,
1946                 P = (noise rate)*1.1
1947             else,
1948                 P = 250
1949         c. Else, P = mean(noise rate, signal rate)
1950 15. Run DRAGANN on the buffered window points using the newly
1951     calculated P.
1952     a. If still no signal points are found, set a dragannError flag.
1953 16. If signal points were found by DRAGANN, for each buffered window
1954     calculate a signal check by dividing the number of signal points found
1955     via DRAGANN by the number of total points in the buffered window.
1956 17. If dragannError has been set, or there are suspect signal statistics, the
1957     following snippet of pseudocode will check those conditionals and try
1958     to iteratively find a better P value to run DRAGANN with:
1959
1960     try_count = 0
1961
1962     While dragannError ...
1963     || ( (noise rate >= 30) ...
1964         && (signal check > noise ratio) ...
1965         && (noise ratio >= 0.15) ) ...
1966     || (signal check < 0.001):
1967
1968         if P < 3,
1969             break
1970         else,
1971             P = P*0.75
1972         end
1973
1974     if try_count < 2
1975         Clear out signal index results from previous DRAGANN run
1976         Re-run DRAGANN with new P value
1977         Recalculate the signal check
1978     end
1979
1980     if no signal index results are returned
1981         P = P*0.75
1982     end
1983

```

1984 try_count = try_count + 1

1985

1986 end

1987

1988

18. If no signal photons are found by DRAGANN because only one

1989

Gaussian was found, set the threshold as $b+c$ (i.e., one standard

1990

deviation away from the Gaussian peak location) for a final DRAGANN

1991

run. Otherwise, set the signal index array to empty and move on to the

1992

next buffered window.

1993

19. Assign the signal values found from DRAGANN for each buffered

1994

window to the original DRAGANN processing window range of points.

1995

20. Combine signal points from each DRAGANN processing window back

1996

into one $L-km$ array of signal points for further processing.

1997

1998 **4.3.3 Iterative DRAGANN processing**

1999

It is possible in processing segments with high noise rates that DRAGANN will

2000

incorrectly identify clusters of noise as signal. One way to reduce these false positive

2001

noise clusters is to run the alternative DRAGANN process (Sec 4.3.1) again with the

2002

input being the signal output photons from the first run through alternative

2003

DRAGANN. Note that this methodology is still being tested, so by default this option

2004

should not be set.

2005

1. If $SNR < 1$ (TBD) from alternative DRAGANN run, run alternative DRAGANN

2006

process again using the output signal photons from first DRAGANN run as the

2007

input to the second DRAGANN run.

2008

2. Recalculate SNR based on output of second DRAGANN run.

2009

2010 **4.4 Is Canopy Present**

- 2011 1. If L -km segment is within an ATL08 region encompassing Antarctica (regions
2012 7, 8, 9, 10) or Greenland (region 11), assume no canopy is present: canopy
2013 flag = 0. Else:
- 2014 2. Determine the center Latitude/Longitude position for the L -km segment.
- 2015 3. Determine the corresponding tile from the Landsat continuous cover
2016 product.
- 2017 4. For each unique XY position in the ATLAS segment, extract the canopy cover
2018 value from the Landsat CC product
- 2019 5. Compute the average canopy cover value for the L -km segment (based on the
2020 Landsat values).
- 2021 6. If canopy cover > 3%, set canopy flag = 1 (assumes canopy is present)
- 2022 7. If canopy cover <= 3%, set canopy flag = 0 (assumes no canopy is present)

2023

2024 **4.5 Compute Filtering Window**

- 2025 1. Next step is to run a surface filter with a variable window size (variable in
2026 that it will change from L -km segment to L -km segment). The window-size is
2027 denoted as Window.
- 2028 2. $Window = \text{ceil}[5 + 46 * (1 - e^{-a*length})]$, where $length$ is the number of
2029 photons in the segment.
- 2030 3. $a = \frac{\log\left(1 - \frac{21}{51-5}\right)}{-28114} \approx 21 \times 10^{-6}$, where a is the shape parameter for the window
2031 span.

2032

2033 **4.6 De-trend Data**

- 2034 1. The input data are the signal photons identified by DRAGANN and the ATL03
2035 classification (signal_conf_ph) values of 3-4.
- 2036 2. Generate a rough surface by connecting all unique (time) photons to each
2037 other. Let's call this surface interp_A.

- 2038 3. Run a median filter through interp_A using the window size set by the
2039 software. Output = Asmooth.
- 2040 4. Define a reference DEM limit (ref_dem_limit) as 120 m (TBD).
- 2041 5. Remove any Asmooth values further than the ref_dem_limit threshold from
2042 the reference DEM, and interpolate the Asmooth surface based on the
2043 remaining Asmooth values. The interpolation method to use is the shape
2044 preserving piecewise cubic Hermite interpolating polynomial – hereafter
2045 labeled as “pchip” (Fritsch & Carlson, 1980).
- 2046 6. Compute the approximate relief of the *L-km* segment using the 95th - 5th
2047 percentile heights of the signal photons. We are going to filter Asmooth again
2048 and the smoothing is a function of the relief.
- 2049 7. Define the SmoothSize using the conditional statements below. The
2050 SmoothSize will be used to detrend the data as well as to create an
2051 interpolated ground surface later.

2052 SmoothSize = 2 * Window

- 2053 • If relief >= 900, SmoothSize = round(SmoothSize/4)
 - 2054 • If relief >= 400 && <= 900, SmoothSize = round(SmoothSize/3)
 - 2055 • If relief >= 200 && <= 400, SmoothSize = round(SmoothSize/2)
- 2056 8. Greatly smooth Asmooth by first running Asmooth 10 times through a
2057 median filter then a smoothing filter with a moving average method on the
2058 result. Both the median filter and the smoothing filter use a window size of
2059 SmoothSize.

2060

2061 **4.7 Filter outlier noise from signal**

- 2062 1. If there are any signal data that are 150 meters above Asmooth, remove them
2063 from the signal data set.

- 2064 2. If the standard deviation of the detrended signal is greater than 10 meters,
2065 remove any signal value from the signal data set that is 2 times the standard
2066 deviation of the detrended signal below Asmooth.
- 2067 3. Calculate a new Asmooth surface by interpolating (pchip method) a surface
2068 from the remaining signal photons and median filtering using the Window
2069 size, then median filter and smooth (moving average method) 10 times again
2070 using the SmoothSize.
- 2071 4. Detrend the signal photons by subtracting the signal height values from the
2072 Asmooth surface height values. Use the detrended heights for surface finding.

2073

2074 **4.8 Finding the initial ground estimate**

- 2075 1. At this point, the initial signal photons have been noise filtered and de-
2076 trended and should have the following format: X, Y, detrended Z, T (T=time).
2077 From this, the input data into the ground finding will be the ATD (along track
2078 distance) metric (such as time) and the detrended Z height values.
- 2079 2. Define a medianSpan as $\text{Window} * 2/3$.
- 2080 3. Calculate the background neighbor density of the subsurface photons using
2081 ALL available photons (the non-detrended data). This step is run on all
2082 photons including noise photons. Histogram the photons in 0.5 m vertical
2083 bins and a 60 m horizontal bin.
- 2084 4. To avoid including zero population bins in the histogram signal tracking
2085 process, identify the bin with the maximum bin count among bins 3 - 7
2086 (starting at the lowest height) across each 60 m within the 10-km processing
2087 window.
- 2088 5. Calculate the mean of those maximum bin values to represent the noise count
2089 for the 10-km window.
- 2090 6. The following steps are run on the detrended signal photons.

2091 7. Calculate the brightness of the surface for each 60 m to be histogrammed via
2092 the calculation in Section 2.4.21. If a bright surface is detected, skip steps 8
2093 and 9

2094 8. Determine the lowest 0.5 m histogram height bin for each 60 m along track,
2095 in the detrended heights where:

2096 a. The neighbor density is 10 x greater than the background density and
2097 b. The neighbor density is greater than the histogram population median
2098 plus 1/3 of the population standard deviation.

2099 9. The photons with detrended heights above this bin are masked from
2100 consideration in the initial ground height estimate. Detrended signal photons
2101 implies that the d_flag photons.

2102 10. Identifying the ground surface is an iterative process. Start by assuming that
2103 all the input signal height photons are the ground. The first goal is the cut
2104 out the lower height excess photons in order to find a lower bound for
2105 potential ground photons. This process is done 5 times and an offset of 4
2106 meters is subtracted from the resulting lower bound. The smoothing filter
2107 uses a moving average again:

2108 for j=1:5
2109 cutOff = median filter (ground, medianSpan)
2110 cutOff = smooth filter (cutOff, Window)
2111 ground = ground((cutOff - ground) > -1)
2112 end
2113 lowerbound = median filter (ground, medianSpan*3)
2114 middlebound = smooth filter (lowerbound, Window)
2115 lowerbound = smooth filter (lowerbound, Window) - 4
2116 end;

2117 11. Create a linearly interpolated surface along the lower bound points and only
2118 keep input photons above that line as potential ground points:

2119 top = input(input > interp(lowerbound))

2120 12. The next goal is to cut out excess higher elevation photons in order to find an
2121 upper bound to the ground photons. This process is done 3 times and an
2122 offset of 1 meter is added to the resulting upper bound. The smoothing filter
2123 uses a moving average:

```
2124     for j = 1:3  
2125         cutOff = median filter (top, medianSpan)  
2126         cutOff = smooth filter (cutOff, Window)  
2127         top = top( (cutOff - top) > -1 )  
2128     end  
2129     upperbound = median filter (top, medianSpan)  
2130     upperbound = smooth filter (upperbound, Window) + 1
```

2131 13. Create a linearly interpolated surface along the upper bound points and
2132 extract the points between the upper and lower bounds as potential ground
2133 points:

```
2134     ground = input( ( input > interp(lowerbound) ) & ...  
2135                   ( input < interp(upperbound) ) )
```

2136 14. Refine the extracted ground points to cut out more canopy, again using the
2137 moving average smoothing:

```
2138     For j = 1:2  
2139         cutOff = median filter (ground, medianSpan)  
2140         cutOff = smooth filter (cutOff, Window)  
2141         ground = ground( (cutOff - ground) > -1 )  
2142     end
```

2143 15. Run the ground output once more through a median filter using window side
2144 medianSpan and a smoothing filter using window size Window, but this time
2145 with the Savitzky-Golay method.

2146 16. Finally, linearly interpolate a surface from the ground points.

- 2147 17. The first estimate of canopy points are those indices of points that are
2148 between 2 and 150 meters above the estimated ground surface. Save these
2149 indices for the next section on finding the top of canopy.
- 2150 18. The output from the final iteration of ground points is temp_interpA – an
2151 interpolated ground estimate.
- 2152 19. Find ground indices that lie within 10 m below and 0.5 m above of
2153 temp_interpA only when the canopy_flag indicates canopy should be present.
2154 Otherwise, (i.e. no canopy) use a threshold of 0.5 m around temp_interpA.
- 2155 20. Apply the ground indices to the original heights (i.e., not the de-trended data)
2156 to label ground photons.
- 2157 21. Interpolate a ground surface using the pchip method based on the ground
2158 photons. Output is interp_Aground.

2159

2160 **4.9 Find the top of the canopy (if canopy_flag = 1)**

- 2161 1. The input are the ATD metric (i.e., time), and the de-trended Z values indexed
2162 by the canopy indices extracted from step 4.8(17).
- 2163 2. Flip this data over so that we can find a canopy “surface” by multiplying the
2164 de-trended canopy heights by -1.0 and adding the mean(heights).
- 2165 3. Finding the top of canopy is also an iterative process. Follow the same steps
2166 described in 4.8(2) – 4.8(16), but use the canopy indexed and flipped Z
2167 values in place of the ground input.
- 2168 4. Final retained photons are considered top of canopy photons. Use the indices
2169 of these photons to define top of canopy photons in the original (not de-
2170 trended) Z values.
- 2171 5. Build a kd-tree on canopy indices.
- 2172 6. If there are less than three canopy indices within a 100m radius, reassign
2173 these photons to noise photons. Initially, a value of 15 m was used for the
2174 search radius. In Release 004 of the algorithm, this value was increased to

2175 100 m to include more top of canopy photons that were not captured in the
2176 initial canopy spline estimate.

2177

2178 **4.10 Compute statistics on de-trended data**

- 2179 1. The input data have been noise filtered and de-trended and should have the
2180 following input format: X, Y, detrended Z, T.
- 2181 2. The input data will contain signal photons as well as a few noise photons
2182 near the surface.
- 2183 3. Compute statistics of heights in the along-track direction using a sliding
2184 window. Using the window size (window), compute height statistics for all
2185 photons that fall within each window. These include max height, median
2186 height, mean height, min height, and standard deviation of all photon heights.
2187 Additionally, in each window compute the median height and standard
2188 deviation of just the initially classified top of canopy photons, and the
2189 standard deviation of just the initially classified ground photon heights.
2190 Currently only the median top of canopy, and all STD variables are being
2191 utilized, but it's possible that other statistics may be incorporated as
2192 changes/improvements are made to the code.
- 2193 4. Slide the window $\frac{1}{4}$ of the window span and recompute statistics along the
2194 entire *L-km* segment. This results in one value for each statistic for each
2195 window.
- 2196 5. Determine canopy index categories for each window based upon the total
2197 distribution of STD values for all signal photons along the *L-km* segment
2198 based on STD quartiles.
- 2199 6. Open canopy have STD values falling within the 1st quartile.
- 2200 7. Canopy Level 1 has STD values falling from 1st quartile to median STD value.
- 2201 8. Canopy Level 2 has STD values falling from median STD value to 3rd quartile.
- 2202 9. Canopy Level 3 has STD values falling from 3rd quartile to max STD.

2203 10. Linearly interpolate the window STD values (both for all photons and
2204 ground-only photons) back to the native along-track resolution and calculate
2205 the interpolated all-photon STD quartiles to create an interpolated canopy
2206 level index. This will be used later for interpolating a ground surface.
2207

2208 **4.11 Refine Ground Estimates**

2209 1. Smooth the interpolated ground surface 10 times. All further ground surface
2210 smoothing use the moving average method:

2211 For j= 1:10

2212 AgroundSmooth = median filter (interp_Aground, SmoothSize*5)

2213 AgroundSmooth = smooth filter (AgroundSmooth, SmoothSize)

2214 End

2215

2216 2. This output (AgroundSmooth) from the filtering/smoothing function is an
2217 intermediate ground solution and it will be used to estimate the final
2218 solution.

2219 3. If there are **no canopy indices** identified along the entire segment (OR
2220 canopy_flag = 0) AND relief >400 m

2221 FINALGROUND = median filter (Asmooth, SmoothSize)

2222 FINALGROUND = smooth filter (FINALGROUND, SmoothSize)

2223 Else

2224 FINALGROUND = AgroundSmooth

2225 end

2226 4. If there are **canopy indices** identified along the segment:

2227 If there is a canopy photon identified at a location along-track above the
2228 ground surface, then at that location along-track

2229 FINALGROUND = AgroundSmooth

```

2230     else if there is a location along-track where the interpolated ground STD has
2231     an interpolated canopy level >= 3
2232         FINALGROUND = Interp_Aground*1/3 + AgroundSmooth*2/3
2233     else
2234         FINALGROUND = Interp_Aground*1/2 + Asmooth*1/2
2235     end
2236 5. Smooth the resulting interpolated ground surface (FINALGROUND) once
2237     using a median filter with window size of 9 then a smoothing filter twice with
2238     window size of 9. Select ground photons that lie within the point spread
2239     function (PSF) of FINALGROUND.
2240 6. PSF is determined by sigma_atlas_land (Eq. 1.2) calculated at the photon
2241     resolution and thresholded between 0.5 to 1 m.
2242     a. Estimate the terrain slope by taking the gradient of FINALGROUND.
2243         Gradient is reported at the center of ((finalground(n+1)-
2244         finalground(n-1))/(dist_x(n+1)-dist_x(n-1)))/2
2245     b. Linearly interpolate the sigma_h values to the photon resolution.
2246     c. Calculate sigma_topo (Eq. 1.3) at the photon resolution.
2247     d. Calculate sigma_atlas_land at the photon resolution using the sigma_h
2248         and sigma_topo values at the photon resolution.
2249     e. Set PSF equal to sigma_atlas_land.
2250         i. Any PSF < 0.5 m is set to 0.5 m as the minimum PSF.
2251         ii. Any PSF > 1 m is set to 1 m as the maximum PSF. Set psf_flag to
2252             true.
2253

```

2254 **4.12 Canopy Photon Filtering**

- 2255 1. The first canopy filter will remove photons classified as top of canopy that
2256 are significantly above a smoothed median top of canopy surface. To
2257 calculate the smoothed median top of canopy surface:
- 2258 a. Linearly interpolate the median and standard deviation canopy
2259 window statistics, calculated from 4.10 (3), to the top of canopy
2260 photon resolution. Output variables: interpMedianC, interpStdC.
 - 2261 b. Calculate a canopy window size using Eq. 3.4, where *length* = number
2262 of top of canopy photons. Output variable: winC.
 - 2263 c. Create the median filtered and smoothed top of canopy surface,
2264 smoothedC, using a locally weighted linear regression smoothing
2265 method, “lowess” (Cleveland, 1979):

```
2266         smoothedC = median filter ( interpMedianC, winC )  
2267  
2268         if SNR > 1, canopySmoothSpan = winC*2;  
2269         else, canopySmoothSpan = smoothSpan;  
2270  
2271         smoothedC = smooth filter ( smoothedC, canopySmoothSpan )  
2272  
2273         d. Add the detrended heights back into the smoothedC surface:
```

```
2273         smoothedC = smoothedC + Asmooth
```

- 2274 2. Set canopy height thresholds based on the interpolated top of canopy STD:

```
2275         If SNR > 1, canopySTDthresh = 3; else, canopySTDthresh = 2;
```

```
2276         canopy_height_thresh = canopySTDthresh*interpStdC
```

```
2277         high_cStd = canopy_height_thresh > 10
```

```
2278         low_cStd = canopy_height_thresh < 3
```

```
2279         canopy_height_thresh(high_cStd) =
```

```
2280         canopy_height_thresh(high_cStd)/2
```

2281 canopy_height_thresh(low_cStd) = 3

2282 3. Relabel as noise any top of canopy photons that are higher than smoothedC +
2283 canopy_height_thresh.

2284 4. Next, interpolate a top of canopy surface using the remaining top of canopy
2285 photons (here we are trying to create an upper bound on canopy points). The
2286 interpolation method used is pchip. This output is named interp_Acanopy.

2287 5. Photons falling below interp_Acanopy and above FINALGROUND+PSF are
2288 labeled as canopy points.

2289 6. For 500 signal photon segments, if number of all canopy photons (i.e., canopy
2290 and top of canopy) is:
2291 < 5% of the total (when SNR > 1), OR
2292 < 10% of the total (when SNR <= 1),
2293 relabel the canopy photons as noise.

2294 7. Interpolate, using the pchip method, a new top of canopy surface from the
2295 filtered top of canopy photons. This output is again named interp_Acanopy.

2296 8. Again, label photons that lie between interp_Acanopy and
2297 FINALGROUND+PSF as canopy photons.

2298 9. Since the canopy points have been relabeled, we need to do a final
2299 refinement of the ground surface:

2300 If canopy is present at any location along-track

2301 FINALGROUND = AgroundSmooth (at that location)

2302 Else if canopy is not present at a location along-track

2303 FINALGROUND = interp_Aground

2304 Smooth the resulting interpolated ground surface (FINALGROUND) once
2305 using a median filter with window size of SmoothSize (SmoothSize = 9), then
2306 a moving average smoothing filter twice with window size of SmoothSize
2307 (SmoothSize = 9)

- 2308 10. Relabel ground photons based on this new (and last) FINALGROUND solution
2309 +/- a recalculated PSF (via steps in 4.11 (6)). Points falling below the buffer
2310 are labeled as noise.
- 2311 11. Using Interp_Acanopy and this last FINALGROUND solution + PSF buffer,
2312 label all photons that lie between the two as canopy photons.
- 2313 12. Repeat the canopy cover filtering: For 500 signal photon segments, if
2314 number of all canopy photons (i.e., canopy and top of canopy) is:
2315 < 5% of the total (when SNR > 1), OR
2316 < 10% of the total (when SNR <= 1),
2317 relabel the canopy photons as noise. This is the last canopy labeling step.

2318

2319 **4.13 Compute individual Canopy Heights**

- 2320 1. At this point, each photon will have its final label assigned in
2321 **classed_pc_flag**: 0 = noise, 1 = ground, 2 = canopy, 3 = top of canopy.
- 2322 2. For each individual photon labeled as canopy or top of canopy, subtract the Z
2323 height value from the interpolated terrain surface, FINALGROUND, at that
2324 particular position in the along-track direction.
- 2325 3. The relative height for each individual canopy or top of canopy photon will
2326 be used to calculate canopy products described in Section 4.16. Additional
2327 canopy products will be calculated using the absolute heights, as described in
2328 Section 4.16.1.

2329

2330 **4.14 Final photon classification QA check**

- 2331 1. Find any ground, canopy, or top of canopy photons that have elevations
2332 further than the ref_dem_limit from the reference DEM elevation value.
2333 Convert these to the noise classification.
- 2334 2. Find any relative heights of canopy or top of canopy photons that are greater
2335 than 150 m above the interpolated ground surface, FINALGROUND. Convert
2336 these to the noise classification.

- 2337 3. Find any FINALGROUND elevations that are further than the ref_dem_limit
2338 from the reference DEM elevation value. Convert those FINALGROUND
2339 elevations to an invalid value, and convert any classified photons at the same
2340 indices to noise.
- 2341 4. If more than 50% of photons are removed in a segment, set ph_removal_flag
2342 to true.

2343

2344 **4.15 Compute segment parameters for the Land Products**

- 2345 1. For each 100 m segment, determine the classed photons (photons classified
2346 as ground, canopy, or top of canopy).
- 2347 a. If there are fewer than 50 classed photons in a 100 m segment, do not
2348 calculate land or canopy products.
- 2349 b. If there are 50 or more classed photons in a 100 m segment, extract
2350 the ground photons to create the land products.
- 2351 2. If the number of ground photons > 5% of the total number of classed photons
2352 within the segment (this control value of 5% can be modified once on orbit):
- 2353 a. Compute statistics on the ground photons: mean, median, min, max,
2354 standard deviation, mode, and skew. These heights will be reported
2355 on the product as **h_te_mean**, **h_te_median**, **h_te_min**, **h_te_max**,
2356 **h_te_mode**, and **h_te_skew** respectively described in Table 2.1.
- 2357 b. Compute the standard deviation of the ground photons about the
2358 interpolated terrain surface, FINALGROUND. This value is reported as
2359 **h_te_std** in Table 2.1.
- 2360 c. Compute the residuals of the ground photon Z heights about the
2361 interpolated terrain surface, FINALGROUND. The product is the root
2362 sum of squares of the ground photon residuals combined with the
2363 **sigma_atlas_land** term in Table 2.5 as described in Equation 1.4. This
2364 parameter reported as **h_te_uncertainty** in Table 2.1.
- 2365 d. Compute a linear fit on the ground photons and report the slope. This
2366 parameter is **terrain_slope** in Table 2.1.

2367 e. Calculate a best fit terrain elevation at the mid-point location of the
2368 100 m segment:

2369 i. Calculate each terrain photon's distance along-track into the
2370 100 m segment using the corresponding ATL03 20 m products
2371 segment_length and dist_ph_along, and determine the mid-
2372 segment distance (expected to be 50 m ± 0.5 m).

2373 1. Use the mid-segment distance to linearly interpolate a
2374 mid-segment time (**delta_time** in Table 2.4). Use the
2375 mid-segment time to linearly interpolate other mid-
2376 segment parameters: interpolated terrain surface,
2377 FINALGROUND, as **h_te_interp** (Table 2.1); **latitude**
2378 and **longitude** (Table 2.4).

2379 ii. Calculate a linear fit, as well as 3rd and 4th order polynomial fits
2380 to the terrain photons in the segment.

2381 iii. Create a slope-adjusted and weighted mid-segment variable,
2382 weightedZ, from the linear fit: Use terrain_slope to apply a
2383 slope correction to each terrain photon by subtracting the
2384 terrain photon heights from the linear fit. Determine the mid-
2385 segment location of the linear fit, and add that height to the
2386 slope corrected terrain photons. Apply a linear weighting to
2387 each photon based on its distance to the mid-segment location:
2388 $1 / \sqrt{(\text{photon distance along} - \text{mid-segment distance})^2}$.
2389 Calculate the weighted mid-segment terrain height, weightedZ:
2390 $\text{sum}(\text{each adjusted terrain height} * \text{its weight}) / \text{sum}(\text{all}$
2391 $\text{weights})$.

2392 iv. Determine which of the three fits is best by calculating the
2393 mean and standard deviation of the fit errors. If one of the fits
2394 has both the smallest mean and standard deviations, use that
2395 fit. Else, use the fit with the smallest standard deviation. If
2396 more than one fit has the same smallest mean and/or standard
2397 deviation, use the fit with the higher polynomial.

2398 v. Use the best fit to define the mid-segment elevation. This
2399 parameter is **h_te_best_fit** in Table 2.1.

2400 1. If **h_te_best_fit** is farther than 3 m from **h_te_interp** (best
2401 fit diff threshold), check if: there are terrain photons on
2402 both sides of the mid-segment location; or the elevation
2403 difference between **weightedZ** and **h_te_interp** is
2404 greater than the best fit diff threshold; or the number of
2405 ground photons in the segment is $\leq 5\%$ of total
2406 number of classified photons per segment. If any of
2407 those cases are present, use **h_te_interp** as the corrected
2408 **h_te_best_fit**. Otherwise use **weightedZ** as the corrected
2409 **h_te_best_fit**.

2410 f. Compute the difference of the median ground height from the
2411 reference DTM height. This parameter is **h_dif_ref** in Table 2.4.

2412

2413 3. If the number of ground photons in the segment $\leq 5\%$ of total number of
2414 classified photons per segment,

2415 a. Report an invalid value for terrain products: **h_te_mean**,
2416 **h_te_median**, **h_te_min**, **h_te_max**, **h_te_mode**, **h_te_skew**, **h_te_std**,
2417 **and h_te_uncertainty** respectively as described in Table 2.1.

2418 b. If the number of ground photons in the segment is $\leq 5\%$ of total
2419 number of classified photons in the segment, compute **terrain_slope**
2420 via a linear fit of the interpolated ground surface, **FINALGROUND**,
2421 instead of the ground photons.

2422 c. Report the mid-segment interpolated terrain surface, **FinalGround**, as
2423 **h_te_interp** as described in Table 2.1, and report **h_te_best_fit** as the
2424 **h_te_interp** value.

2425

2426 **4.16 Compute segment parameters for the Canopy Products**

- 2427 1. For each 100 m segment, determine the classed photons (photons classified as
2428 ground, canopy, or top of canopy).
- 2429 a) If there are fewer than 50 classed photons in a 100 m segment, do not
2430 calculate land or canopy products.
- 2431 b) If there are 50 or more classed photons in a 100 m segment, extract all
2432 canopy photons (i.e., canopy and top of canopy; henceforth referred to
2433 as “canopy” unless otherwise noted) to create the canopy products.
- 2434 2. Only compute canopy height products if the number of canopy photons is >
2435 5% of the total number of classed photons within the segment (this control
2436 value of 5% can be modified once on orbit).
- 2437 a) If the number of ground photons is also > 5% of the total number of
2438 classed photons within the segment, set **canopy_rh_conf** to 2.
- 2439 b) If the number of ground photons is < 5% of the total number of classed
2440 photons within the segment, continue with the relative canopy height
2441 calculations, but set **canopy_rh_conf** to 1.
- 2442 c) If the number of canopy photons is < 5% of the total number of classed
2443 photons within the segment, regardless of ground percentage, set
2444 **canopy_rh_conf** to 0 and report an invalid value for each canopy height
2445 variable.
- 2446 3. Again, the relative heights (height above the interpolated ground surface,
2447 FINALGROUND) have been computed already. All parameters derived in the
2448 section are based on relative heights.
- 2449 4. Sort the heights and compute a cumulative distribution of the heights. Select
2450 the height associated with the 98% maximum height. This value is **h_canopy**
2451 listed in Table 2.2.
- 2452 5. Compute statistics on the relative canopy heights. Min, Mean, Median, Max and
2453 standard deviation. These values are reported on the product as
2454 **h_min_canopy**, **h_mean_canopy**, **h_max_canopy**, and **canopy_openness**
2455 respectively in Table 2.2.

- 2456 6. Using the cumulative distribution of relative canopy heights, select the heights
 2457 associated with the **canopy_h_metrics** percentile distributions (10, 15, 20, 25,
 2458 30, 35, 40, 45, 50, 55, 60, 65, 70, 75, 80, 85, 90, 95), and report as listed in Table
 2459 2.2.
- 2460 7. Compute the difference between h_canopy and canopy_h_metrics(50). This
 2461 parameter is **h_dif_canopy** reported in Table 2.2 and represents an amount of
 2462 canopy depth.
- 2463 8. Compute the standard deviation of all photons that were labeled as Top of
 2464 Canopy (flag 3) in the photon labeling portion. This value is reported on the
 2465 data product as **toc_roughness** listed in Table 2.2.
- 2466 9. The quadratic mean height, **h_canopy_quad** is computed by

2467
$$qmh = \sqrt{\frac{\sum_{i=1}^{N_{ca}} h_i^2}{N_{ca}}}$$

2468 where N_{ca} is the number of canopy photons in the segment and h_i are the
 2469 individual canopy heights.

2470

2471 **4.16.1 Canopy Products calculated with absolute heights**

- 2472 1. The absolute canopy height products are calculated if the number of canopy
 2473 photons is > 5% of the total number of classed photons within the segment.
 2474 No number of ground photons threshold is applied for these. Absolute
 2475 canopy heights are first determined as the relative heights of individual
 2476 photons above the estimated terrain surface. Once those cumulative
 2477 distribution is made, the absolute heights are the relative heights plus the
 2478 best fit terrain height (h_te_bestfit).
- 2479 2. The **centroid_height** parameter in Table 2.2 is represented by all the classed
 2480 photons for the segment (canopy & ground). To determine the centroid
 2481 height, compute a cumulative distribution of all absolute classified heights
 2482 and select the median height.
- 2483 3. Calculate **h_canopy_abs**, the 98th percentile of the absolute canopy heights.

- 2484 4. Compute statistics on the absolute canopy heights: Min, Mean, Median, and
2485 Max. These values are reported on the product as **h_min_canopy_abs**,
2486 **h_mean_canopy_abs**, and **h_max_canopy_abs**, respectively, as described in
2487 Table 2.2.
- 2488 5. Again, using the cumulative distribution of relative canopy heights, select the
2489 heights associated with the **canopy_h_metrics_abs** percentile distributions
2490 (10, 15, 20, 25, 30, 35, 40, 45, 50, 55, 60, 65, 70, 75, 80, 85, 90, 95) and then
2491 added to the h_te_bestfit, and report as listed in Table 2.2.

2492 **4.17 Record final product without buffer**

- 2493 1. Now that all products have be determined via processing of the *L-km*
2494 segment with the buffer included, remove the products that lie within the
2495 buffer zone on each end of the *L-km* segment.
- 2496 2. Record the final *L-km* products and move on to process the next *L-km*
2497 segment.

2498

2499

2500 **5 DATA PRODUCT VALIDATION STRATEGY**

2501 Although there are no Level-1 requirements related to the accuracy and precision
2502 of the ATL08 data products, we are presenting a methodology for validating terrain
2503 height, canopy height, and canopy cover once ATL08 data products are created.
2504 Parameters for the terrain and canopy will be provided at a fixed size of 100 m along
2505 the ground track referred to as a segment. Validation of the data parameters should
2506 occur at the 100 m segment scale and residuals of uncertainties are quantified (i.e.
2507 averaged) at the 5-km scale. This 5-km length scale will allow for quantification of
2508 errors and uncertainties at a local scale which should reflect uncertainties as a
2509 function of surface type and topography.

2510

2511 **5.1 Validation Data**

2512 Swath mapping airborne lidar is the preferred source of validation data for the
2513 ICESat-2 mission due to the fact that it is widely available and the errors associated
2514 with most small-footprint, discrete return data sets are well understood and
2515 quantified. Profiling airborne lidar systems (such as MABEL) are more challenging to
2516 use for validation due to the low probability of exact overlap of flightlines between
2517 two profiling systems (e.g. ICESat-2 and MABEL). In order for the ICESat-2 validation
2518 exercise to be statistically relevant, the airborne data should meet the requirements
2519 listed in Table 5.1. Validation data sets should preferably have a minimum average
2520 point density of 5 pts/m². In some instances, however, validation data sets with a
2521 lower point density that still meet the requirements in Table 5.1 may be utilized for
2522 validation to provide sufficient spatial coverage.

2523 Table 5.1. Airborne lidar data vertical height (*Z* accuracy) requirements for validation data.

ICESat-2 ATL08 Parameter	Airborne lidar (rms)
Terrain height	<0.3 m over open ground (vertical) <0.5 m (horizontal)

Canopy height	<2 m temperate forest, < 3 m tropical forest
Canopy cover	n/a

2524

2525 Terrain and canopy heights will be validated by computing the residuals between the
2526 ATL08 terrain and canopy height value, respectively, for a given 100 m segment and
2527 the terrain height (or canopy height) of the validation data for that same
2528 representative distance. Canopy cover on the ATL08 data product shall be validated
2529 by computing the relative canopy cover ($cc = \text{canopy returns}/\text{total returns}$) for the
2530 same representative distance in the airborne lidar data.

2531 It is recommended that the validation process include the use of ancillary data sets
2532 (i.e. Landsat-derived annual forest change maps) to ensure that the validation results
2533 are not errantly biased due to non-equivalent content between the data sets.

2534 Using a synergistic approach, we present two options for acquiring the required
2535 validation airborne lidar data sets.

2536

2537 **Option 1:**

2538 We will identify and utilize freely available, open source airborne lidar data as the
2539 validation data. Potential repositories of this data include OpenTopo (a NSF
2540 repository or airborne lidar data), NEON (a NSF repository of ecological monitoring
2541 in the United States), and NASA GSFC (repository of G-LiHT data). In addition to
2542 small-footprint lidar data sets, NASA Mission data (i.e. ICESat and GEDI) can also be
2543 used in a validation effort for large scale calculations.

2544

2545 **Option 2:**

2546 Option 2 will include Option 1 as well as the acquisition of additional airborne lidar
2547 data that will benefit multiple NASA efforts.

2548 GEDI: With the launch of the Global Ecosystems Dynamic Investigation
2549 (GEDI) mission in 2018, there are tremendous synergistic activities for
2550 data validation between both the ICESat-2 and GEDI missions. Since the
2551 GEDI mission, housed on the International Space Station, has a
2552 maximum latitude of 51.6 degrees, much of the Boreal zone will not be
2553 mapped by GEDI. The density of GEDI data will increase as latitude
2554 increases north to 51.6 degrees. Since the data density for GEDI would
2555 be at its highest near 51.6 degrees, we would propose to acquire
2556 airborne lidar data in a “GEDI overlap zone” that would ample
2557 opportunity to have sufficient coverage of benefit to both ICESat-2 and
2558 GEDI for calibration and validation.

2559 We recommend the acquisition of new airborne lidar collections that will meet our
2560 requirements to best validate ICESat-2 as well as be beneficial for the GEDI mission.
2561 In particular, we would like to obtain data over the following two areas:

- 2562 1) Boreal forest (as this forest type will NOT be mapped with GEDI)
- 2563 2) GEDI high density zone (between 50 to 51.6 degrees N). Airborne lidar data
2564 in the GEDI/ICESat-2 overlap zone will ensure cross-calibration between
2565 these two critical datasets which will allow for the creation of a global,
2566 seamless terrain, canopy height, and canopy cover product for the
2567 ecosystem community.

2568 In both cases, we would fly data with the following scenario:

2569 Small-footprint, full-waveform, dual wavelength (green and NIR), high point density
2570 (>20 pts/m²) and, over low and high relief locations. In addition, the newly acquired
2571 lidar data must meet the error accuracies listed in Table 5.1.

2572 Potential candidate acquisition areas include: Southern Canadian Rocky Mountains
2573 (near Banff), Pacific Northwest mountains (Olympic National Park, Mt. Baker-
2574 Snoqualmie National Forest), and Sweden/Norway. It is recommended that the

2575 airborne lidar acquisitions occur during the summer months to avoid snow cover in
 2576 either 2016 or 2017 prior to launch of ICESat-2.

2577

2578 **5.2 Internal QC Monitoring**

2579 In addition to the data product validation, internal monitoring of data
 2580 parameters and variables is required to ensure that the final ATL08 data quality
 2581 output is trustworthy. Table 5.2 lists a few of the computed parameters that should
 2582 provide insight into the performance of the surface finding algorithm within the
 2583 ATL08 processing chain.

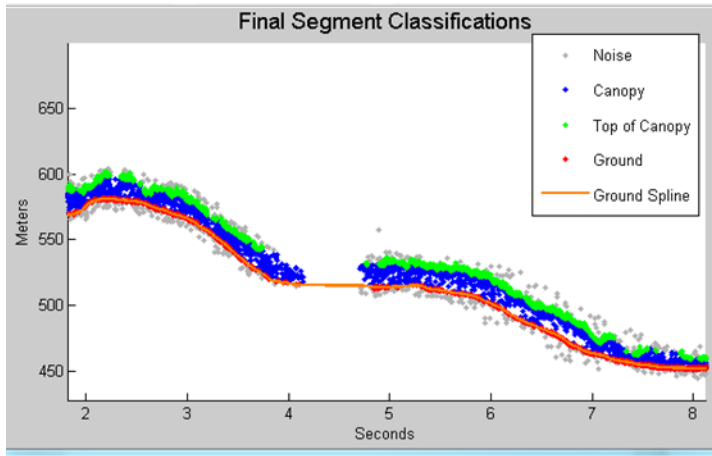
2584 Table 5.2. ATL08 parameter monitoring.

Group	Description	Source	Monitor	Validate in Field
h_te_median	Median terrain height for segment	computed		Yes against airborne lidar data. The airborne lidar data should have an absolute accuracy of <30 cm rms.
n_te_photons n_ca_photons n_toc_photons	Number of classed (sum of terrain, canopy, and top of canopy) photons in a 100 m segment	computed	Yes. Build an internal counter for the number of segments in a row where there aren't enough photons (currently a minimum of 50 photons	

h_te_interp	Interpolated terrain surface height, FINALGROUND	computed	per 100 m segment is used) Difference h_te_interp and h_te_median and determine if the value is > a specified threshold. 2 m is suggested as the threshold value. This is an internal check to evaluate whether the median elevation for a segment is roughly the same as the interpolated surface height.	
h_dif_ref	Difference between h_te_median and ref_dem	computed	This value will be computed and flagged if the difference is > 25 m. The reference DEM is the onboard DEM.	
h_canopy	95% height of individual canopy heights for segment	computed	Yes, > a specified threshold (e.g. 60 m)	Yes against airborne lidar data. The

				canopy heights derived from airborne lidar data should have a relative accuracy <2 m in temperate forest, <3 m in tropical forest
h_dif_canopy	Difference between h_canopy and canopy_h_metrics(50)	computed	Yes, this is an internal check to make sure the calculations on canopy height are not suspect	
psf_flag	Flag is set if computed PSF exceeds 1m	computed	Yes, this is an internal check to make sure the calculations are not suspect	
ph_removal_flag	Flag is set if more than 50% of classified photons in a segment is removed during final QA check	computed		
dem_removal_flag	Flag is set if more than 20% of classified photons in a segment is removed due to a large distance from the reference DEM	computed	Yes, this will check if bad results are due to bad DEM values or because too much noise was labeled as signal	

2586 In addition to the monitoring parameters listed in Table 5.2, a plot such as what is
2587 shown in Figure 5.1 would be helpful for internal monitoring and quality
2588 assessment of the ATL08 data product. Figure 5.1 illustrates in graphical form what
2589 the input point cloud look like in the along-track direction, the classifications of each
2590 photon, and the estimated ground surface (FINALGROUND).



2591

2592 Figure 5.1. Example of *L-km* segment classifications and interpolated ground surface.

2593

2594 The following parameters are to be calculated and placed in the QA/QC group on the
 2595 HDF5 data file, based on Table 5.2 of the ATL08 ATBD. Statistics shall be computed
 2596 on a per-granule basis and reported on the data product. If any parameter meets the
 2597 QA trigger conditional, an alert will be sent to the ATL08 ATBD team for product
 2598 review.

2599 Table 5.3. QA/QC trending and triggers.

QA/QC trending description	QA trigger conditional
Percentage of segments with > 50 classed photons	None
Max, median, and mean of the number of contiguous segments with < 50 classed photons	None
Number and percentage of segments with difference in $h_{te_interp} - h_{te_median}$ is greater than a specified threshold (2 m TBD)	> 50 segments in a row
Max, median, and mean of h_{diff_ref} over all segments	None
Percentage of segments where $h_{diff_ref} > 25$ m	Percentage > 75%
Percentage of segments where the h_{canopy} is > 60m	None
Max, median, and mean of h_{diff}	None
Number and percentage of Landsat continuous tree cover pixels per processing (L-km) segment with values > 100	None
Percentage of segments where psf_flag is set	Percentage > 75%
Percentage of classified photons removed in a segment during final photon QA check	Percentage > 50% (i.e., $ph_removal_flag$ is set to true)

Percentage of classified photons removed in a segment during the reference DEM threshold removal process	Percentage > 20% (i.e., dem_removal_flag is set to true)
--	--

2600

2601

2602 **6 REFERENCES**

2603

2604 Carroll, M. L., Townshend, J. R., DiMiceli, C. M., Noojipady, P., & Sohlberg, R. A.
2605 (2009). A new global raster water mask at 250 m resolution. *International Journal of*
2606 *Digital Earth*, 2(4), 291–308. <http://doi.org/10.1080/17538940902951401>

2607 Channan, S., K. Collins, and W. R. Emanuel (2014). Global mosaics of the standard
2608 MODIS land cover type data. University of Maryland and the Pacific Northwest
2609 National Laboratory, College Park, Maryland, USA.

2610 Chauve, Adrien, et al. (2008). Processing full-waveform lidar data: modelling raw
2611 signals. *International archives of photogrammetry, remote sensing and spatial*
2612 *information sciences 2007*, 102-107.

2613 Cleveland, W. S. (1979). Robust Locally Weighted Regression and Smoothing
2614 Scatterplots. *Journal of the American Statistical Association*, 74(368), 829–836.
2615 <http://doi.org/10.2307/2286407>

2616 Friedl, M.A., D. Sulla-Menashe, B. Tan, A. Schneider, N. Ramankutty, A. Sibley and X.
2617 Huang (2010). MODIS Collection 5 global land cover: Algorithm refinements and
2618 characterization of new datasets, 2001-2012, Collection 5.1 IGBP Land Cover,
2619 Boston University, Boston, MA, USA.

2620 Fritsch, F.N., and Carlson, R.E. (1980). Monotone Piecewise Cubic Interpolation.
2621 *SIAM Journal on Numerical Analysis*, 17(2), 238–246.
2622 <http://doi.org/10.1137/0717021>

2623 Goshtasby, A., and O’Neill, W.D. (1994). Curve fitting by a Sum of Gaussians.
2624 *Graphical Models and Image Processing*, 56(4), 281-288.

2625 Goetz and Dubayah (2011). Advances in remote sensing technology and
2626 implications for measuring and monitoring forest carbon stocks and change. *Carbon*
2627 *Management*, 2(3), 231-244. doi:10.4155/cmt.11.18

2628 Hall, F.G., Bergen, K., Blair, J.B., Dubayah, R., Houghton, R., Hurtt, G., Kellndorfer, J.,
2629 Lefsky, M., Ranson, J., Saatchi, S., Shugart, H., Wickland, D. (2011). Characterizing 3D
2630 vegetation structure from space: Mission requirements. *Remote sensing of*
2631 *environment*, 115(11), 2753-2775

2632 Harding, D.J., (2009). Pulsed laser altimeter ranging techniques and implications for
2633 terrain mapping, in *Topographic Laser Ranging and Scanning: Principles and*
2634 *Processing*, Jie Shan and Charles Toth, eds., CRC Press, Taylor & Francis Group, 173-
2635 194.

2636 Neuenschwander, A.L. and Magruder, L.A. (2016). The potential impact of vertical
2637 sampling uncertainty on ICESat-2/ATLAS terrain and canopy height retrievals for
2638 multiple ecosystems. *Remote Sensing*, 8, 1039; doi:10.3390/rs8121039

2639 Neuenschwander, A.L. and Pitts, K. (2019). The ATL08 Land and Vegetation Product
2640 for the ICESat-2 Mission. *Remote Sensing of Environment*, 221, 247-259.
2641 <https://doi.org/10.1016/j.rse.2018.11.005>

2642 Neumann, T., Brenner, A., Hancock, D., Robbins, J., Saba, J., Harbeck, K. (2018). ICE,
2643 CLOUD, and Land Elevation Satellite – 2 (ICESat-2) Project Algorithm Theoretical
2644 Basis Document (ATBD) for Global Geolocated Photons (ATL03).

2645 Olson, D. M., Dinerstein, E., Wikramanayake, E. D., Burgess, N. D., Powell, G. V. N.,
2646 Underwood, E. C., D'Amico, J. A., Itoua, I., Strand, H. E., Morrison, J. C., Loucks, C. J.,
2647 Allnutt, T. F., Ricketts, T. H., Kura, Y., Lamoreux, J. F., Wettengel, W. W., Hedao, P.,
2648 Kassem, K. R. (2001). Terrestrial ecoregions of the world: a new map of life on Earth.
2649 *Bioscience*, 51(11), 933-938.

2650 Sexton, J.O., Song, X.-P., Feng, M. Noojipady, P., Anand, A., Huang, C., Kim, D.-H.,
2651 Collins, K.M., Channan, S., DiMiceli, C., Townshend, J.R.G. (2013). Global, 30-m
2652 resolution continuous fields of tree cover: Landsat-based rescaling of MODIS
2653 Vegetation Continuous Fields with lidar-based estimations of error. *International*
2654 *Journal of Digital Earth*, 130321031236007. doi:10.1080/17538947.2013.786146.

2655

2656 **Appendix A**

2657 **DRAGANN Gaussian Deconstruction**

2658 John Robbins

2659 20151021

2660

2661 Updates made by Katherine Pitts:

2662 20170808

2663 20181218

2664

2665 **Introduction**

2666 This document provides a verbal description of how the DRAGANN (Differential,
2667 Regressive, and Gaussian Adaptive Nearest Neighbor) filtering system deconstructs
2668 a histogram into Gaussian components, which can also be called *iteratively fitting a*
2669 *sum of Gaussian Curves*. The purpose is to provide enough detail for ASAS to create
2670 operational ICESat-2 code required for the production of the ATL08, Land and
2671 Vegetation product. This document covers the following Matlab functions within
2672 DRAGANN:

- 2673 • mainGaussian_dragann
- 2674 • findpeaks_dragann
- 2675 • peakWidth_dragann
- 2676 • checkFit_dragann
- 2677

2678 Components of the k-d tree nearest-neighbor search processing and histogram
2679 creation were covered in the document, *DRAGANN k-d Tree Investigations*, and have
2680 been determined to function consistently with UTexas DRAGANN Matlab software.

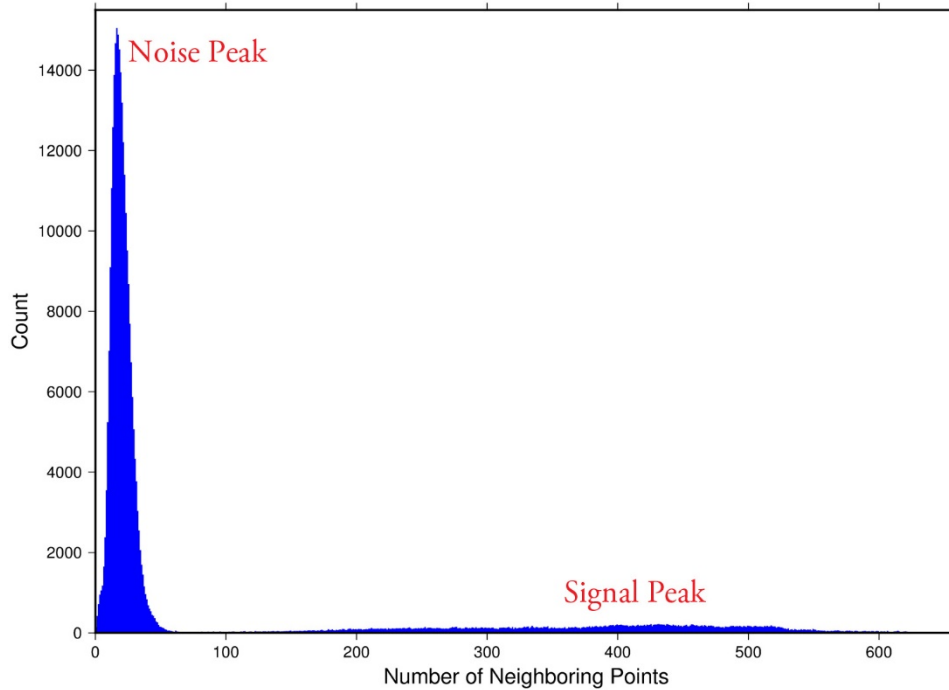
2681

2682 **Histogram Creation**

2683 Steps to produce a histogram of nearest-neighbor counts from a normalized photon
2684 cloud segment have been completed and confirmed. Figure A.1 provides an example
2685 of such a histogram. The development, below, is specific to the two-dimensional
2686 case and is provided as a review.

2687 The histogram represents the frequency (count) of the number of nearby photons
2688 within a specified radius, as ascertained for each point within the photon cloud. The
2689 radius, R , is established by first normalizing the photon cloud in time (x-axis) and in
2690 height (y-axis), i.e., both sets of coordinates (time & height) run from 0 to 1; then an
2691 average radius for finding 20 points is determined based on forming the ratio of 20
2692 to the total number of the photons in the cloud (N_{total}): $20/N_{total}$.

2693



2694

2695 **Figure A.1.** Histogram for Mabel data, channel 43 from SE-AK flight on July 30, 2014
 2696 at 20:16.

2697 Given that the total area of the normalized photon cloud is, by definition, 1, then this
 2698 ratio gives the average area, A , in which to find 20 points. A corresponding radius is
 2699 found by the square root of A/π . A single equation describing the radius, as a
 2700 function of the total number of photons in the cloud (remembering that this is done
 2701 in the cloud normalized, two-dimensional space), is given by

2702
$$R = \sqrt{\frac{20/N_{total}}{\pi}} \quad (A.1)$$

2703 For the example in Figure A.1, R was found to be 0.00447122. The number of
 2704 photons falling into this radius, at each point in the photon cloud, is given along the
 2705 x-axis; a count of their number (or frequency) is given along the y-axis.

2706

2707 **Gaussian Peak Removal**

2708

2709 At this point, the function, `mainGaussian_dragann`, is called, which passes the
 2710 histogram and the number of peaks to detect (typically set to 10).

2711 This function essentially estimates (i.e., fits) a sequence of Gaussian curves, from
 2712 larger to smaller. It determines a Gaussian fit for the highest histogram peak, then
 2713 removes it before determining the fit for the next highest peak, etc. In concept, the
 2714 process is an iterative sequential-removal of the ten largest Gaussian components
 2715 within the histogram.

2716 In the process of *sequential least-squares*, parameters are re-estimated when input
2717 data is incrementally increased and/or improved. The present problem operates in
2718 a slightly reverse way: the data set is fixed (i.e., the histogram), but components
2719 within the histogram (independent Gaussian curve fits) are removed sequentially
2720 from the histogram. The paper by *Goshtasby & O'Neill* (1994) outlines the concepts.

2721 Recall that a Gaussian curve is typically written as

$$2722 \quad y = a \cdot \exp(-(x - b)^2 / 2c^2) \quad (\text{A.2})$$

2723 where a = the height of the peak; b = position of the peak; and c = width of the bell
2724 curve.

2725 The function, `mainGaussian_dragann`, computes the $[a, b, c]$ values for the ten
2726 highest peaks found in the histogram. At initialization, these $[a, b, c]$ values are set to
2727 zero. The process begins by locating histogram peaks via the function,
2728 `findpeaks_dragann`.

2729

2730 **Peak Finding**

2731 As input arguments, the `findpeaks_dragann` function receives the histogram and a
2732 minimum peak size for consideration (typically set to zero, which means all peaks
2733 will be found). An array of index numbers (i.e., the “number of neighboring points”,
2734 values along x-axis of Figure A.1) for all peaks is returned and placed into the
2735 variable `peaks`.

2736 The methodology for locating each peak goes like this: The function first computes
2737 the derivatives of the histogram. In Matlab there is an intrinsic function, called `diff`,
2738 which creates an array of the derivatives. `Diff` essentially computes the differences
2739 along sequential, neighboring values. “ $Y = \text{diff}(X)$ calculates differences between
2740 adjacent elements of X .” [from Matlab Reference Guide] Once the derivatives are
2741 computed, then `findpeaks_dragann` enters a loop that looks for changes in the sign
2742 of the derivative (positive to negative). It skips any derivatives that equal zero.

2743 For the k th derivative, the “*next*” derivative is set to $k+1$. A test is made whereby if
2744 the $k+1$ derivative equals zero and $k+1$ is less than the total number of histogram
2745 values, then increment “*next*” to $k+2$ (i.e., find the next negative derivative). The test
2746 is iterated until the start of the “down side” of the peak is found (i.e., these iterations
2747 handle cases when the peak has a flat top to it).

2748 When a sign change (positive to negative) is found, the function then computes an
2749 approximate index location (variable *maximum*) of the peak via

$$2750 \quad \text{maximum} = \text{round}\left(\frac{\text{next}-k}{2}\right) + k \quad (\text{A.3})$$

2751 These values of *maximum* are retained in the peaks array (which can be *grown* in
2752 Matlab) and returned to the function mainGaussian_dragann.

2753 Next, back within mainGaussian_dragann, there are two tests to determine whether
2754 the first or last elements of the histogram are peaks. This is done since the
2755 findpeaks_dragann function will not detect peaks at the first or last elements, based
2756 solely on derivatives. The tests are:

2757 If (histogram(1) > histogram(2) && max(histogram)/histogram(1) < 20) then
2758 insert a value of 1 to the very first element of the peaks array (again, Matlab can
2759 easily “grow” arrays). Here, max(histogram) is the highest peak value across the
2760 whole histogram.

2761 For the case of the last histogram value (say there are N-bins), we have

2762 If (histogram(N) > histogram(N-1) && max(histogram)/histogram(N) < 4) then
2763 insert a value of N to the very last element of the peaks array.

2764 One more test is made to determine whether there any peaks were actually found
2765 for the whole histogram. If none were found, then the function,
2766 mainGaussian_dragann, merely exits.

2767

2768 **Identifying and Processing upon the Ten Highest Peaks**

2769 The function, mainGaussian_dragann, now begins a loop to analyze the ten highest
2770 peaks. It begins the n^{th} loop (where n goes from 1 to 10) by searching for the largest
2771 peak among all remaining peaks. The index number, as well as the magnitude of the
2772 peak, are retained in a variable, called maximum, with dimension 2.

2773 In each pass in the loop, the $[a,b,c]$ values (see eq. 2) are retained as output of the
2774 function. The values of a and b are set equal to the index number and peak
2775 magnitude saved in maximum(1) and maximum(2), respectively. The c -value is
2776 determined by calling the function, peakWidth_dragann.

2777 *Determination of Gaussian Curve Width*

2778 The function, peakWidth_dragann, receives the whole histogram and the index
2779 number (maximum(1)) of the peak for which the value c is needed, as arguments.
2780 For a specific peak, the function essentially searches for the point on the histogram
2781 that is about $\frac{1}{2}$ the size of the peak and that is furthest away from the peak being
2782 investigated (left and right of the peak). If the two sides (left and right) are
2783 equidistant from the peak, then the side with the smallest value is chosen ($> \frac{1}{2}$
2784 peak).

2785 Upon entry, it first initializes c to zero. Then it initializes the index values left, xL and
2786 right, xR as index-1 and index+1, respectively (these will be used in a loop,

2787 described below). It next checks whether the n^{th} peak is the first or last value in the
2788 histogram and treats it as a special case.

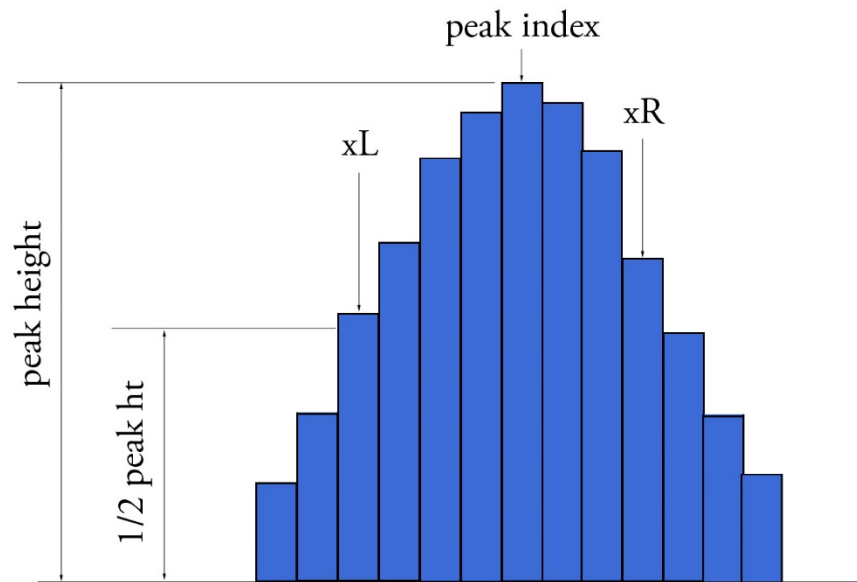
2789 At initialization, first and last histogram values are treated as follows:

2790 If first bin of histogram (peak = 1), set left = 1 and xL = 1.

2791 If last bin of histogram, set right = m and xR = m , where m is the final index of the
2792 histogram.

2793 Next, a search is made to the left of the peak for a nearby value that is smaller than
2794 the peak value, but larger than half of the peak value. A while-loop does this, with
2795 the following conditions: (a) left > 0, (b) histogram value at left is \geq half of histo
2796 value at peak and (c) histo value at left is \leq histo value at peak. When these
2797 conditions are all true, then xL is set to left and left is decremented by 1, so that the
2798 test can be made again. When the conditions are no longer met (i.e., we've moved to
2799 a bin in the histogram where the value drops below half of the peak value), then the
2800 program breaks out of the while loop.

2801 This is followed by a similar search made upon values to the right of the peak. When
2802 these two while-loops are complete, we then have the index numbers from the
2803 histogram representing bins that are above half the peak value. This is shown in
2804 Figure A.2.



2805

2806 **Figure A.2.** Schematic representation of a histogram showing xL and xR parameters
2807 determined by the function peakWidth_dragann.

2808 A test is made to determine which of these is furthest from the middle of the peak. In
2809 Figure A.2, xL is furthest away and the variable x is set to equal xL. The histogram

2810 “height” at x , which we call V_x , is used (as well as x) in an inversion of Equation A.2
2811 to solve for c :

$$2812 \quad c = \sqrt{\frac{-(x-b)^2}{2\ln\left(\frac{V_x}{a}\right)}} \quad (\text{A.4})$$

2813 The function, `peakWidth_dragann`, now returns the value of c and control returns to
2814 the function, `mainGaussian_dragann`.

2815 The `mainGaussian_dragann` function then picks-up with a test on whether the
2816 returned value of c is zero. If so, then use a value of 4, which is based on an *a priori*
2817 understanding that c usually falls between 4 and 6. If the value of c is not zero, then
2818 add 0.5 to c .

2819 At this point, we have the $[a,b,c]$ values of the Gaussian for the n^{th} peak. Based on
2820 these values, the Gaussian curve is computed (via Equation A.2) and it is removed
2821 (subtracted) from the current histogram (and put into a new variable called
2822 `newWave`).

2823 After a Gaussian curve is removed from the current histogram, the following peak
2824 width calculations could potentially have a V_x value less than 1 from a . This would
2825 cause the width, c , to be calculated as unrealistically large. Therefore, a check is put
2826 in place to determine if $a - V_x < 1$. If so, V_x is set to a value of $a - 1$.

2827 *Numeric Optimization Steps*

2828 The first of the optimization steps utilizes a Full Width Half Max (*FWHM*) approach,
2829 computed via

$$2830 \quad FWHM = 2c\sqrt{2\ln 2} \quad (\text{A.5})$$

2831 A left range, L_r , is computed by $L_r = \text{round}(b - FWHM/2)$. This tested to make sure it
2832 doesn't go off the left edge of the histogram. If so, then it is set to 1.

2833 Similarly, a right range, R_r , is computed by $R_r = \text{round}(b + FWHM/2)$. This is also tested
2834 to be sure that it doesn't go off the right edge of the histogram. If so, then it is set to
2835 the index value for the right-most edge of the histogram.

2836 Using these new range values, create a temporary segment (between L_r and R_r) of
2837 the `newWave` histogram, this is called `errorWave`. Also, set three delta parameters
2838 for further optimization:

2839 $\Delta C = 0.05;$ $\Delta B = 0.02;$ $\Delta A = 1$

2840 The temporary segment, `errorWave` is passed to the function `checkFit_dragann`,
2841 along with a set of zero values having the same number of elements as `errorWave`,
2842 the result, at this point, is saved into a variable called `oldError`. The function,
2843 `checkFit_dragann`, computes the sum of the squares of the difference between two

2844 histogram segments (in this case, errorWave and zeros with the same number of
2845 elements as errorWave). Hence, the result, oldError, is the sum of the squares of the
2846 values of errorWave. This function is applied in optimization loops, to refine the
2847 values of b and c , described below.

2848 *Optimization of the b -parameter.* The do-loop operates at a maximum of 1000 times.
2849 It's purpose is to refine the value of b , in 0.02 increments. It increments the value of
2850 b by DeltaB, to the right, and computes a new Gaussian curve based on $b+\Delta b$, which
2851 is then removed from the histogram with the result going into the variable
2852 newWave. As before, checkFit_dragann is called by passing the range-limited part of
2853 newWave (errorWave) and returning a new estimate of the error (newError) which
2854 is then checked against oldError to determine which is smaller. If newError is \geq
2855 oldError, then the value of b that produced oldError is retained, and the testing loop
2856 is exited.

2857 *Optimization of the c -parameter.* Now the value of c is optimized, first to the left,
2858 then to the right. It is performed independently of, but similarly, to the b -parameter,
2859 using do-loops with a maximum of 1000 passes. These loops increment (to right) or
2860 decrement (to left) by a value of 0.05 (DeltaC) and use checkFit_dragann to, again,
2861 check the quality of the fit. The loops (right and left) kick-out when the fit is found to
2862 be smallest.

2863 The final, optimized Gaussian curve is now removed (subtracted) from the
2864 histogram. After removal, a statement "corrects" any histogram values that may
2865 drop below zero, by setting them to zero. This could happen due to any mis-fit of the
2866 Gaussian.

2867 The n^{th} loop is concluded by examining the peaks remaining in the histogram
2868 without the peak just processed by sending the n^{th} -residual histogram back into the
2869 function findpeaks_dragann. If the return of peak index numbers from
2870 findpeaks_dragann reveals more than 1 peak remaining, then the index numbers for
2871 peaks that meet these three criteria are retained in an array variable called these:

- 2872 1. The peak must be located above $b(n)-2*c(n)$, and
 - 2873 2. The peak must be located below $b(n)+2*c(n)$, and
 - 2874 3. The height of the peak must be $< a(n)/5$.
- 2875

2876 The peaks meeting all three of these criteria are to be eliminated from further
2877 consideration. What this accomplishes is eliminate the nearby peaks that have a size
2878 lower than the peak just previously analyzed; thus, after their elimination, only
2879 leaving peaks that are further away from the peak just processed and are
2880 presumably "real" peaks. The n^{th} iteration ends here, and processing begins with the
2881 revised histogram (after having removed the peak just analyzed).

2882

2883 **Gaussian Rejection**

2884 The function `mainGaussian_dragann` returns the $[a,b,c]$ parameters for the ten
2885 highest peaks from the original histogram. The remaining code in `dragann` examines
2886 each of the ten Gaussian peaks and eliminates the ones that fail to meet a variety of
2887 conditions. This section details how this is accomplished.

2888 First, an approximate area, $area1=a*c$, is computed for each found peak and b , for all
2889 ten peaks, being the index of the peaks, are converted to an actual value via
2890 $b+\min(\text{numptsinrad})-1$ (call this $allb$).

2891 Next, a rejection is made for all peaks that have any component of $[a,b,c]$ that are
2892 imaginary (Matlab `isreal` function is used to confirm that all three components are
2893 real, in which case it passes).

2894 To check for a narrow noise peak at the beginning of the histogram in cases of low
2895 noise rates, such as during nighttime passes, a check is made to first determine if the
2896 highest Gaussian amplitude, a , within the first 5% of the histogram is $\geq 1/10$ * the
2897 maximum amplitude of all Gaussians. If so, that peak's Gaussian width, c , is checked
2898 to determine if it is ≤ 4 bins. If neither of those conditions are met in the first 5%,
2899 the conditions are rechecked for the first 10% of the histogram. This process is
2900 repeated up to 30% of the histogram, in 5% intervals. Once a narrow noise peak is
2901 found, the process breaks out of the incremental 5% histogram checks, and the
2902 noise peak values are returned as $[a0, b0, c0]$.

2903 If a narrow noise peak was found, the remaining peak area values, $area1 (a*c)$, then
2904 pass through a descending sort; if no narrow noise peak was found, all peak areas go
2905 through the descending sort. So now, the $[a,allb,c]$ -values are sorted from largest
2906 "area" to smallest, these are placed in arrays $[a1, b1, c1]$. If a narrow noise peak was
2907 found, it is then appended to the beginning of the $[a1, b1, c1]$ arrays, such that $a1 =$
2908 $[a0 a1]$, $b1 = [b0 b1]$, $c1 = [c0 c1]$.

2909 In the case that a narrow noise peak was not found, a test is made to check that at
2910 least one of the peaks is within the first 10% of the whole histogram. It is done
2911 inside a loop that works from peak 1 to the number of peaks left at this point. This
2912 loop first tests whether the first (sorted) peak is within the first 10% of the
2913 histogram; if so, then it simply kicks out of the loop. If not, then it places the loop's
2914 current peak into a holder (`ihold`) variable, increments the loop to the next peak and
2915 runs the same test on the second peak, etc. Here's a Matlab code snippet:

```
2916     inds = 1:length(a1);  
2917     for i = 1:length(b1)  
2918         if b1(i) <= min(numptsinrad) + 1/10*max(numptsinrad)  
2919             if i==1  
2920                 break;  
2921             end  
2922             ihold = inds(i);  
2923             for j = i:-1:2  
2924                 inds(j) = inds(j-1);  
2925             end  
2926             inds(1) = ihold;
```

```

2927         break
2928     end
2929 end
2930

```

2931 The j-loop expression gives the `init_val:step_val:final_val`. The semi-colon at the end
 2932 of statements causes Matlab to execute the expression without printout to the user's
 2933 screen. When this loop is complete, then the indexes (`inds`) are re-ordered and
 2934 placed back into the `[a1,b1,c1]` and `area1` arrays.

2935 Next, are tests to reject any Gaussian peak that is entirely encompassed by another
 2936 peak. A Matlab code snippet helps to describe the processing.

```

2937 % reject any gaussian if it is fully contained within another
2938 isR = true(1,length(a1));
2939 for i = 1:length(a1)
2940     ai = a1(i);
2941     bi = b1(i);
2942     ci = c1(i);
2943     aset = (1-(c1/ci).^2);
2944     bset = ((c1/ci).^2*2*bi - 2*b1);
2945     cset = -(2*c1.^2.*log(a1/ai)-b1.^2+(c1/ci).^2*bi^2);
2946     realset = (bset.^2 - 4*aset.*cset >= 0) | (a1 > ai);
2947     isR = isR & realset;
2948 end
2949 a2 = a1(isR);
2950 b2 = b1(isR);
2951 c2 = c1(isR);
2952

```

2953 The logical array `isR` is initialized to all be true. The i-do-loop will run through all
 2954 peaks. The computations are done in array form with the variables `aset,bset,cset` all
 2955 being arrays of `length(a1)`. At the bottom of the loop, `isR` remains "true" when
 2956 either of the conditions in the expression for `realset` is met (the single "|" is a logical
 2957 "or"). Also, the nomenclature, "." and ".", denote element-by-element array
 2958 operations (not matrix operations). Upon exiting the i-loop, the array variables
 2959 `[a2,b2,c2]` are set to the `[a1,b1,c1]` that remain as "true." [At this point, in our test
 2960 case from channel 43 of East-AK Mable flight on 20140730 @ 20:16, six peaks are
 2961 still retained: 18, 433, 252, 33, 44.4 and 54.]

2962 Next, reject Gaussian peaks whose centers lay within 3σ of another peak, unless only
 2963 two peaks remain. The code snippet looks like this:

```

2964 isR = true(1, length(a2));
2965 for i = 1:length(a2)
2966     ai = a2(i);
2967     bi = b2(i);
2968     ci = c2(i);
2969     realset = (b2 > bi+3*ci | b2 < bi-3*ci | b2 == bi);
2970     realset = realset | a2 > ai;
2971     isR = isR & realset;
2972 end
2973 if length(a2) == 2
2974     isR = true(1, 2);
2975 end
2976 a3 = a2(isR);

```

```
2977     b3 = b2(isR);
2978     c3 = c2(isR);
2979
```

2980 Once again, the isR array is initially set to “true.” Now, the array, realset, is tested
2981 twice. In the first line, one of three conditions must be true. In the second line, if
2982 realset is true or $a2 > ai$, then it remains true. At this point, we’ve pared down, from
2983 ten Gaussian peaks, to two Gaussian peaks; one represents the noise part of the
2984 histogram; the other represents the signal part.

2985 If there are less than two peaks left, a thresholding/histogram error message is
2986 printed out. If the lastTryFlag is not set, DRAGANN ends its processing and an empty
2987 IDX value is returned. The lastTryFlag is set in the preprocessing function which
2988 calls DRAGANN, as multiple DRAGANN runs may be tried until sufficient signal is
2989 found.

2990 If there are two peaks left, then set the array [a,b,c] to those two peaks. [At this
2991 point, in our test case from channel 43 of East-AK Mable flight on 20140730 @
2992 20:16, the two peaks are: 18 and 433.]

2993

2994 **Gaussian Thresholding**

2995 With the two Gaussian peaks identified as noise and signal, all that is left is to
2996 compute the threshold value between the Gaussians.

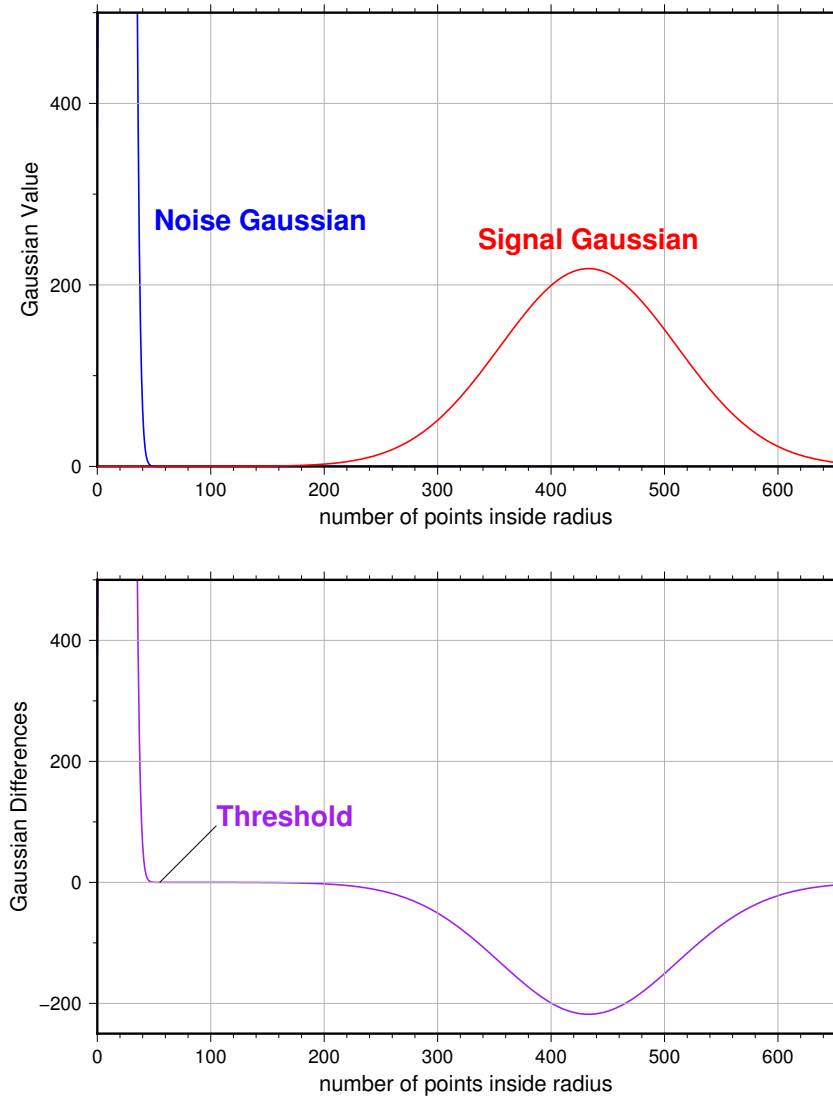
2997 An array of xvals is established running from $\min(\text{numptsinrad})$ to
2998 $\max(\text{numptsinrad})$. In our example, xvals has indices between 0 and 653. For each
2999 of these xvals, Gaussian curves (allGauss) are computed for the two Gaussian peaks
3000 [a,b,c] determined at the end of the previous section. This computation is performed
3001 via a function called gaussmaker which receives, as input, the xvals array and the
3002 [a,b,c] parameters for the two Gaussian curves. An array of heights of the Gaussian
3003 curves is returned by the function, computed with Equation A.2. In Matlab, the
3004 allGauss array has dimension 2×654 . An array, noiseGauss is set to be equal to the
3005 1st column of allGauss.

3006 An if-statement checks whether the b array has more than 1 element (i.e., consisting
3007 of two peaks), if so, then nextGauss is set to the 2nd column of allGauss, and a
3008 difference, noiseGauss-nextGauss, is computed.

3009 The following steps are restricted to be between the two main peaks. First, the first
3010 index of the absolute value of the difference that is near-zero (defined as $1e-8$) is
3011 found, if it exists, and put into the variable diffNearZero. This is expected to be found
3012 if the two Gaussians are far away from each other in the histogram.

3013 Second, the point (i.e., index) is found of the minimum of the absolute value of the
3014 difference; this index is put into variable, signchanges. This point is where the sign
3015 changes from positive to negative as one moves left-to-right, up the Gaussian curve

3016 differences (noise minus next will be positive under the peak of the noise curve, and
3017 negative under the next (signal) curve). Figure A.3 (top) shows the two Gaussian
3018 curves. The bottom plot shows their differences.



3019

3020 **Figure A.3.** Top: two remaining Gaussian curves representing the noise (blue) and
3021 signal (red) portions of the histogram in F1gure A.1. Bottom: difference noise -
3022 signal of the two Gaussian curves. The threshold is defined as the point where the
3023 sign of the differences change.

3024 If there is any value stored in `diffNearZero`, that value is now saved into the variable
3025 `threshNN`. Else, the value of the threshold in `signchanges` is saved into `threshNN`,
3026 concluding the if-statement for `b` having more than 1 element.

3027 An else clause ($b \neq 1$), merely sets threshNN to $b+c$, i.e., 1-standard deviation away
3028 from mean of the (presumably) noise peak.

3029 The final step is mask the signal part of the histogram where all indices above the
3030 threshNN index are set to logical 1 (true). This is applied to the numptsinrad array,
3031 which represents the photon cloud. After application, dragann returns the cloud
3032 with points in the cloud identified as “signal” points.

3033 The Matlab code has a few debug statements that follow, along with about 40 lines
3034 for plotting.

3035

3036 **References**

3037 Goshtasby, A & W. D. O’Neill, Curve Fitting by a Sum of Gaussians, *CVGIP: Graphical*
3038 *Models and Image Processing*, V. 56, No. 4, 281-288, 1994.